Cross-cultural ethnobotanical knowledge of *Sandoricum koetjape* (Burm.f.) Merr. supported by multi-target ethnopharmacological evidence

Nur Anisa, Asril Burhan, Hersan Bayu Kurnia, Ulfa Febiana Whatin, I Gusti Ngurah Sentana Putra, M. Salman Nuryahya, Dyah Ayu Puspitasari, Fajar Dini, Rosa Amelia, Rati Lestari, Arman Arman, Muh Akbar Idris, Fitmawati, Silmi Mariya, Berry Juliandi

Correspondence

Nur Anisa[1], Asril Burhan[2,3], Hersan Bayu Kurnia[4], Ulfa Febiana Whatin[5], I Gusti Ngurah Sentana Putra[6], M. Salman Nuryahya[7], Dyah Ayu Puspitasari[5], Fajar Dini[8], Rosa Amelia[8], Rati Lestari[7], Arman Arman[7], Muh Akbar Idris[6,9], Fitmawati[4], Silmi Mariya[10], Berry Juliandi[1*]

[1]Animal Biosciences Study Program, Department of Biology, IPB University, Bogor, Indonesia
[2]Plant Biology Study Program, Department of Biology, IPB University, Bogor, Indonesia
[3]Department of Pharmaceutical Biology, Faculty of Health Science, Universitas Almarisah Madani, Makasar, Indonesia
[4]Department of Biology, Riau University, Pekanbaru, Indonesia
[5]Biotechnology Study Program, Graduate School, IPB University, Bogor, Indonesia
[6]Department of Statistics and Data Sciences, IPB University, Bogor, Indonesia
[7]Integrated Pest Management Study Program, Department of Plant Protection, IPB University, Bogor, Indonesia
[8]Microbiology Study Program, Department of Biology, IPB University, Bogor, Indonesia
[9]Department of Mathematics, Faculty of Mathematics and Natural Sciences, Universitas Sulawesi Barat, Majene, Indonesia
[10]Laboratory Microbiology and Immunology, Primate Research Center (PSSP), IPB University, Bogor, Indonesia

*Corresponding Author: bjuliandi@apps.ipb.ac.id

Ethnobotany Research and Applications 35:23 (2026) - http://dx.doi.org/10.32859/era.35.23.1-86
Manuscript received: 04/05/2026 - Revised manuscript received: 13/07/2026 - Published: 14/07/2026

Research

Abstract

Background: *Sandoricum koetjape* (Burm.f.) Merr is embedded in Southeast Asian ethnobotanical knowledge, where bark, leaves, roots, and fruit pericarps are used for digestive disorders, fever, inflammation, postpartum recovery, wounds, and functional beverages. Although these practices are culturally diverse, they converge around symptom clusters associated with inflammatory and metabolic imbalance. This study examined whether cross-cultural plant-part selection and preparation patterns can be linked with supporting ethnopharmacological evidence.

Methods: Published ethnobotanical records were synthesized to map plant parts, traditional uses, preparation practices, and reported bioactive constituents. Based on documented use, leaves and fruit pericarps were evaluated using α-glucosidase inhibition as a limited supporting assay. Reported triterpenoids and limonoids were further assessed through drug-likeness screening, target prediction, network pharmacology, PPI analysis, GO/KEGG enrichment, and molecular docking to explore plausible mechanisms related to inflammation, metabolic regulation, and cancer-associated pathways.

Results: Ethnobotanical records showed repeated cross-cultural use of bark, leaves, roots, and fruit-derived materials, with decoction, infusion, topical application, and functional beverages. Leaf extract showed moderate alpha-glucosidase inhibition (IC_{50} = 228.27 ± 0.91 ppm), whereas fruit pericarp activity was weak (>500 ppm). Network analyses identified IL6, TNF, PPARG, and TP53 as key inflammatory and metabolic-oncogenic regulators connecting traditional symptom categories between selected compounds and these proteins.

Conclusions: *S. koetjape* use appears to reflect culturally transmitted plant-part selection associated with inflammation, digestive disturbance, and metabolic regulation. Laboratory and computational findings should be interpreted as supportive, hypothesis-generating evidence rather than direct therapeutic proof.

Keywords: Ethnobotany, Ethnopharmacology, Traditional knowledge, Triterpenoid, *Sandoricum koetjape*.

Background

Sandoricum koetjape (Burm.f.) Merr. is a tropical tree of the Meliaceae family that has long been embedded in ethnobotanical knowledge systems across Southeast Asia (Powell *et al.* 1991). The species is known by different local names, including *krathon* or *santhon* in Thailand and *sentul* or *kecapi* in Indonesia, reflecting its cultural familiarity and diverse uses among local communities (Kaneda *et al.* 1992; Wijaya 2022). Ethnobotanical records from Thailand, Malaysia, the Philippines, Indonesia, and Myanmar show that different plant parts, including bark, leaves, roots, and fruit pericarps, are selectively used for digestive disorders, diarrhea, fever, inflammation, postpartum recovery, wounds, skin-related conditions, and functional beverages (Perry & Metzger 1980; Kaneda *et al.* 1992; Lim 2012; Adnyana 2020; Agapin 2020; Izazah & Anisa 2021; Bailly 2022; Wijaya 2022).

The ethnobotanical value of *S. koetjape* is not limited to a single plant part or therapeutic indication. In Thailand, bark decoctions are ethnobotanically prepared to relieve diarrhea, while in Malaysia, aqueous bark extracts are consumed as a restorative tonic after childbirth (Kaneda *et al.* 1992; Wijaya 2022). In the Philippines, leaves are used not only for diarrhea but also for fever and inflammation, either as decoctions, topical applications, or bathing preparations, while roots are used as general tonics and to treat dysentery (Perry & Metzger 1980; Lim 2012; Agapin 2020). In Indonesia, stem bark preparations are used for colic, leucorrhea, stomach disorders, and skin infections, including ringworm (Perry & Metzger 1980; Novaryatiin & Indah 2019). The cultural relevance of this species is also further reflected in Balinese traditional healing traditions such as *Taru Pramana*, as well as among the Baduy community, where root and leaf preparations are used as herbal drinks (*loloh*) for digestive disorders (Adnyana 2020; Igiastini *et al.* 2021). In Riau, Indonesia, fruit peel is traditionally consumed as a daily herbal infusion, reflecting its local use as a functional beverages (Izazah & Anisa 2021).

The repeated use of different plant parts across cultural settings suggests that traditional knowledge of *S. koetjape* may reflect a cumulative process of empirical selection based on perceived efficacy, availability, and preparation suitability. Bark and roots are commonly associated with digestive and restorative uses, leaves are frequently linked to fever and inflammation, while fruit-derived materials are often consumed as infusions or functional beverages (Perry & Metzger 1980; Kaneda *et al.* 1992; Lim 2012; Adnyana 2020; Agapin 2020; Izazah & Anisa 2021; Yadana *et al.* 2021; Bailly 2022; Wijaya 2022). Decoction, infusion, topical application, bathing preparation, and direct consumption represent dominant preparation modes (Bailly 2022; Wijaya 2022). This pattern is important from an ethnobotanical perspective because it shows how communities adapt the same species to different health needs while maintaining recurring themes related to digestive disturbance, inflammatory symptoms, and general body restoration.

Although traditional communities do not classify illness using modern biomedical categories such as diabetes or cancer, many reported uses of *S. koetjape* converge around symptom clusters associated with inflammation, digestive imbalance, fever, wounds, and metabolic discomfort. These conditions may be linked to broader biological processes such as inflammatory signaling, oxidative stress, and metabolic regulation (Sahoo *et al.* 2023; Shao *et al.* 2024). Therefore, the ethnobotanical relevance of *S. koetjape* should not be interpreted as direct traditional evidence for treating modern chronic diseases, but as a culturally grounded indication that the species may influence physiological processes shared across several disease contexts.

Within this framework, diabetes- and breast cancer-related targets were used as modern biomedical pathway models rather than as direct traditional disease claims. Both disease contexts involve processes that overlap with traditional symptom categories documented for *S. koetjape*, including inflammation, metabolic imbalance, oxidative stress, tissue dysregulation, and altered cell survival (Sahoo *et al.* 2023; Guo *et al.* 2024). Exploring these pathway models therefore provides a

mechanistic context for examining whether culturally selected plant parts and reported compounds may correspond to multi-target biological networks. This approach is particularly relevant because inflammatory and metabolic regulation commonly involve interconnected pathways, including PI3K/AKT, AMPK, and NF-κB signaling, which are also implicated in metabolic dysfunction, cytokine signaling, and cell-survival regulation (Hopkins *et al.* 2018; Shao *et al.* 2024).

Phytochemical studies provide supporting evidence for this interpretation. Previous reports have identified triterpenoids and limonoids as major constituents of *S. koetjape*, including compounds with reported α-glucosidase inhibitory, anti-inflammatory, antibacterial, cytotoxic, and other bioactivities (Bailly 2022; Hang *et al.* 2024; Anisa *et al.* 2026). Cycloartane-type triterpenes and related compounds, such as 16R,22R-dihydroxycycloartenone, katononic acid, and koetjapic acid, have shown α-glucosidase inhibitory activity, while koetjapic acid has also been reported to affect breast cancer cell behavior, including cell viability, invasion, migration, and colony formation (Nassar *et al.* 2012; Hang *et al.* 2024). These findings do not replace ethnobotanical evidence, but they provide a biological basis for exploring how traditionally selected plant parts may contain compounds relevant to inflammatory, metabolic, and cancer-associated pathways.

Most previous studies on *S. koetjape* have focused on isolated metabolites or single bioactivity endpoints. However, ethnobotanical use usually involves crude preparations, mixed constituents, and multiple modes of application. Such practices are more consistent with a multi-component and multi-target framework than with a single-compound, single-target model. From an ethnopharmacological perspective, integrating traditional knowledge with limited experimental and computational evidence can help explain how culturally transmitted plant-use patterns may correspond to broader biological mechanisms without overstating therapeutic claims.

In this study, *S. koetjape* was examined as a culturally embedded medicinal plant whose plant-part selection and preparation practices vary across Southeast Asian knowledge systems. Rather than treating traditional use merely as a rationale for pharmacological screening, this work places ethnobotanical knowledge as the central interpretive framework. Published records were synthesized to identify recurring patterns of plant use, preparation methods, therapeutic indications, and reported bioactive constituents. Leaves and fruit pericarps were selected based on documented traditional use and evaluated through a limited α-glucosidase inhibition assay, while reported triterpenoids and limonoids were explored using drug-likeness screening, target prediction, network pharmacology, protein–protein interaction analysis, GO/KEGG enrichment, and molecular docking to generate mechanistic hypotheses. By integrating ethnobotanical synthesis with supporting in vitro and in silico evidence, this study aims to clarify how culturally transmitted knowledge of *S. koetjape* may correspond to multi-target biological pathways related to inflammatory and metabolic regulation.

Materials and Methods

Ethnobotanical records of *S. koetjape* were systematically compiled from published literature to document local names, geographic context, plant parts, traditional indications, preparation methods, and routes of administration. These data were used to identify cross-cultural patterns of plant-part selection and to guide the interpretation of the experimental and computational analyses. The review was not treated as background information only, but as the primary framework for evaluating the cultural relevance of subsequent ethnopharmacological evidence.

Plant material collection, voucher deposition, and Nagoya Protocol compliance

Leaves and fruit pericarps of *S. koetjape* were collected from Pekanbaru, Riau, Indonesia. The plant was identified by Prof. Fitmawati, M.Si., a botanist at Riau University, Indonesia, and verified by the Directorate of Scientific Collection Management, BRIN, Cibinong, Bogor, Indonesia, under Certificate No. B-3142/II.6.2/IR.01.02/9/2024. A voucher specimen was deposited at Herbarium Bogoriense (BO), BRIN, under accession number BO-1331006. The collection and use of plant material complied with applicable institutional, national, and international regulations, including the Nagoya Protocol on Access and Benefit-Sharing.

Preparation of Plant Extracts

Sample preparation and extraction followed the maceration standard of BPOM RI (2023). Fresh leaves and fruit pericarps of *S. koetjape* were wet sorted to remove impurities and foreign materials. Leaves were air-dried under shade, while fruit pericarps were sun-dried until completely dry. The dried materials were ground into powder, and 100 g of each powdered simplicia was macerated with 96% ethanol at a 1:5 ratio (w/v). Maceration was performed for 6 h with occasional stirring, followed by standing for 24 h. The macerate was filtered using Whatman No. 42 filter paper, and the extraction was repeated

three times using the same solvent type and ratio. All filtrates were pooled and concentrated using a rotary evaporator at 40°C to obtain crude extracts. The extraction yield was calculated as:

Total extract yield (%) = (weight of crude extract / weight of powdered plant material) × 100.

In vitro α-glucosidase inhibition assay

An inhibitory assay of α-glucosidase enzyme was employed as a relevant *in vitro* model to evaluate the potential of *S. koetjape* in supporting its traditional use related to metabolic and digestive disorders, particularly diabetes. The antidiabetic assay was performed in a 96-well microplate following a modified method from Munshif (2014). 50 µL of phosphate buffer (0.1 M, pH 7.0) was combined with 25 µL of p-nitrophenyl-α-D-glucopyranoside (0.5 mM) as a substrate. The combination was kept for 5 minutes at 37°C in the incubator before adding 10 µL of test sample. Crude extracts were prepared at concentrations of 500, 250, 200, 100, 50, and 10 ppm, while acarbose, used as the positive control, was prepared at concentrations of 10, 5, 1, 0.5, and 0.1 ppm. The reaction was initiated by adding 25 µL of α-glucosidase from *Saccharomyces cerevisiae* (Sigma-Aldrich, USA; Cat. No. G5003) and incubated at 37°C for 30 min. 100 µL of Na_2CO_3 (0.2 M) was added to end the reaction. The optical density (OD) was assessed with a microplate reader at 410 nm. Inhibition was calculated as:

Inhibition (%) = [(A0 - A1) / A0] x 100,

A_o represents the optical density of the blank control, while A_1 represents the optical density of the test sample. Dose-response curves were generated by plotting inhibition percentage against sample concentration.

Statistical Analysis

IC_{50} values were calculated using the logarithmic regression equation (Fang & Zhou 2024; Chen *et al.* 2025):

$$Y = a \ln(X) + b; \text{ therefore,}$$
$$IC_{50} = \exp^{((50 - b)/a)}$$

Because the IC_{50} values were not normally distributed, differences among samples were analyzed using the Kruskal-Wallis test followed by Dunn's post-hoc test. Statistical significance was set at $p < 0.05$ and the analyses were performed in RStudio Version 2025.09.2+418.

Drug-likeness and Target Prediction Dataset Selection

Triterpenoid and limonoid compounds previously reported from *S. koetjape* were compiled from published literature and open-access chemical databases, including PubChem, MOLBASE, and KNApSAcK Family. The collected information included compound name, chemical class, reported plant part, documented bioactivity, and available structural identifiers. Only compounds with complete molecular structures, represented by SMILES or InChI codes, were included. Duplicate entries and inconsistent structures were cross-checked across databases before further analysis. The verified compounds were screened for drug-likeness using SwissADME (http://www.swissadme.ch/) and Molsoft (https://molsoft.com/). The screening criteria included Lipinski's rule of five, consisting of molecular weight ≤500 Da, LogP ≤5, hydrogen bond acceptors ≤10, and hydrogen bond donors ≤5, and Veber's rule, consisting of rotatable bonds ≤10 and topological polar surface area ≤140 Å² (Veber *et al.* 2002; Lipinski *et al.* 2012). Oral bioavailability (OB (%) ≥ 30%) and drug-likeness score (DL > 0.18) were also considered (Xu *et al.* 2012). Compounds with no more than one Lipinski violation, no Veber violation, and fulfilling the OB and DL thresholds were retained for target prediction.

Potential protein targets of the selected compounds were predicted using SwissTargetPrediction (http://www.swisstargetprediction.ch/), with *Homo sapiens* selected as the target organism. Predicted targets with probability scores >0.1 were retained, and duplicate entries were removed. To ensure nomenclature consistency across databases, all target names were standardized into official gene symbols using the UniProt database mapping tool with *Homo sapiens* as the reference organism. The resulting compound–target dataset was used for subsequent network pharmacology, protein–protein interaction, enrichment, and molecular docking analyses.

Network Pharmacology & Network Topology Modeling

Network pharmacology was conducted as a hypothesis-generating approach to explore whether ethnobotanically relevant compounds of *S. koetjape* may correspond to multi-target biological pathways associated with inflammatory, metabolic, and cancer-related regulation. Disease-related targets associated with "diabetes" and "breast cancer" used here as modern

biomedical pathway models rather than direct traditional disease claims, were retrieved from GeneCards (https://www.genecards.org/), DrugBank (https://go.drugbank.com/), ClinPGx (https://www.clinpgx.org/), DisGeNET (https://disgenet.com/), and the Therapeutic Target Database (TTD) (https://ttd.idrblab.cn/). Overlapping targets between compound-predicted targets and disease-associated targets were identified using the Draw Venn Diagram tool (https://bioinformatics.psb.ugent.be/webtools/Venn/). The intersected genes were further assessed using TTD (https://db.idrblab.org/ttd/) and the Comparative Toxicogenomics Database (CTD) (http://ctdbase.org/) to identify related diseases and signaling pathways, following a modified method by Umar *et al.* (2025).

Compound–target–disease–pathway interaction networks were constructed and visualized using Cytoscape 3.10.1 (https://cytoscape.org/). Network topology was evaluated using Network Analyzer based on degree, betweenness centrality, and closeness centrality to identify central compounds and regulatory targets. Protein–protein interaction (PPI) networks of the intersecting targets were constructed using STRING version 11.0 (https://string-db.org/), with *Homo sapiens* selected as the reference organism and a minimum confidence score of 0.900. PPI data were exported to Cytoscape 3.10.1 using the "Send network to Cytoscape" feature for further visualization and analysis (Doncheva *et al.* 2018). Hub targets were identified using the CytoHubba plugin based on degree, betweenness centrality, and proximity centrality values (Chin *et al.* 2014). Functional enrichment analysis was performed using STRING version 11.0 (https://string-db.org/) and DAVID Bioinformatics Resources 6.8 (https://davidbioinformatics.nih.gov/) to classify targets according to biological process (BP), cellular component (CC), and molecular function (MF) categories (Babichev *et al.* 2025). Gene Ontology (GO) results were processed and visualized using SRplot (https://bioinformatics.com.cn/en), while Kyoto Encyclopedia of Genes and Genomes (KEGG) enrichment was used to identify relevant biological pathways. GO and KEGG terms with false discovery rate (FDR) and p-values <0.01 were considered statistically significant, and the top 15 enriched terms were prioritized for interpretation (Umar *et al.* 2025).

In Silico Molecular Docking Simulations

Molecular docking was performed as a supporting in silico approach to explore possible ligand–target interactions between selected *S. koetjape* compounds and key regulatory proteins identified from the network analysis. The selected proteins represented diabetes- and breast cancer-associated pathway models rather than direct traditional disease claims, and were used to generate mechanistic hypotheses related to inflammatory, metabolic, and cancer-associated regulation. Molecular docking is commonly applied to predict ligand–protein binding affinity and interaction profiles and may provide supportive evidence for bioactivity interpretation (Nursyarah *et al.* 2023; Umar *et al.* 2023).

Ligand structures were prepared in PyRx by energy minimization using the Universal Force Field (UFF) and converted into PDBQT format. Protein structures were obtained from the RCSB Protein Data Bank, including IL6 (PDB ID: 1ALU), TNF-α (PDB ID: 1TNF), PPARG (PDB ID: 2PRG), and TP53 (PDB ID: 2OCJ). Prior to docking, protein structures were prepared by removing water molecules and native co-crystallized ligands, followed by the addition of polar hydrogen atoms and appropriate charges. Docking simulations were carried out using AutoDock Vina through the PyRx Vina Wizard interface. Blind docking was initially performed to identify putative ligand-binding regions, followed by focused docking on the predicted active or interaction sites. The grid box parameters were set as follows: IL6, center x = -8.3974, y = -14.5448, z = 0,000, size x = 66.8933, y = 56.0027, z = 58.7352; TNF-α, center x = 12.2333, y = 4.8834, z = 13.2635, size x = 61.2191, y = 63.3345, z = 58.6316; PPARG, center x = 18.5829, y = -0.8460, z = 7.3589, size x = 51.6282, y = 58.2826, z = 52.3024; and TP53, center x = -40.329, y = 27.5613, z = -18.6874, size x = 94.0926, y = 101.8465, z = 57.9952. The exhaustiveness value was set to 8. Binding poses with RMSD ≤ 2.0 Å were considered reliable, and ligand–protein complexes with binding affinity values of ΔGbind ≤ −6.0 kcal/mol were considered to show potential interactions (Hendrarti *et al.* 2024). The highest-ranking complexes were visualized using PyMOL 3.0 and BIOVIA Discovery Studio 2024 Client to examine hydrogen bonds, hydrophobic interactions, and key amino acid residues within the binding site.

Results

Cross-cultural ethnobotanical patterns of *S. koetjape*

The ethnobotanical synthesis in Table 1 revealed that *S. koetjape* is used across Southeast Asian knowledge systems, particularly in Indonesia, Malaysia, Thailand, the Philippines, and Myanmar (Perry & Metzger 1980; Kaneda *et al*. 1992; Lim 2012; Adnyana 2020; Agapin 2020; Izazah & Anisa 2021; Yadana *et al*. 2021; Bailly 2022; Wijaya 2022). Reported uses involved multiple plant parts, including bark, stem bark, leaves, roots, and fruit-derived materials, for gastrointestinal disorders, diarrhea, fever, inflammation, postpartum recovery, wounds, skin-related conditions, and functional beverages. This indicates that the ethnobotanical relevance of *S. koetjape* is distributed across different plant parts and cultural contexts rather than being limited to a single use category.

A recurring pattern of plant-part selection was observed. Bark and stem bark were mainly associated with digestive complaints, diarrhea, colic, stomach disorders, postpartum recovery, and skin-related applications. Leaves were frequently linked to fever, inflammation, diarrhea, swelling, coughs, and colds, while roots were reported as tonics and remedies for digestive disorders or dysentery. Fruit peels or fruit pericarps were commonly consumed as infusions, herbal teas, or functional beverages. Across these records, decoction and infusion were the dominant preparation methods, followed by topical application, bathing preparations, chewing, and direct consumption.

The reported uses converged around recurring symptom categories, particularly digestive disturbance, inflammatory conditions, fever, wound care, skin-related disorders, and restorative use. These patterns provided the ethnobotanical basis for selecting leaves and fruit pericarps for supporting α-glucosidase inhibition testing and for exploring reported triterpenoids and limonoids in the subsequent in silico analyses.

Plant-part-associated reported compounds and bioactivities

The ethnobotanical patterns summarized in Table 1 were further supported by the distribution of reported compounds and bioactivities across different plant parts of *S. koetjape*. Leaves have been associated with several limonoids and triterpenoids, including koetjapin A–D, phellochin, sandoripins, sanjecumins, 16R,22R-dihydroxycycloartenone, and 4,10,11-trihydroxy guaiane (Bailly 2022; Hang *et al*. 2024; Anisa *et al.* 2026). Several of these compounds have been reported to show α-glucosidase inhibitory, anti-inflammatory, nitric oxide inhibitory, or cytotoxic-related activities, which are relevant to the traditional use of leaves for fever, inflammation, diarrhea, swelling, coughs, and colds (Perry & Metzger 1980; Lim 2012; Agapin 2020; Bailly 2022; Hang *et al.* 2024). Fruit-derived materials, particularly fruit peels or fruit pericarps, have been linked to triterpenoid constituents such as bryonolic acid and bryononic acid (Bailly 2022). These compounds have been reported for bioactivities related to cytotoxicity, antibacterial activity, cholesterol regulation, and neuroprotection. This supports the ethnobotanical relevance of fruit-derived materials as infusions, herbal teas, and functional beverages, especially in communities where fruit peel is consumed as a daily herbal preparation (Izazah & Anisa 2021). Bark and stem bark also represent important ethnobotanical sources of bioactive compounds. Several triterpenoids, including koetjapic acid, katonic acid, katononic acid, 3-oxo-olean-12-en-29-oic acid, sentulic acid, sandorinic acids, secobryononic acid, and secoisobryononic acid, have been reported from these plant parts (Kaneda *et al*. 1992; Nassar *et al*. 2012; Bailly 2022; Hang *et al*. 2024; Anisa *et al.* 2026). Among them, katonic acid, katononic acid, and koetjapic acid appear to be the most consistently evaluated in previous ethnopharmacological studies, with reported anti-inflammatory, antibacterial, α-glucosidase inhibitory, and cytotoxic-related activities (Nassar *et al.* 2012; Bailly 2022; Hang *et al.* 2024). These findings correspond with the traditional use of bark and stem bark for digestive disorders, colic, postpartum recovery, skin infections, and other restorative applications (Perry & Metzger 1980; Kaneda *et al.* 1992; Novaryatiin & Indah 2019; Wijaya 2022).

Although bark, stem bark, and roots are prominent in the ethnobotanical record, leaves and fruit pericarps were prioritized for the supporting in vitro assay because they are directly associated with documented traditional use, commonly prepared as decoctions or infusions, and represent less destructive plant materials compared with bark or roots (Perry & Metzger 1980; Lim 2012; Agapin 2020; Izazah & Anisa 2021; Bailly 2022). The selection of leaves was supported by their repeated use for fever, inflammation, diarrhea, and swelling, while fruit pericarps were selected because of their local use in Riau as a daily herbal infusion or functional beverages (Perry & Metzger 1980; Lim 2012; Agapin 2020; Izazah & Anisa 2021). Thus, the experimental focus on leaves and fruit pericarps was intended to evaluate culturally relevant and sustainably accessible plant parts, rather than to exclude the ethnobotanical importance of other organs. The correspondence between traditional plant-part selection and reported compound bioactivities suggests that ethnobotanical practices may reflect empirical recognition of plant parts containing biologically active metabolites. The compiled compound data were therefore used as supporting evidence for subsequent hypothesis-generating in silico analyses, rather than as direct proof of therapeutic efficacy.

Ethnobotanically selected plant parts and α-glucosidase inhibition

The extraction of 100 g dried powdered simplicia yielded 0.5132 g of crude leaf extract and 3.0165 g of crude fruit pericarp extract, corresponding to extraction yields of 0.51% and 3.02%, respectively. The higher yield of the fruit pericarp extract indicates that fruit pericarps contained a greater proportion of ethanol-soluble constituents than leaves under the same maceration conditions. However, extraction yield does not directly reflect biological activity, as the leaf extract showed stronger α-glucosidase inhibitory activity despite its lower yield. The bioactivity of *S. koetjape* extracts may depend more on the composition and potency of extracted metabolites than on the total amount of crude extract obtained.

Table 1. Reported ethnobiological knowledge across some country (plant parts, traditional uses, and preparation practices), related to triterpenoid and limonoid compounds, and known its bioactivities from *S. koetjape.*

Source (part)	Traditional Uses	Preparation Practices	Compound Name	Chemical Class	Reported Bioactivity	References
Bark	Diarrhea (Indonesia, Thailand, Malaysia), stomach ache (Indonesia), gastrointestinal disorders and postpartum tonic (Malaysia), treating ringworm,	Chewed and sprayed into stomach (Indonesia), decoction (Indonesia, Thailand, Malaysia), aqueous extract (Malaysia)	3-oxo-olean-12-en- 27-oic acid	Oleane-type triterpenoid	Cytotoxicity against HL-60 cells (IC_{50} = 27.4 µm)	(Perry & Metzger *et al.* 1980; Kaneda *et al.* 1992; Nassar *et al.* 2010; Efdi *et al.* 2012; Novaryatiin & Indah 2019)
			Sentulic acid	A-seco triterpenoid	Cytotoxicity against HL-60 cells (IC_{50} = 37.0 µm)	(Efdi *et al.* 2012)
			Indicic acid	Triterpenoid acid	Not reported	(King & Morgan 1960)
Stem Bark	colic, leucorrhoea (Indonesia)	Decoction (Indonesia)	(–)-alloaromadendrene	Sesquiterpene	Potential antifungal	(Kaneda *et al.* 1992; Kosela *et al.* 1995; Warsinah *et al.* 2015)
			(–)-caryophyllene oxide	Sesquiterpene	Cytotoxic against U-937 cells (CC_{50} = 24.25±0.37 µg/ml), anticancer against A549 (IC_{50} = 124.1 g/ml, antilymphoma (ED50 = 6.14±0.52 mg/kg), Toxicity (LD_{50} >1000 mg/kg), Proapoptosis (CC50 = 24.25 µg/ml)	(Ram *et al.* 2024; Shabana, *et al.,* 2023)
			(+)-spathulenol	Sesquiterpene	Neuroprotective by reducing the ROS production validated through SH-SY5Y cells, antimycobacterial against Mtb H37Rv (MIC_{50} = 167.5±6.8 µm), dan Mtb M299 (MIC_{50} = 191.0±2.2 µm)	(Kaneda *et al.* 1992; Babu *et al.* 2021; Francisca *et al.* 2021)
			3-Oxo-olean-12-en-29-oic acid	Ring-A secotriterpene	Cytotoxicity against cell lines: A-431 (ED_{50} >20 µg/ml), BC1 (ED_{50} >20 µg/ml), Col2 (ED_{50} >20 µg/ml), KB (ED_{50} = 4.9 µg/ml), HT-1080 (ED_{50} >20 µg/ml), KB-VI (ED_{50} = 8.5 µg/ml), LNCaP (ED_{50} = 10 µg/ml), Lu1 (ED_{50} = 10 µg/ml), Mel2 (ED_{50} = 12 µg/ml), ZR-75-	(Kaneda *et al.* 1992)

					1 (ED_{50} = 5.2 µg/ml), P-388 (ED_{50} = 0.61 µg/ml)	
			20-epikoetjapic acid	Oleane-type triterpenoid	Antibacterial (MIC 3.25-6.25 µg/ml), Antiinflammatory (IC_{50} = 0.5-1.9 µm), Cytotoxic against P388 cells (IC_{50} > 25 µg/ml)	(Tanaka *et al.* 2001; Muhammad *et al.* 2000)
			3-epikatonic acid	Oleane-type triterpenoid	Cytotoxic against P388 cells (IC_{50} > 25 µg/ml)	(Tanaka *et al.* 2001)
			Brionononic acid	Oleane-type triterpenoid	Not reported	(Tukiran *et al.* 2006)
			Sandorinic acid A	12β-hydroxymultiflorane triterpenoid acids	Cytotoxic against P388 cells (IC_{50} = 9-16 µg/ml)	(Tanaka *et al.* 2001)
			Sandorinic acid B	12β-hydroxymultiflorane triterpenoid acids	Cytotoxic against P388 cells (IC_{50} = 16-25 µg/ml)	(Tanaka *et al.* 2001)
			Sandorinic acid C	12β-hydroxymultiflorane triterpenoid acids	Cytotoxic against P388 cells (IC_{50} > 25 µg/ml)	(Tanaka *et al.* 2001)
			Secobryononic acid	Ring-A secotriterpenoid	Not reported	(Kosela *et al.* 1995)
			Secoisobryononic acid	Ring-A secotriterpenoid	Not reported	(Kosela *et al.* 1995)
Bark, Fruit pericaps	Toothache, Bedsore, Chickenpox, Prickly Heat, Wounds, Diarrhea (Myanmar)	ground with rice water and applied topically to treat skin-related conditions, while dried fruit peel is consumed for diarrhea (Myanmar)	Bryononic acid	Ring-A secotriterpenoids were	Antibacterial (MIC = 6.0 µg/ml)	(Sim & Lee 1972; Kosela *et al.* 1995; Heliawati *et al.* 2019; Yadana *et al.* 2021)
Bark, Leaves	Diarrhea (Indonesia)	Chewed and sprayed into stomach (Indonesia),	Katonic Acid	Triterpenoid acid	Anti-inflammatory (oedema inhibition = 81±12%), cytotoxic against P-388 cells (ED_{50} = 0.11 µg/ml, IC_{50} = 16-25 µg/ml), cytotoxicity against A549 cells (IC_{50} 81.2±10.3 µm), cytotoxicity against cell lines: A-431 (ED_{50} = 12	(Rasadah *et al.* 2004; Kaneda *et al.* 1992; Tanaka *et al.* 2001; Nassar *et al.* 2010; Hang *et al.* 2024; King & Morgan

					µg/ml), BC1 (ED_{50} = 7.8 µg/ml), Col2 (ED_{50} > 20 µg/ml), HT-1080 (ED_{50} = 19 µg/ml), KB (ED_{50} = 8.3 µg/ml), KB-VI (ED_{50} = 15 µg/ml), LNCaP (ED_{50} = 10 µg/ml), Lu1 (ED_{50} = 11 µg/ml), Mel2 (ED_{50} = 12 µg/ml), ZR-75-1 (ED_{50} = 2.2 µg/ml), P-388 (ED_{50} = 0.11 µg/ml), α-glucosidase inhibitory activity (IC_{50} = 49.2±1.7 µm), inhibits Epstein-Barr virus early	1960; Ismail *et al.* 2003; Khastini *et al.* 2021; Hang 2022)
			Katononic acid	Triterpenoid acid	Anti-inflammatory (oedema inhibition = 94±8 %), cytotoxic against P-388 cells (ED_{50} = 0.61 µg/ml, IC_{50} = 12-25 µg/ml), α-glucosidase inhibitory activity (IC_{50} = 15.7±0.8 µm), Ichthyotoxic and inhibits Epstein-Barr virus early	(Rasadah *et al.* 2004; Kaneda *et al.* 1992; Tanaka *et al.* 2001; Hang *et al.* 2024; Ismail *et al.* 2003)
			Koetjapic Acid	Ring-A secotriterpene	Anti-inflammatory (oedema inhibition = 13±12 %), Antibacterial (MIC 6.25-12.5 µg/ml), cytotoxic against P388 cells (IC_{50} > 25 µg/ml), cytotoxic against MCF-7 cells (IC_{50} 68.88±6.075 µg/ml), α-glucosidase inhibitory activity (IC_{50} = 34.2±2.8 µm), proapoptotic and antimetastatic effect against HCT 116 cells, skin cancer chemopreventive, ichthyotoxic and Inhibit Epstein-Barr virus early antigen (EBV-EA)	(Rasadah *et al.* 2004; Muhammad *et al.* 2000; Kaneda *et al.* 1992; Tanaka *et al.* 2001; Jafari *et al.* 2024; Hang *et al.* 2024; Ismail *et al.* 2003; Nassar *et al.* 2012)
Fruit pericarps	Herbal tea (Indonesia, Philippines), fever (Philippines)	Infused in hot water (Indonesia), consumed raw or processed into various food preparations (Philippines, Indonesia)	Bryonolic acid	Pentacyclic triterpenes	Cytotoxic against MCF-7 (1.4–1.7 times than the control group), against Saos-2 cells (1.1–1.3 times than the control group), inhibit cholesterol esterification (ACAT activity) (IC_{50} =	(Sim & Lee 1972; Khallouki *et al.* 2018; Que *et al.* 2016; Lim *et al.* 2012; Lertphadungkit *et al.*

					12.6±2.4 µm), neuroprotective effects against NMDA in PC12 cells	2020; Izazah & Anisa 2021)
Leaves, seed	-	-	6-hydroxysandoricin	Andirobin-type limonoids	Potential antifeedant	(Powell *et al.* 1991)
			Koetjapin A	Andirobin-class limonoid	Cytotoxic against P388 cells (IC_{50} = 46.8±1.9 µg/ml), α-glucosidase inhibitory activity (IC_{50} = 13.1±0.7 µm)	(Bumi *et al.* 2019; Hang *et al.* 2024; Hang 2022)
			Koetjapin B	Andirobin-class limonoid	Cytotoxic against P388 cells (IC_{50} = 52.0±1.6 µg/ml), α-glucosidase inhibitory activity (IC_{50} = 7.9±0.6 µm)	(Bumi *et al.* 2019; Hang *et al.* 2024; Hang 2022)
			Koetjapin C	Andirobin-class limonoid	Cytotoxic against P388 cells (IC_{50} = 59.2±6.2 µg/ml), α-glucosidase inhibitory activity (IC_{50} = 14.8±0.3 µm)	(Bumi *et al.* 2019; Hang *et al.* 2024; Hang 2022)
			Koetjapin D	Trijugin-class limonoid	Cytotoxic against P388 cells (IC_{50} = 16.8±1.8 µg/ml), α-glucosidase inhibitory activity (IC_{50} = 17.5±1.7 µm)	(Bumi *et al.* 2019; Hang *et al.* 2024; Hang 2022)
			Sandoricin	Andirobin-type limonoids	Potential antifeedant	(Powell *et al.* 1991)
Leaves	Coughs and colds (Philippines), diarrhea and swelling (Indonesia), fever and inflammation (Indonesia, Philippines)	Decoction and poultice (Indonesia, Philippines), consumed raw (Indonesia), extract, taken orally, and apply directly on skin (Philippines)	[21α-methylmelianol (21R,23R) epoxy-24- hydroxy-21α-methoxyl]triucalla-7,25-dien-3-one	Tirucallane triterpenoids	A-glucosidase inhibitory activity (IC_{50} = 23.1±1.4 µm)	(Perry & Metzger *et al.* 1980; Agapin 2020; Belgica *et al.* 2021; Banua 2022; Hang *et al.* 2024;)
			[2α-(2-methylbutanoyl)oxy]sandoricin	Limonoid	Not reported	(Pancharoen & Haboonmee 2006)
			[2α-(2-methylpropanoyl)oxy]sandoricin	Limonoid	Not reported	(Pancharoen & Haboonmee 2006)
			16R,22R-dihydroxycycloartenone	Cycloartane triterpenoids	A-glucosidase inhibitory activity (IC_{50} = 14.0±1.1 µm)	(Hang *et al.* 2024)
			4,10,11-trihydroxy guaiane	Sesquiterpenoid	α-glucosidase inhibitory activity (IC_{50} = 26.5±1.1 µm)	(Hang 2022)
			Phellochin	Cycloartane triterpenoids	α-glucosidase inhibitory activity (IC_{50} = 34.7±1.5 µm), cytotoxicity against A549 cells (IC_{50} 16.1±2.4 µm)	(Hang *et al.* 2024; Hang 2022)

			Sandoripin A	Andirobin-type limonoids	Inhibit NO production (IC_{50} = 16.4 µm)	(Pancharoen *et al.* 2009; Nagakura *et al.* 2013)
			Sandoripin B	Andirobin-type limonoids	Inhibit NO production (IC_{50} = 30.4 µm)	(Pancharoen *et al.* 2009; Nagakura *et al.* 2013)
			Sandrapins A	Trijugin-type limonoids	Not reported	(Ismail *et al.* 2003)
			Sandrapins B	Trijugin-type limonoids	Not reported	(Ismail *et al.* 2003)
			Sandrapins C	Trijugin-type limonoids	Not reported	(Ismail *et al.* 2003)
			Sandrapins D	Trijugin-type limonoid	Not reported	(Ismail *et al.* 2004)
			Sandrapins E	Trijugin-type limonoid	Not reported	(Ismail *et al.* 2004)
			Sanjecumin A	Limonoids/ tetranorterpenoid	α-glucosidase inhibitory activity (IC_{50} = 22.0±1.2 µm)	(Nagakura *et al.* 2013; Hang *et al.* 2024)
			Sanjecumin B	Limonoids/ tetranorterpenoid	α-glucosidase inhibitory activity (IC_{50} = 28.3±1.3 µm)	(Nagakura *et al.* 2013; Hang *et al.* 2024)
Roots	Diarrhea (Indonesia), digestive disorders, tonic (Indonesia, Philippines)	Decoction or infusion (Indonesia, Philippines)	-	-	-	(Perry & Metzger *et al.* 1980)

The crude extracts of *S. koetjape* leaves and fruit pericarps were evaluated for their α-glucosidase inhibitory activity as a limited supporting assay for interpreting traditionally selected plant parts (Table 2). The leaf extract showed moderate inhibitory activity, with an IC_{50} value of 228.27 ± 0.91 ppm, whereas the fruit pericarp extract did not reach 50% inhibition at the highest tested concentration, indicating an IC_{50} value >500 ppm. At 500 ppm, the leaf extract showed 63.67 ± 0.00% inhibition, while the fruit pericarp extract showed only 27.135 ± 0.43% inhibition. Acarbose, used as the positive control, showed stronger inhibition with an IC_{50} value of 0.135 ± 0.002 ppm. Kruskal-Wallis analysis showed significant differences among samples (P = 0.0273), and Dunn's post-hoc test indicated that acarbose differed significantly from the fruit pericarp extract, while the leaf extract showed intermediate activity. These results suggest that leaves provide stronger supporting α-glucosidase inhibitory evidence than fruit pericarps, consistent with the repeated ethnobotanical use of leaves in conditions associated with fever, inflammation, and digestive disturbance.

Table 2. Inhibition percentage and IC_{50} values of leaves and fruit pericarps crude extract against α-glucosidase.

Sample	Concentration (ppm)	%Inhibition				IC_{50} (ppm)
		R1	R2	R3	Mean	
Leaves extract	500	63.670	63.670	63.670	63.670±0.00	228.27±0.91[ab]
	250	53.571	53.695	52.956	53.407±0.39	
	200	46.675	46.552	46.429	46.552±0.12	
	100	35.837	35.468	36.33	35.878±0.43	
	50	23.645	23.276	23.645	23.522±0.21	
	10	5.172	5.049	4.926	5.049±0.12	
Fruit pericarp extract	500	27.586	27.094	26.724	27.135±0.43	>500[b]
	250	9.483	10.714	9.236	9.811±0.79	
	200	7.02	6.65	7.512	7.061±0.43	
	100	3.325	3.695	2.833	3.284±0.43	
	50	2.463	2.833	2.463	2.586±0.21	
	10	1.355	0.739	0.616	0.903±0.39	
Acarbose	10	96.296	96.296	96.801	96.465±0.29	0.135±0.002[a]
	5	92.256	91.582	91.246	91.695±0.51	
	1	73.906	73.232	73.401	73.513±0.35	
	0.5	68.013	68.182	68.182	68.126±0.09	
	0.1	43.771	43.603	44.108	43.827±0.25	

Note: R1–R3 represent triplicate measurements (n = 3). The data is presented as mean ± SD. Different superscript letters (a-b) indicate significant differences among samples based on Dunn's post-hoc test following Kruskal-Wallis analysis (P < 0.05).

The IC_{50} values differed significantly among samples based on the Kruskal–Wallis test (P = 0.0273) (Table S1). Dunn's post-hoc test showed that acarbose differed significantly from the fruit pericarp extract, as indicated by different superscript letters, while the leaf extract showed intermediate activity and was not significantly different from either group.

Drug-likeness profile of reported triterpenoids and limonoids

Drug-likeness screening was conducted to prioritize reported *S. koetjape* compounds for target prediction and network-based analyses. Of the 41 triterpenoids and limonoids identified from the database, 15 compounds fulfilled the drug-likeness criteria, indicating acceptable physicochemical profiles for inclusion in the in silico dataset (Tables 1 and 3).

Table 3. Drug-likeness parameters of selected *S. koetjape* bioactive chemicals

Compound name	Pubchem ID	Lipinski/Veber Violations	OB (%)	DL
20-epikoetjapic acid	10790564	1/0	84	0.42
3-epikatonic acid	10434225	1/0	85	0.42
3-Oxo-olean-12-en-29-oic acid	11970027	1/0	85	0.42
Bryonolic acid	159970	1/0	85	0.46
Bryononic acid	472768	1/0	86	0.46
Katonic acid	9804114	1/0	85	0.42
Katononic acid	9981416	1/0	85	0.42

Koetjapic acid	15513441	1/0	85	0.42
Phellochin	14021541	1/0	55	0.48
Sandorinic acid A	10323147	0/0	56	0.57
Sandorinic acid B	10323148	0/0	56	0.63
Sandorinic acid C	11048975	1/0	85	0.51
Secobryononic acid	78101312	1/0	85	0.48
Secoisobryononic acid	85082262	1/0	85	0.35
Sentulic acid	70683988	1/0	85	0.26

Network pharmacology and central regulatory nodes

Network pharmacology analysis was used to explore whether reported compounds of *S. koetjape* correspond to multi-target biological pathways related to the ethnobotanical symptom categories documented for this species. Using diabetes- and breast cancer-associated target sets as modern biomedical pathway models, the intersection between predicted compound targets and disease-related genes identified 65 shared targets for the diabetes model and 62 shared targets for the breast cancer model (Fig. S1). These overlapping targets represent potential biological links between reported *S. koetjape* compounds and pathways involved in inflammatory, metabolic, and cancer-associated regulation.

In the diabetes-related network (Fig. 1), the most connected compounds were 3-oxo-olean-12-en-29-oic acid (degree = 38), sandorinic acid B (degree = 37), sandorinic acid A (degree = 36), and 20-epikoetjapic acid (degree = 36) (Table S3). The main regulatory targets were PIK3CA (degree = 173), TP53 (degree = 129), EGFR (degree = 123), TNF (degree = 72), IL6 (degree = 60), and PPARG (degree = 35) (Table S4). In the breast cancer-related network (Fig. 2), katonic acid (degree = 34), phellochin (degree = 33), sentulic acid (degree = 32), sandorinic acid A (degree = 32), and katononic acid (degree = 31) were the most connected compounds (Table S8), while MAPK3 (degree = 243), PIK3CA (degree = 174), TP53 (degree = 137), PRKCA (degree = 130), and EGFR (degree = 126) were the main target nodes (Table S9). These topology values indicate that several reported compounds of *S. koetjape*, particularly 3-oxo-olean-12-en-29-oic acid, sandorinic acids, katonic acid, and phellochin, occupied central positions within the compound–target networks. Their connections with regulatory proteins such as PIK3CA, TP53, EGFR, IL6, TNF, and PPARG suggest possible links with metabolic regulation, inflammatory signaling, immune response, signal transduction, and altered cell-survival pathways. Rather than indicating direct therapeutic efficacy against diabetes or breast cancer, the network structure supports a multi-component and multi-target interpretation of *S. koetjape*, in which compounds reported from ethnobotanically relevant plant parts may interact with biological pathways overlapping with traditional indications such as digestive disturbance, fever, inflammation, wound care, and restorative use.

PPI and enrichment analysis of inflammatory–metabolic pathway models

PPI analysis further supported the central role of inflammatory and metabolic regulatory proteins in both biomedical pathway models (Fig. 3; Table S7). In the diabetes-related PPI network, IL6 showed the highest connectivity (degree = 43), followed by TNF and PPARG (degree = 41 each), TP53 (degree = 29), PPARA (degree = 28), PTGS2 and REN (degree = 27 each), and EGFR (degree = 26). In the breast cancer-related PPI network, TNF and IL6 were also the most connected hubs (degree = 45 each), followed by TP53 (degree = 43), MAPK3 (degree = 39), PTGS2 (degree = 38), EGFR and PPARG (degree = 37 each), and ESR1 (degree = 35) (Table S12). The repeated appearance of IL6, TNF, PPARG, TP53, EGFR, and PTGS2 across both networks suggests that the predicted targets of *S. koetjape* compounds are concentrated around inflammatory signaling, metabolic regulation, and altered cell-survival processes.

Functional enrichment analysis showed that the intersecting targets were mainly associated with signal transduction, lipid metabolism, immune response, cytokine and interleukin signaling, nuclear receptor-related regulation, PI3K-AKT signaling, AMPK signaling, insulin resistance, PPAR signaling, TNF signaling, and cancer-associated pathways (Fig. 4). These enriched terms indicate that the diabetes- and breast cancer-related models share overlapping inflammatory–metabolic regulatory networks. In the context of this study, these findings should not be interpreted as direct evidence of therapeutic efficacy against diabetes or breast cancer, but as hypothesis-generating support that traditionally selected plant parts and reported compounds of *S. koetjape* may correspond to biological pathways relevant to fever, inflammation, digestive disturbance, wound care, and restorative use.

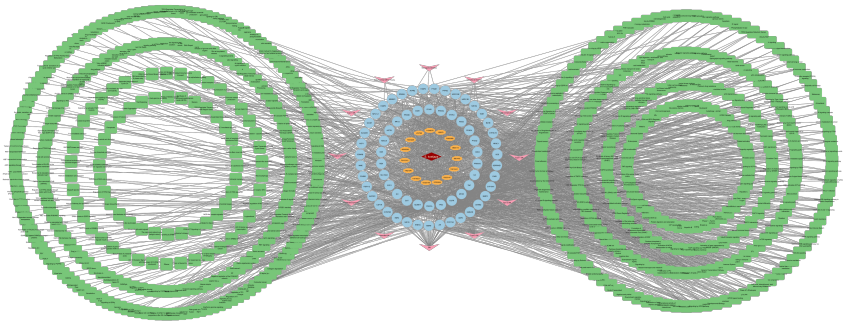

Figure 1. Pharmacological network visualization illustrates *S. koetjape's* interactions with diabetes across multiple compounds, gene targets, disease, and pathways, with nodes labelled brown (plant), orange (compound), blue (target), pink (disease), and green (pathway).

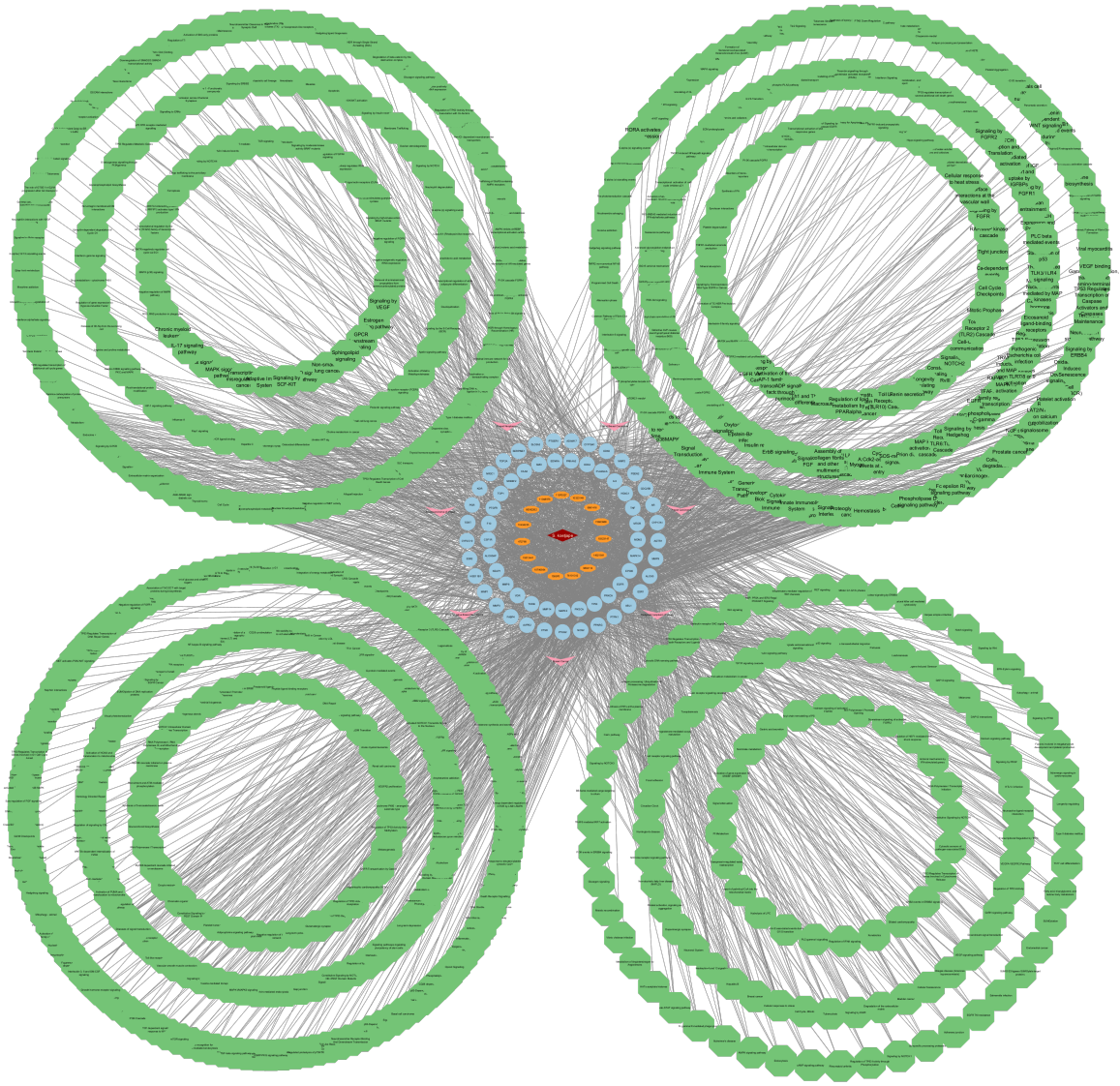

Figure 2. Pharmacological network visualization illustrates *S. koetjape's* interactions with breast cancer across multiple compounds, gene targets, disease, and pathways, with nodes labelled brown (plant), orange (compound), blue (target), pink (disease), and green (pathway).

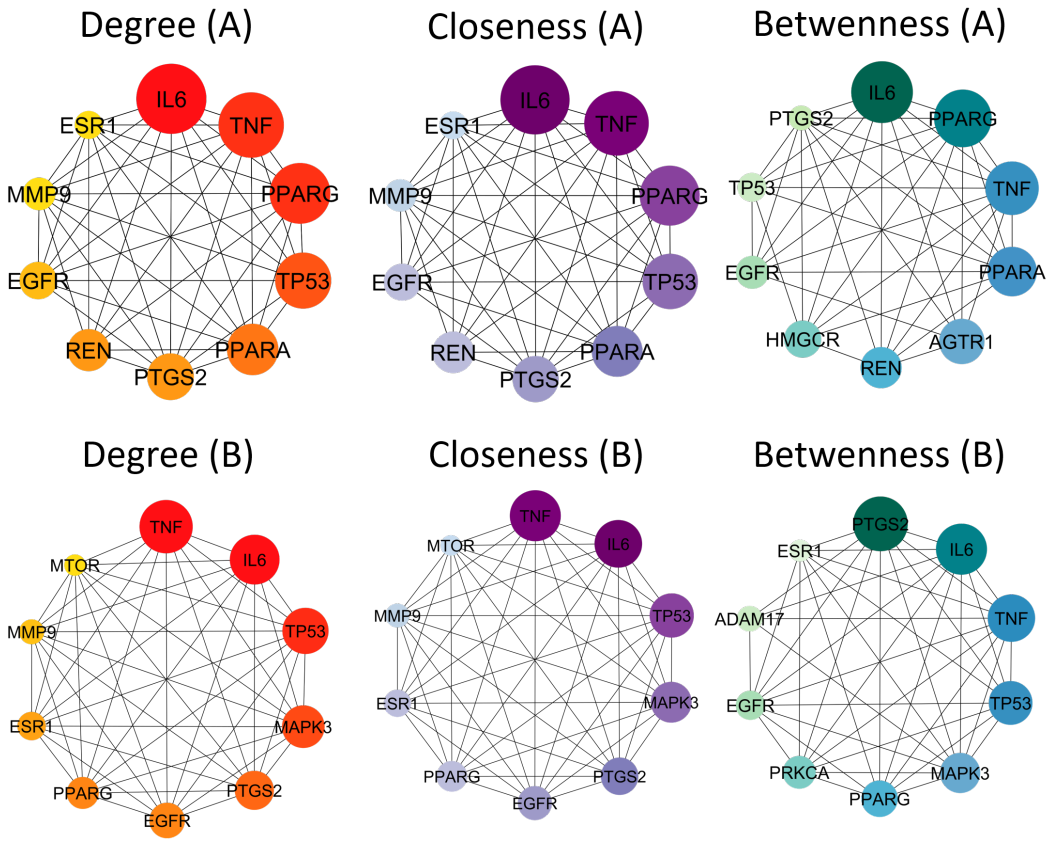

Figure 3. PPI network formed in diabetes (A) and breast cancer (B). The greater the circle and the lighter the color, the more degrees the node possesses.

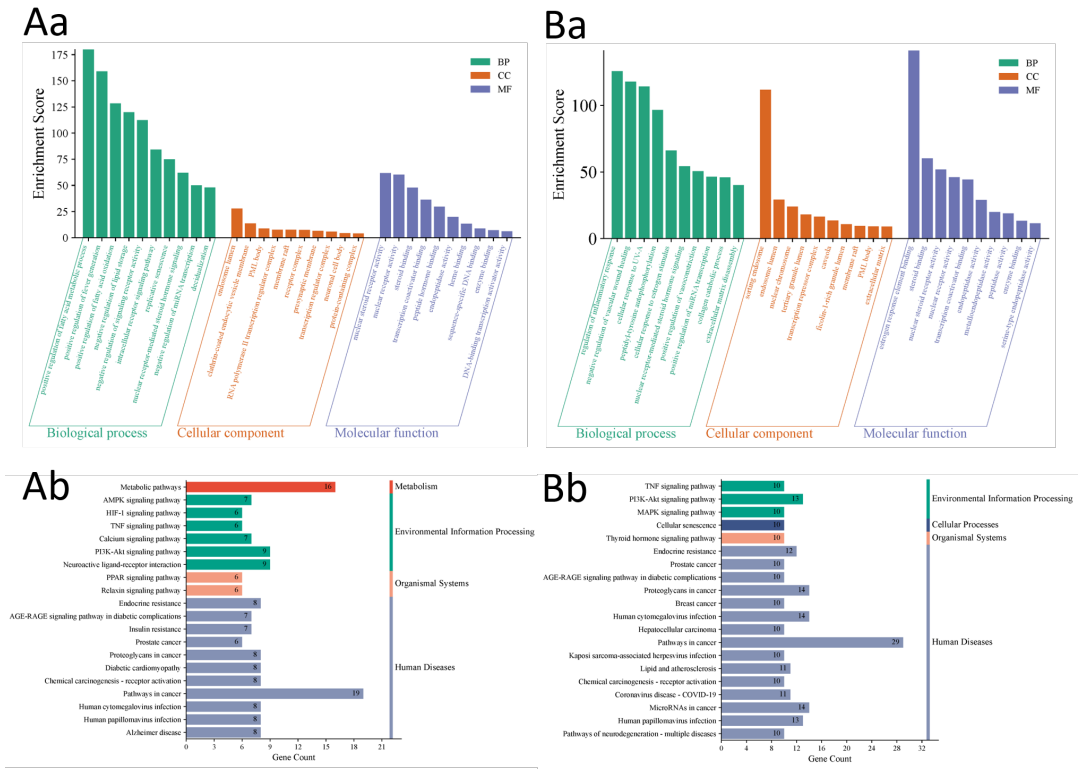

Figure 4. GO of CC, MF, BP (a), and KEGG pathways (b) are associated with diabetes (A) and breast cancer (B).

Molecular docking as supporting interaction evidence

Molecular docking was used to provide supporting evidence for possible interactions between selected *S. koetjape* compounds and key regulatory targets identified from the network analysis. In the diabetes-related pathway model, several compounds showed binding affinity values below the interaction threshold of ΔGbind ≤ −6.0 kcal/mol. The strongest interaction was observed for 3-oxo-olean-12-en-29-oic acid with PPARG (ΔGbind = −8.0 kcal/mol), followed by 3-oxo-olean-12-en-29-oic acid with IL6 (ΔGbind = −7.9 kcal/mol), sandorinic acid B with TNF-α (ΔGbind = −7.4 kcal/mol), sandorinic acid B with IL6 (ΔGbind = −7.3 kcal/mol), and sandorinic acid A with PPARG (ΔGbind = −7.6 kcal/mol). These values indicate favorable predicted interactions with proteins involved in inflammatory and metabolic regulation.

In the breast cancer-related pathway model, selected compounds also showed favorable binding affinities toward inflammatory and cell-survival regulatory targets. Phellochin showed the strongest interaction with TNF-α (ΔGbind = −7.9 kcal/mol), while katonic acid interacted with IL6 (ΔGbind = −7.7 kcal/mol) and TP53 (ΔGbind = −7.5 kcal/mol). Sentulic acid showed lower but still acceptable interactions with IL6 and TNF-α (ΔGbind = −6.5 and −6.3 kcal/mol, respectively). Doxorubicin, used as a reference compound, showed binding affinities of −7.2 kcal/mol with IL6, −6.9 kcal/mol with TNF-α, and −7.9 kcal/mol with TP53.

Table 4. Molecular docking result of diabetes and breast cancer–related targets

Target	Compound	ΔG_{bind}(kcal/mol)	RMSD	Amino acid residue
Molecular docking result of diabetic-related targets				
IL6*	3-Oxo-olean-12-en-29-oic acid	-7.9	3.44	**Arg (A:42),** Lys (A:43)
	Sandorinic acid B	-7.3	1.56	**Glu (B:25),** Tyr (A:33), Lys (A:29), Arg (A:32)
	Sandorinic Acid A	-7.2	24.81	**Glu (A:174), Lys (A:68), Ser (A:178), Gln (A:177), Ser (A:54),** Met (A:69), Phe (A:76)
	Acarbose	-6.6	1.37	**Ser (B:54), Met (A:69), Gln (A:177),** Ser (B:55), Glu (A:174), Lys (A:68)
TNF-α*	3-Oxo-olean-12-en-29-oic acid	-7.3	2.89	**Ser (C:95), Gln (B:149),** Leu (C:75)
	Sandorinic acid B	-7.4	29.73	**Arg (A:82),** Ala (C:38), Ala (C:33)
	Sandorinic Acid A	-7.1	2.42	Ala (A:109), Pro (A:106)
	Acarbose	-5.8	1.41	**Lys (B:65), Gln (B:67), Tyr (B:141), Cys (B:69), Pro (B:139),** Leu (B:142), Gly (B:24)
PPARG	3-Oxo-olean-12-en-29-oic acid	-8	1.61	**Asp (A:131),** Phe (A:141), Val (A:42)
	Sandorinic acid B	-7.1	1.58	**Ser (B:76), Ser (A:19)**, Pro (A:21)
	Sandorinic Acid A	-7.6	23.44	**Glu (A:85),** Pro (A:21), Lys (A:59)
	Acarbose	-6.6	1.29	**Cys (A:79), Ser (A:83), Tyr (A:121), Tyr (A:267),** Leu (A:134), Gly (A:78), Arg (A:82)
Molecular docking results of breast cancer-related targets				
IL6*	Katonic acid	-7.7	1.72	Phe (A:80), Lys (B:43), Asn (B:47)
	Phellochin	-6.3	1.82	**Arg (A:184), Arg (B:32),** Lys (B:29), Tyr (B:33)
	sentulic acid	-6.5	1.62	**Ser (B:39), Arg (B:42),** Phe (A:80), Ala (B:40), Lys (B:43)
	Doxorubicin	-7.2	2.35	**Lys (B:68), Ser (B:178), Arg (B:181), Glu (B:71),** Ala (B:70), Phe (B:76), Met (B:69), Arg (A:181)
TNF-α*	Katonic acid	-7.3	19.34	**Tyr (B:141), Asp (B:140), Pro (B:70),** Leu (B:142)
	Phellochin	-7.9	1.84	**Lys (A:112), Thr (A:105), Glu (C:107), Gly (C:108),** Pro (A:106), Cys (A:69), Ala (A:109)
	sentulic acid	-6.3	4.83	**Glu (A:135), Ser (A:81), Lys (A:90), Thr (A:79)**

	Doxorubicin	-6.9	2.82	**Glu (C:127), Arg (B:32), Ala (B:35), Asn (B:34), Arg (C:82),** Ala (B:33), Val (C:91), Tyr (C:87)
TP53	Katonic acid	-7.5	2.95	**Asp (A:115),** Val (A:4)
	Phellochin	-6	19.42	**Asn (A:175),** Tyr (A:33), Pro (A:35), His (A:22)
	sentulic acid	-6	4.05	Arg (C:65), Met (C:67), Ile (C:161), Pro (C:5), Leu (C:171)
	Doxorubicin	-7.9	3.07	**Ser (A:6),** Thr (B:138), Glu (B:131), Met (A:67), Pro (A:5), Ile (A:161)

* IL6 and TNF are shared targets between diabetes and breast cancer networks, and amino acid residue in bold are hydrogen bonds.

Visualization of the ligand–protein complexes showed that the selected compounds formed hydrogen bonds and hydrophobic interactions with key amino acid residues within the predicted binding regions. Representative interactions included sandorinic acid B with IL6, 3-oxo-olean-12-en-29-oic acid with PPARG, phellochin with TNF-α, and katonic acid with TP53 (Fig. 5-6). These docking results should be interpreted as hypothesis-generating support for the network pharmacology findings, suggesting that reported compounds from ethnobotanically relevant plant parts may interact with upstream inflammatory and regulatory proteins such as IL6, TNF-α, PPARG, and TP53. However, these results do not provide direct evidence of therapeutic efficacy and require further experimental validation.

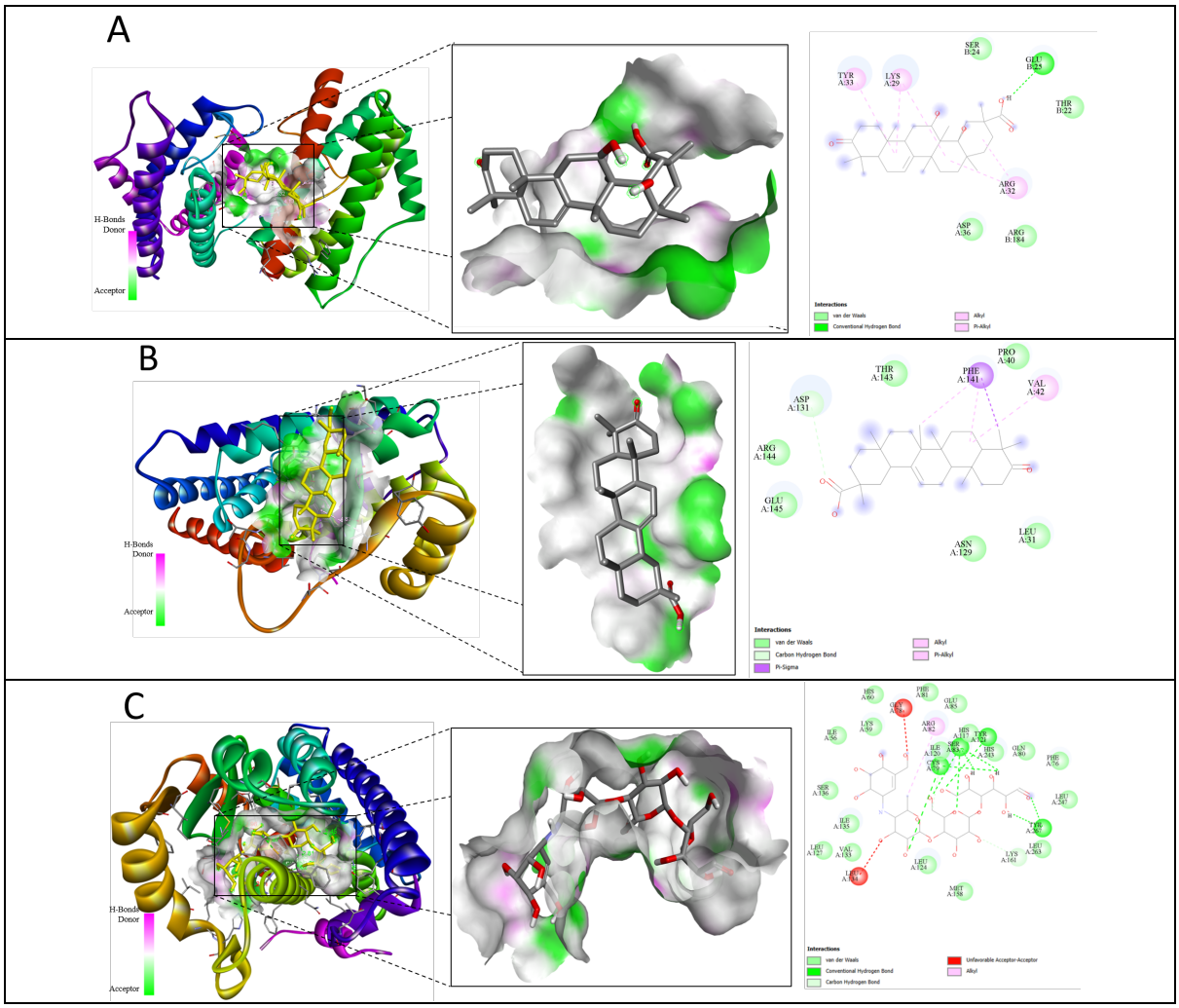

Figure 5. Binding pose and binding interaction in diabetic-related target of IL6 – sandorinic acid B (A), PPARG – 3-oxo-olean-12-en-29-oic acid (B), and PPARG – acarbose (C).

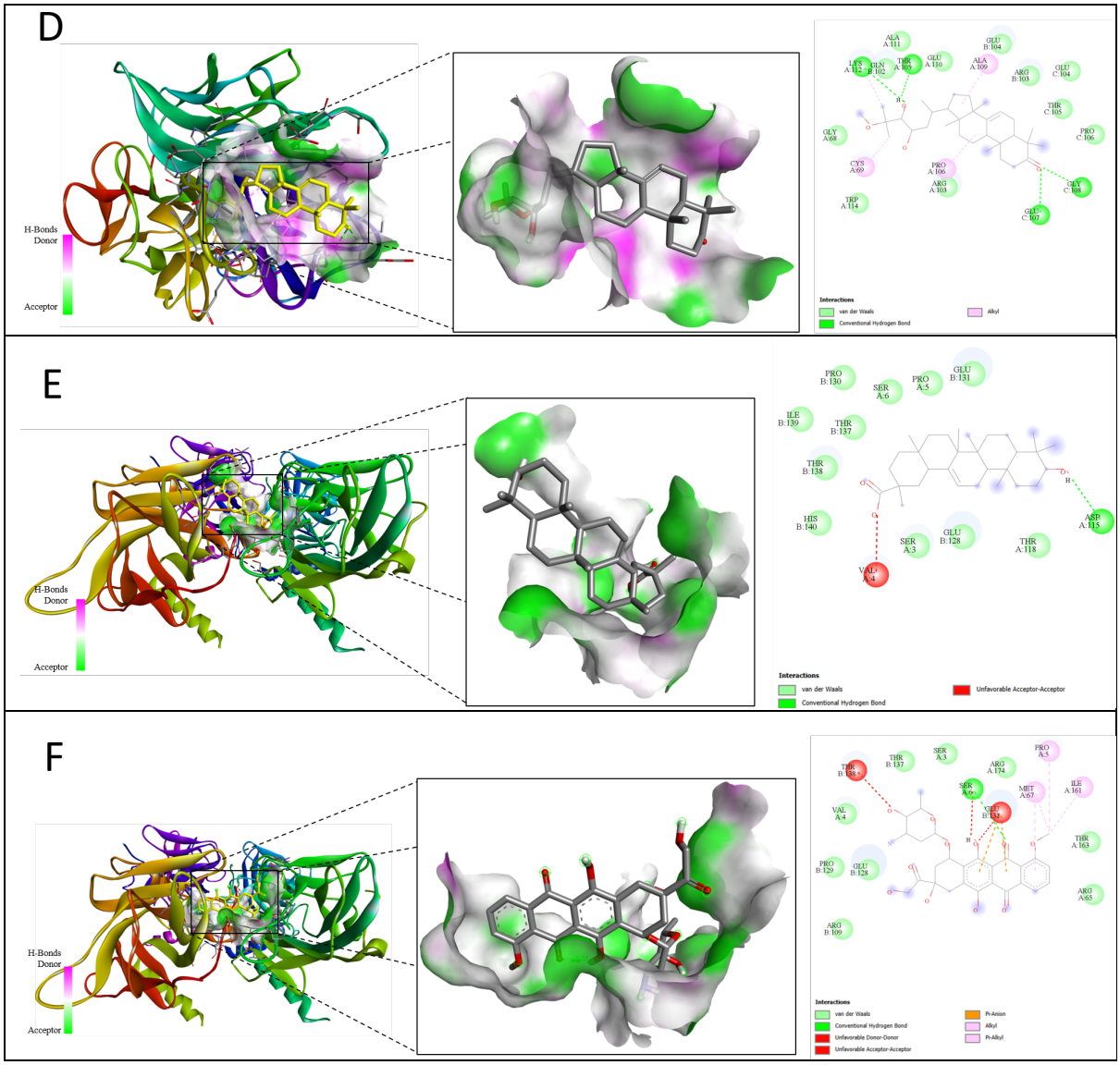

Figure 6. Binding pose and binding interaction in breast cancer-related target of TNF-α – Phellochin (D), TP53 – katonic acid (E), and TP53 – doxorubicin (F).

Discussion

The findings of this study show that *S. koetjape* represents a culturally embedded medicinal plant whose uses are shaped by cross-cultural variation in plant-part selection, preparation practices, and therapeutic indications across Southeast Asia. In this context, the laboratory and computational findings are best understood as supporting evidence for interpreting ethnobotanical patterns, rather than as standalone pharmacological validation. The records summarized in Table 1 show that *S. koetjape* is not used in a single uniform way. Bark decoctions for diarrhea and stomach disorders, leaves for fever, swelling, coughs, colds, inflammation, roots as tonics or digestive remedies, and fruit pericarps as infusions or food-based beverages represent locally adapted solutions shaped by available plant parts, preparation technologies, symptom categories, and community experience (Perry & Metzger 1980; Kaneda *et al.* 1992; Lim 2012; Adnyana 2020; Agapin 2020; Igiastini *et al.* 2021; Izazah & Anisa 2021). Thus, *S. koetjape* functions as a mobile ethnobotanical resource whose meanings and applications are adjusted as it moves through ecological, linguistic, and therapeutic contexts.

Cross-cultural consistency in this case does not imply identical use, but rather patterned variation. Communities repeatedly associate *S. koetjape* with bodily states involving digestive disturbance, fever, inflammation, skin irritation, postpartum recovery, and general restoration, yet each community assigns emphasis differently. This pattern suggests adaptive convergence, different knowledge systems may arrive at partially overlapping uses because they interact with similar sensory cues, illness experiences, and outcomes while filtering them through distinct cultural taxonomies of illness (Cotton 1996; Martin 2004; Heinrich & Jäger 2015; Albuquerque et al. 2019). The ethnobotanical value of the plant therefore lies not only

in the presence of bioactive compounds, but in the culturally mediated rules that determine which plant part is selected, how it is prepared, and for whom it is used.

Plant-part selection appears to be a central mechanism of this adaptation. Bark and roots are generally connected with decoction-based remedies for gastrointestinal or tonic purposes, leaves are associated with acute or visible conditions such as fever, swelling, coughs, and inflammation, while fruit pericarps are incorporated into beverage or food-related practices, including daily infusion in Riau (Perry & Metzger 1980; Kaneda et al. 1992; Lim 2012; Agapin 2020; Igiastini et al. 2021; Izazah & Anisa 2021; Bailly 2022; Wijaya 2022). These distinctions suggest a practical ethnobotanical classification system in which therapeutic function is distributed across the plant body rather than concentrated in a single organ. The preference for leaves in many traditional preparations may be related to their accessibility and harvesting sustainability, as leaves and fruit pericarps are easily obtained and can be collected without killing the plant (Wang *et al.* 2025). In contrast, roots and whole-plant materials are generally less sustainable to harvest, although they are often culturally associated with stronger or more systemic effects (Wang *et al.* 2025). Such plant-part selection is therefore shaped not only by perceived pharmacological efficacy, but also by ecological availability, preparation burden, taste, dose familiarity, and the social context in which the remedy is prepared and administered. More broadly, plant-based healthcare practices are culturally mediated rather than determined solely by pharmacology, they may change through migration, community integration, healthcare access, and the persistence of more traditional lifestyles (Ceuterick *et al.* 2008; Teixidor-Toneu *et al.* 2018; Maleki *et al.* 2024).

Preparation practices add another layer to this cultural adaptation. Decoction, infusion, topical application, chewing, bathing, and consumption as food or drink are not merely delivery routes, but cultural technologies that transform plant material into socially acceptable remedies (Lamxay *et al.* 2011; Wang *et al.* 2025). The same species may therefore function as a household beverage, postpartum tonic, topical preparation, or digestive decoction (Degbe *et al.* 2025). This flexibility helps explain why *S. koetjape* persists across multiple knowledge systems without being fixed to one disease category. Its use is continually reinterpreted according to local therapeutic logic rather than transferred as a single standardized pharmacological indication.

Traditional illness categories documented for *S. koetjape* are experiential rather than biomedical (Isyaka *et al.* 2024). They include fever, swelling, diarrhea, stomach discomfort, wound-related conditions, skin irritation, postpartum weakness, and general tonic use (Perry & Metzger 1980; Kaneda *et al.* 1992; Lim 2012; Adnyana 2020; Agapin 2020; Igiastini *et al.* 2021; Izazah & Anisa 2021). From a biomedical perspective, many of these signs can be linked to disruption of cellular and tissue homeostasis, including inflammatory cytokine release, overproduction of reactive oxygen species (ROS), oxidative stress, metabolic imbalance, and tissue repair responses (Lopes *et al.* 2024). Therefore, the traditional relevance of *S. koetjape* should not be read as direct historical evidence for treating modern chronic diseases, but as a culturally grounded indication that the plant may influence physiological processes shared across multiple disease contexts (Kolac *et al.* 2026).

The α-glucosidase assay should be understood within this ethnobotanical framework. It was not intended to redefine *S. koetjape* as a diabetes drug, but to provide a limited biochemical checkpoint for one process suggested by the ethnobotanical record, digestive and metabolic regulation (Khastini *et al.* 2021). The leaf extract showed moderate α-glucosidase inhibition, whereas the fruit pericarp extract showed weak activity. This difference supports the possibility of plant-part-specific functional variation, especially because leaves are repeatedly reported for fever, inflammation, diarrhea, and swelling, while fruit pericarps are more strongly associated with infusion or functional beverages use (Perry & Metzger 1980; Kaneda *et al.* 1992; Lim 2012; Adnyana 2020; Agapin 2020; Igiastini *et al.* 2021; Izazah & Anisa 2021). However, the moderate potency of the leaf extract and weak activity of fruit pericarps also indicate that crude extracts may contain inactive, competing, or antagonistic constituents that reduce apparent activity in a single-enzyme assay (Caesar *et al.* 2019; Ru *et al.* 2019).

This interpretation is important because traditional preparations rarely involve isolated compounds. Crude extracts contain mixtures of metabolites that may interact additively, synergistically, or antagonistically (Aisha *et al.* 2009; Caesar *et al.* 2019; Ru *et al.* 2019; Nassar *et al.* 2012). Therefore, a moderate IC_{50} value does not necessarily invalidate ethnobotanical relevance; instead, it reflects the complexity of plant preparations used in cultural practice. Conversely, as reported in historical literature, stronger cytotoxic or bioactivity profiles have been observed in stem bark extracts or isolated bark-derived compounds (Aisha *et al.* 2009; Nassar *et al.* 2012). However, stem bark was not tested in the present in vitro assay, which focused specifically on leaves and fruit pericarps because these parts are culturally relevant, commonly prepared as decoctions or infusions, and less destructive to harvest than bark or roots (Saadah *et al.* 2022; Armaghan *et al.* 2024; Febriyanti *et al.* 2025).

The chemical data support this plant-part interpretation. Leaves have been associated with limonoids and triterpenoids such as koetjapin derivatives, phellochin, sandoripins, sanjecumins, 16R,22R-dihydroxycycloartenone, and 4,10,11-trihydroxy guaiane, while fruit-derived materials have been linked with triterpenoids such as bryonolic acid and bryononic acid (Sim & Lee 1972; Hang 2022). Bark and stem bark contain several well-studied triterpenoids, including koetjapic acid, katonic acid, katononic acid, sandorinic acids, and related compounds (Bailly 2022; Wijaya 2022). These metabolites help explain why different plant parts may show distinct bioactivity profiles (Saadah *et al.* 2022; Anisa *et al.* 2026). Nevertheless, compounds should not be treated as the sole explanation for traditional knowledge, because traditional use also involves preparation methods, dose familiarity, sensory evaluation, social context, and intergenerational transmission (Zakaria 2026).

The network pharmacology, PPI, enrichment, and docking analyses provide a systems-level interpretation of the plant-part and compound diversity documented for *S. koetjape*. Diabetes- and breast cancer-related target sets were used as modern biomedical pathway models, not as direct substitutes for local illness categories. The identification of shared targets in the diabetes-related and breast cancer-related model suggests that reported *S. koetjape* compounds may intersect with pathways related to inflammation, metabolic regulation, immune response, signal transduction, lipid metabolism, and altered cell survival (Meehan & Wang 2022). This interpretation was further supported by the repeated appearance of IL6 and TNF as inflammatory cytokine hubs, together with PPARG and TP53 as metabolic and cell-survival regulatory nodes (Itoh *et al.* 2018). IL6 and TNF may represent upstream inflammatory mediators linked to cytokine amplification, oxidative stress, insulin resistance, and tissue remodeling (Engin *et al.* 2019; Diep *et al.* 2022), while PPARG and TP53 connect the network to lipid/glucose regulation, inflammatory modulation, stress response, cell-cycle control, and apoptosis (Cataldi *et al.* 2021; Frkic *et al.* 2021; Duffy *et al.* 2018; Marvalim *et al.* 2023; Wang *et al.* 2023). These findings do not provide definitive evidence of therapeutic efficacy but serve as heuristic maps showing that culturally documented uses of *S. koetjape* for fever, inflammation, digestive disturbance, wound care, and restoration may correspond to broad regulatory systems recognized in contemporary biology.

This cytokine- and receptor-centered interpretation helps connect the ethnobotanical symptom categories of *S. koetjape* with downstream signaling systems. Fever, swelling, inflammation, wound-related conditions, and digestive disturbance can be understood as experiential signs of inflammatory activation and disruption of cellular or tissue homeostasis (Chen *et al.* 2024; Wang *et al.* 2024). In medicinal plant network studies, cytokine–receptor interaction, TNF signaling, NF-κB, and JAK-STAT pathways often appear together, indicating that inflammatory mediators act through interconnected regulatory modules rather than isolated targets (Shawky *et al.* 2020). The enrichment of PI3K/AKT, AMPK, NF-κB, PPAR, TNF, mTOR, and VEGF-related pathways in this study therefore suggests that predicted *S. koetjape* targets are involved in broader inflammatory, metabolic, and stress-response cascades (Shawky *et al.* 2020; Merecz-Sadowska *et al.* 2025). This interpretation is consistent with reports that medicinal plants may modulate PI3K/AKT and AKT1-centered anti-inflammatory pathways (Merecz-Sadowska 2025), as well as TLR4/NF-κB, PI3K-AKT, MAPK, and microbiota–immune interactions in intestinal inflammation (Yang 2023). Natural products have also been reported to reduce TNF-α, IL-1β, and IL-6 while suppressing NF-κB and JAK/STAT3 signaling in inflammatory bowel disease models (Gandhi *et al.* 2023), and traditional decoctions may regulate IL-10, IL-1β, and IL-6 through EGFR-dependent MAPK/ERK1/2 signaling (Wang *et al.* 2022). Together, these findings support the view that traditional uses of *S. koetjape* may correspond to physiological states now recognized as inflammation-, metabolism-, and stress-response-related processes (Naidu *et al.* 2024).

The docking results provide supporting interaction evidence for this systems-level interpretation. Selected compounds showed favorable predicted binding affinities with upstream regulatory targets, including IL6, TNF-α, PPARG, and TP53. For example, 3-oxo-olean-12-en-29-oic acid showed strong predicted interaction with PPARG and IL6, sandorinic acid B interacted with TNF-α and IL6, phellochin showed favorable interaction with TNF-α, and katonic acid interacted with IL6 and TP53. Visualization of ligand–protein complexes indicated hydrogen bonds and hydrophobic interactions with key amino acid residues in the predicted binding regions. These interactions should not be interpreted as proof of therapeutic efficacy, but they support the network-based observation that *S. koetjape* compounds may interact with upstream inflammatory and regulatory proteins that crosstalk with downstream cascades such as NF-κB, PI3K/AKT, AMPK, mTOR, and VEGF-related signaling.

An important point in interpreting the network results is that network centrality does not necessarily equal experimental potency. Koetjapic acid, for example, has been widely reported for α-glucosidase inhibitory and cytotoxic-related activities, yet it did not consistently appear as the most dominant compound node in the constructed networks. This does not contradict previous experimental findings. Network centrality reflects the number and position of predicted target connections within a defined dataset, whereas experimental potency reflects the strength of activity in a specific assay,

concentration range, extract matrix, or cellular context (Noor *et al.* 2022). Therefore, compounds with strong reported bioactivity may not always rank as the most central network nodes, and highly connected compounds may function more as broad interaction candidates than as the most potent bioactive agents.

The biomedical disease labels used in this study should therefore be understood as analytic translations rather than replacements for local illness categories. Traditional records describe diarrhea, fever, swelling, skin irritation, stomach discomfort, postpartum weakness, and general restorative use, not modern diagnostic entities such as diabetes or breast cancer (Saadah *et al.* 2022; Wijaya 2022). The relevance of diabetes- and cancer-associated pathways emerges through shared biological processes, particularly inflammation, oxidative stress, metabolic imbalance, immune regulation, and altered cell survival (Itoh *et al.* 2018). This distinction is essential because the study does not claim that traditional communities historically used *S. koetjape* specifically for diabetes or breast cancer. Rather, it suggests that traditional symptom-based applications may correspond to physiological networks that are also implicated in these chronic disease models.

Consequently, the major contribution of this study is not the identification of a single candidate compound or a single therapeutic target. Its main contribution is an integrative model for studying a culturally distributed medicinal plant without reducing traditional knowledge to pharmacological pre-screening. In this model, ethnobotanical evidence guides the research frame, laboratory and computational findings provide partial mechanistic support, and interpretation returns to the cultural system that selected, maintained, and adapted the plant in the first place. This approach allows *S. koetjape* to be discussed as both a culturally meaningful medicinal plant and a source of compounds with plausible multi-target biological relevance.

This study has several limitations. The ethnobotanical synthesis was based on published sources, which may underrepresent local variation, practitioner knowledge, gendered knowledge transmission, and changes in contemporary use. The α-glucosidase assay evaluated only one biochemical activity and only two selected plant parts. Network pharmacology and molecular docking depend on database completeness, algorithmic prediction, target availability, and structural assumptions, and therefore cannot replace experimental validation. Future studies should prioritize community-based ethnographic validation, comparative analysis of culturally specific preparation methods, metabolomic profiling of traditional preparations, expanded bioassays across plant parts, and in vivo or clinical studies only after the ethnobotanical context has been clearly established. Such work would allow laboratory validation to remain supportive and context-dependent, rather than replacing the knowledge system that gives *S. koetjape* its medicinal significance.

Conclusion

This study shows that *Sandoricum koetjape* (Burm.f.) Merr. is embedded in diverse Southeast Asian ethnobotanical knowledge systems, where plant-part selection and preparation practices are culturally adapted to digestive disturbance, fever, inflammation, wound care, postpartum recovery, and functional beverages use. The repeated use of bark, leaves, roots, and fruit pericarps across different communities suggests that traditional knowledge of this species reflects patterned empirical selection rather than arbitrary plant use. Supporting α-glucosidase inhibition, compound profiling from published records, network pharmacology, enrichment analysis, and molecular docking indicate that reported *S. koetjape* compounds may correspond to biological processes related to inflammatory, metabolic, immune, and cell-survival regulation. However, these laboratory and computational findings should be interpreted as hypothesis-generating support, not as direct proof of therapeutic efficacy against diabetes or breast cancer. Overall, this study provides an ethnobotanical framework for understanding how culturally transmitted knowledge of *S. koetjape* can guide mechanistic exploration while keeping traditional plant-use systems as the central interpretive context.

Declarations

List of abbreviations: PPI – Protein–Protein Interaction; GO – Gene Ontology; KEGG – Kyoto Encyclopedia of Genes and Genomes; PDB – Protein Data Bank; RMSD – Root Mean Square Deviation; TTD – Therapeutic Target Database; BP – Biological Process; CC – Cellular Component; MF – Molecular Function; OB (%)– Oral Bioavailability; DL – Drug-Likeness; IL6 – Interleukin 6; PPARG – Peroxisome Proliferator-Activated Receptor Gamma; TNF-α – Tumor Necrosis Factor Alpha; TP53 – Tumor Protein p53; $\Delta G_{bind}^{(kcal/mol)}$ – Binding Affinity.

Ethics approval and consent to participate: Not applicable**.**

Consent for publication: Not applicable.

Availability of data and materials: All data generated or analyzed during this study are included in this published article and its supplementary information files.
Competing interests: The authors declare that they have no competing interests.
Funding: This research was supported by the Indonesia Endowment Fund for Education (LPDP) scholarship.
Author contributions: N.A. conceived and designed the study, conducted the majority of experiments and data analysis, and drafted the manuscript. A.B. performed to illustrated the network pharmacology, PPI interactions, GO, and KEGG pathway analyses. H.B.K. carried out plant sampling and conducted the α-glucosidase inhibitory assay. I.G.N.S.P. and M.A.I collected *in silico* data and performed statistical analysis. D.A.P. and U.F.W. analyzed α-glucosidase inhibition data and PPI results. M.S.N. conducted plant sampling and compiled compound data. F.D. and R.A. analyzed and interpreted α-glucosidase inhibition results and contributed to writing this section. R.L. and A. prepared plant materials, performed extraction, and collected compound data. F. assisted with taxonomic identification of the plant sample. S.M. supervised the study and refined the manuscript. B.J. supervised the research, served as the principal investigator, and refined the manuscript. All authors have reviewed and approved the final version of the manuscript.

Acknowledgements

This research was supported by graduate's scholarship funding from the Indonesia Endowment Fund for Education (Lembaga Pengelola Dana Pendidikan/LPDP) and center for Higher Education Funding and Assessment, the Indonesian Education Scholarship Program (BPI), Ministry of Finance of the Republic of Indonesia. The scholarship recipients contributing to this study include Nur Anisa (NIB: 202406111503410), Asril Burhan (NIB: 202209091341), Ulfa Febiana Whatin (NIB: 202501110000527), I Gusti Ngurah Sentana Putra (NIB: 202404110201596), M. Salman Nuryahya (NIB: 202406110304557), Dyah Ayu Puspitasari (NIB: 202501110000427), Fajar Dini (NIB: 202405111501931), Rosa Amelia (NIB: 202406111504035), Rati Lestari (NIB: 202406110304200), and Arman (NIB: 202407110304895). The authors also acknowledge the facilities, scientific and technical support from Botanical Characterization Laboratories, National Research and Innovation Agency through E Layanan Sains, Badan Riset dan Inovasi Nasional (BRIN).

Literature cited

Adnyana PES. 2020. Lontar taru pramana: pelestarian budaya pengobatan tradisional Bali. Jurnal Yoga Dan Kesehatan 2: 178. 10.25078/jyk.v2i2.1572.

Agapin JS. 2020. Medicinal plants used by traditional healers in Pagadian City, Zamboanga del Sur, Philippines. Philippine Journal of Science 14: 83-89. doi: 10.2139/ssrn.3625332.

Aisha AFA, Alrokayan SA, Abu-Salah KM, Darwis Y, Majid AMS. 2009. *In vitro* cytotoxic and apoptotic properties of the stem bark extract of *Sandoricum koetjape* on breast cancer cells. International Journal of Cancer Research 5: 123–129. doi: 10.3923/ijcr.2009.123.129.

Albuquerque UP, Cruz da Cunha LVF, de Lucena RFP, Alves RRN. 2019. Methods and techniques in ethnobiology and ethnoecology. Springer, New York.

Anisa N, Juliandi B, Mariya S, Widayati KA, Widarto TH. 2026. Metabolite profiling and preliminary biological assessment of *Sandoricum koetjape* (Burm. f.) Merr. Bark extracts from Pekanbaru, Indonesia. Journal of Multidisciplinary Applied Natural Science 20: 1-19. doi: 10.47352/jmans.2774-3047.378.

Armaghan M, Khan K, Irfan M, Hafeez A, Zafar ZJ, Sharifi-Rad J, Butnariu M, Sarac I, Bagiu JC, Bagiu RV. 2024. Koetjapic acid: unveiling its potential as a saviour in the realm of biological and medicinal properties, with a focus on anticancer mechanism of action. European Journal of Medical Research 29: 1-11. doi: 10.1186/s40001-024-01699-6.

Babichev S, Yarema O, Liakh I. 2025. A Gene ontology-based pipeline for selecting significant gene subsets in biomedical applications. Applied Science 15: 1–16. doi: 10.3390/app15084471.

Babu R, Ramya S, Kavithaa K, Paulpandi M, Saranya T, Babu S, Winster H, Balachandar V, Arul N. 2021. Spathulenol attenuates 6-hydroxydopamine induced neurotoxicity in SH-SY5Y neuroblastoma cells. Gene Reports 25: 101396. doi: 10.1016/j.genrep.2021.101396.

Bailly C. 2022. The health benefits of santol fruits and bioactive products isolated from *Sandoricum koetjape* Merr.: A scoping review. Journal of Food Biochemistry 46: 1–11. doi: 10.1111/jfbc.14152.

Banua AS. 2022. Medicinal plants utilized by the traditional healers and their patients in Bicol Region, Philippines. BU R&D Journal 25: 21-35. doi: 10.47789/burdj.mbtcbbgs.20222502.03.

Belgica TH, Suba MD, Alejandro GJD. 2021. Quantitative ethnobotanical study of medicinal flora used by local inhabitants in slected Barangay of Malinao, Albay, Philippines. Biodiversitas 22: 2711-2721. doi: 10.13057/biodiv/d220720.

BPOM RI. 2023. Pedoman penyiapan bahan baku obat bahan alam berbasis ekstrak/ fraksi. Badan Pengawas Obat dan Makanan RI, Jakarta.

Bumi MB, Heliawaty L, Hermawati E, Syah YM. 2019. Four limonoids from the seeds extract of *Sandoricum koetjape*. Journal of Natural Medicines 73: 641–647. doi: 10.1007/s11418-019-01303-w.

Caesar LK, Cech NB, Caesar LK, Cech NB. 2019. Synergy and antagonism in natural product extracts: when 1 + 1 does not equal 2. Natural Product Reports 36. doi: 10.1039/c9np00011a.

Cataldi S, Costa V, Ciccodicola A. 2021. PPAR γ and diabetes: beyond the genome and towards personalized medicine. Current Diabetes Reports 21.

Ceuterick M, Vandebroek I, Torry B, Pieroni A. 2008. Cross-cultural adaptation in urban ethnobotany: The Colombian folk pharmacopoeia in London. Journal of Ethnopharmacology 120: 342-359. doi: 10.1016/j.jep.2008.09.004.

Chen Y, Zhang J, Zhang B, Lee HK, Xie S, Shen W, Chen X, You M, Shen C, Xia B, Xing H. 2025. Optimizing drug sensitivity assays in patient-derived tumor organoids: a comparison of IC_{50} estimation methods and experimental parameters. Biology Methods and Protocols 10: 1–8.

Chin C, Chen S, Wu H, Ho C, Ko M, Lin C. 2014. CytoHubba: identifying hub objects and sub-networks from complex interactome. BMC Systems Biology 8: 1–7. doi: 10.1101/438192.

Cotton CM. 1996. Ethnobotany: principles and applications. John Wiley & Sons, Chichester.

Debge M, Gbekley EH, Kantati YT, Akakpo AWM, Tetebenissan A, Toubate BB, Metowogo K. 2025. Ethnonutritional and medicinal plant knowledge and practices for postpartum maternal healthcare in Yoto Prefecture, Togo: An ethnopharmacological study. European Journal of Medicinal Plants 36: 52-69. doi: 10.9734/ejmp/2025/v36i61306.

Doncheva NT, Morris JH, Gorodkin J, Jensen LJ. 2018. Cytoscape stringApp: network analysis and visualization of proteomics data. BioRxiv 8: 1-21. doi: 10.1101/438192.

Efdi M, Ninomiya M, Suryani E, Tanaka K, Ibrahim S, Watanabe K, Koketsu M. 2012. Sentulic acid: A cytotoxic ring A-seco triterpenoid from *Sandoricum koetjape* Merr. Bioorganic & Medicinal Chemistry Letters 22: 4242–4245. doi: 10.1016/j.bmcl.2012.05.043.

Fang X, Zhou S. 2024. A comparative study of *in vitro* dose-response estimation under extreme observations. Biometric Journal 66: 2200092. doi: 10.1002/bimj.202200092.

Francisca I, Borges DJ, Lopes T, Ventura B, Calixto SD, Pereira RV, Ungaretti T, Konno P, Pinto SC, Tinoco LW, Lasunskaia E,

Frkic RL, Richter K, Bruning JB. 2021. The therapeutic potential of inhibiting PPAR γ phosphorylation to treat type 2 diabetes. Journal of Biological Chemistry 297: 101030. doi: 10.1016/j.jbc.2021.101030.

Hang TXH, Jarupinthusophon S, Hairani R, Nguyen VK, Chavasiri W. 2024. Cycloartane-type triterpenoids from the leaves of *Sandoricum koetjape* and their efficacy on α-glucosidase inhibition activity. Journal of Natural Medicines 78: 655–663. doi: 10.1007/s11418-023-01778-8.

Hang, TXH. 2022. Bioactive compounds from leaves and heartwoods of santol *Sandoricum koetjape* Merr. PhD dissertation, Chulalongkorn University.

Heliawati L, Syah YM, Bumi MB. 2019. Bryononic acid: antibacterial compound from fruit hulls of *S. koetjape* Merr extract. Journal of Chemical and Pharmaceutical Sciences 12: 14–18. doi: 10.30558/jchps.20191201004.

Hendrarti W, Umar AH, Syahruni R, Rafi M, Kusuma WA. 2024. Deciphering the mechanism of action *Cosmos caudatus* compounds against breast neoplasm: a combination of pharmacological networking and molecular docking approach with bibliometric analysis. Indonesian Journal of Science & Technology 9: 527–556. doi: 10.17509/ijost.v9i2.71856.

Heinrich M, Jäger AK. 2015. Ethnopharmacology. Wiley-Blackwell, Oxford.

Hopkins BD, Pauli C, Du X, Wang DG, Li X, Wu D, Amadiume SC, Goncalves MD, Hodakoski C, Lundquist MR, Bareja R, Ma Y, Harris EM, Sboner A, Beltran H, Rubin MA, Mukherjee S, Cantley LC. 2018. Suppression of insulin feedback enhances the

efficacy of PI3K inhibitors. Research Letter 560: 499. doi: 10.1038/s41586-018-0343-4.

Igiastini RO, Wahyuni I, Saraswati I. 2021. Ethnobotanical study of digestive systems disorders in Baduy Ethnic Indonesia. Biotropia 28: 54–63. doi: 10.11598/btb.0.0.0.1055.

Ismail IS, Ito H, Hatano T, Taniguchi S, Yoshida T. 2003. Modified limonoids from the leaves of *Sandoricum koetjape*. Phytochemistry 64: 1345–1349. doi: 10.1016/S0031-9422(03)00500-4.

Isyaka SM, Akintayo AH, Abdullahi AM. 2024. A review of ethnomedicinal uses, phytochemistry and pharmacology of Nigerian *Crotons.* Archives of Current Research International 24: 250-274. doi: 10.9734/acri/2024/v24i121016.

Ito T, Katsurayama K, Efdi M, Ninomiya M, Koketsu M. 2018. Sentulic acid isolated from *sandoricum koetjape* Merr attenuates lipopolysaccharide and interferon gamma co-stimulated nitric oxide production in murine macrophage RAW264 cells. Bioorganic & Medical Chemistry Letters 28: 3496-3501. doi: 10.1016/j.bmcl.2018.10.008.

Izazah N, Anisa N. 2021. Potensi kecapi (*Sandoricum koetjape*) pohon larat nan kaya manfaat asal Riau. Taman Karya, IKAPI, Pekanbaru.

Jafari SF, Keshavarzi M, Abdulmajid AMS, Al-Suede FSR, Asif M, Ahamed MBK, Khan MSS, Hassan LAE, Majid ASA, Naseri M. 2024. Evaluation of *in vitro* and *in vivo* anticancer activities of potassium koetjapate: a solubility improved formulation of koetjapic acid against human colon cancer. Research in Pharmaceutical Sciences 19: 203–216. doi: 10.4103/RPS.RPS_247_22.

Kaneda N, Pezzuto JM, Kinghorn D, Farnsworth NR, Santisuk T, Tuchinda P, Udchachon J, Reutrakul V. 1992. Plant anticancer agents, l. cytotoxic triterpenes from *Sandoricum koetjape* stems. Journal of Natural Products 55: 654–659. doi: 10.1021/np50083a016.

Khallouki F, Owen RW, Silvente-Poirot S, Poirot M. 2018. Bryonolic acid blocks cancer cell clonogenicity and invasiveness through the inhibition of fatty acid: cholesteryl ester formation. Biomedicines 6: 1–9. doi: 10.3390/biomedicines6010021.

Khastini RO, Wahyuni I, Saraswati I. 2021. Ethnobotanical study of digestive systems disorders in Baduy Ethnic, Indonesia. Biotropia 28: 54-63. doi: 10.11598/btb.2021.28.1.1055.

King FE, Morgan JWW. 1960. The Chemistry of extractives from hardwoods. Part XXX. The constitution of katonic acid, a triterpene from *Sandoricum indicum*. Journal of the Chemical Society 0: 4738–4747.

Kosela S, Yulizar Y, Chairul, Tori M, Asakawat Y. 1995. Secomultiflorane-type triterpenoid acids from stem bark of *Sandoricum koetjape*. Phytochemistry 38: 691–694.

Lamxay V, de Boer HJ, Bjork L. 2011. Traditions and plant use during pregnancy, childbirth and postpartum recovery by the Kry ethnic group in Lao PDR. Journal of Ethnobiology and Ethnomedicine 7: 1-15.

Lertphadungkit P, Suksiriworapong J, Satitpatipan V, Sirikantaramas S, Wongrakpanich A, Bunsupa S. 2020. Enhanced production of bryonolic acid in *Trichosanthes cucumerina* L. (Thai Cultivar) cell cultures by elicitors and their biological activities. Plants 9: 1–11.

Lim TK. 2012. *Sandoricum koetjape* in edible medicinal and non-medicinal plants, Springer Dordrecht, US.

Lipinski CA, Lombardo F, Dominy BW, Feeney PJ. 2012. Experimental and computational approaches to estimate solubility and permeability in drug discovery and development settings. Advanced Drug Delivery Reviews 64: 4–17. doi: 10.1016/j.addr.2012.09.019.

Lopes FB, Sarandy MM, Novaes RD, Valacchi G, Goncalves RV. 2024. Oxinflammatory responses in the wound healing process: A systematic review. Antioxidants 13: 1-23. doi: 10.3390/antiox13070823.

Maleki T, Leonti M, Cero MD, Sonboli A, Weckerle CS. 2025. Kurdish ethnomedicine in the context of historic migration. Journal of Ethnopharmacology 339: 119431. doi: 10.1016/j.ep.2024.119132.

Martin GJ. 2004. Ethnobotany: a methods manual. Earthscan Publications, London.

Merecz-Sadowska A, Sadowski A, Zielinska-Blizniewska H, Zajdel K, Zajdel R. 2025. Network pharmacology as a tool to investigate the antioxidant and anti-inflammatory potential of plant secondary metabolites – a review and perspectives. Molecular Sciences 26: 1-25. doi: 10.3390/ijms26146678.

Meehan EV, Wang K. 2022. Interleukin-17 family cytokines in metabolic disorders and cancer. Genes 13: 1-27. doi: 10.3390/genes13091643.

Muhammad I, Sayed KA, El Mossa JS, Al-said MS, El-feraly FS, Clark AM, Hufford CD, Oh S, Mayer AMS. 2000. Bioactive 12-oleanene triterpene and secotriterpene acids from *Maytenus undata*. Journal of Natural Products 63: 605–610. doi: 10.1021/np990456y.

Munshif AA. 2014. Aktivitas inhibisi α-glukosidase dan sitotoksisitas ekstrak xantorizol temulawak (*Curcuma xanthorriza* Roxb.) dari berbagai daerah. Thesis, IPB University.

Nagakura Y, Nugroho AE, Hirasawa Y, Hosoya T, Rahman A, Kusumawati I, Zaini NC, Morita H. 2013. Sanjecumins A and B: New limonoids from *Sandoricum koetjape*. Journal of Natural Medicines 67: 381–385. doi: 10.1007/s11418-012-0677-4.

Nassar ZD, Aisha AFA, Al Suede FSR, Majid ASA, Majid AMSA. 2012. *In vitro* antimetastatic activity of koetjapic acid against breast cancer cells. Biological and Pharmaceutical Bulletin 35: 503–508. doi: 10.1248/bpb.35.503.

Nassar ZD, Aisha AAF, Majid AMSA. 2010. The pharmacological properties of triterpenoids from *Sandoricum koetjape.* WebmedCentral Complementary Medicine. 1: WMC001311.

Noor F, Tahir M, Ashfaq UA, Albutti A, Alwashmi ASS, Aljasir MA. 2022. Network pharmacology approach for medicinal plants: review and assessment. Pharmaceuticals 15: 1–33.

Novaryatiin S, Indah I. 2019. The medicinal plants used in Anjir Pulang Pisau, Cental Kalimantan-Indonesia. Pharmacognosy Journal 11: 1572-1579. doi: 10.5530/pj.2019.11.240.

Nursyarah AT, Safithri M, Andrianto D. 2023. Red betel leaf bioactive compounds as ERα receptor inhibitors *in silico* and MCF-7 cell anticancer *in vitro*. HAYATI Journal of Biosciences 30: 789–796. doi: 10.4308/hjb.30.5.789-796.

Pancharoen O, Haboonmee P. 2006. Chemical constituents from the leaves of *Sandoricum koetjape*. Perspectives in Natural Product Chemistry 3: 51–55.

Pancharoen O, Pipatanapatikarn A, Taylor WC, Bansiddhi J. 2009. Two new limonoids from the leaves of *Sandoricum koetjape*. Natural Product Research 23: 10–16. doi: 10.1080/14786410601133426.

Perry LM, Metzger J. 1980. Medicinal plants of East and Southeast Asia: attributed properties and uses. MIT Press, Cambridge.

Powell RG, Mikolajczak KL, Zilkowski BW. 1991. Limonoid antifeedants from seed of *Sandoricum koetjape*. Journal of Natural Product 54: 241–246.

Que J, Ye M, Zhang Y, Xu W, Li H, Xu W, Chu K. 2016. Bryonolic acid, a triterpenoid, protect against n-methyl-d-aspartate-induced neurotoxicity in PC12 Cells. Molecules 21. doi: 10.3390/molecules21040418.

Ram J, Calzada F, Garc N, Barbosa E, Vel C, Valdes M. 2024. Caryophyllene oxide, a bicyclic terpenoid isolated from *Annona macroprophyllata* with antitumor activity: *in vivo*, *in vitro*, and *in silico* studies. International Journal of Molecular Sciences 25: 1–24. doi: 10.3390/ijms252413355.

Rasadah MA, Khozirah S, Aznie AA, Nik MM. 2004. Anti-inflammatory agents from *Sandoricum koetjape* Merr. Phytomedicine 11: 261–263. doi: 0944-7113/04/11/02–03-261.

Ru J, Del Valle P, De Arriaga De, Fernandez-Alvarez L, Garcia-Armesto MR. 2019. Combination of carvacrol and thymol: Antimicrobial activity against *Staphylococcus aureus*. Foodborne Pathogens and Disease XX: 1–8. doi: 10.1089/fpd.2018.2594.

Saadah S, Tulandi SM, Rohman RA. 2022. Phytochemical and gas chromatography-mass spectrometry profiling of two plant parts of *Sandoricum koetjape*. Biodiversitas 23: 6199-6207. doi: 10.13057/biodiv/d231214.

Sahoo DK, Heilmann RM, Paital B, Patel A, Yadav VK, Wong D, Jergens AE. 2023. Oxidative stress, hormones, and effects of natural antioxidants on intestinal inflammation in inflammatory bowel disease. Frontiers in Endocrinology 14: 1217165. doi: 10.3389/fendo.2023.1217165.

Shabana SM, Gad NS, Othman AI, Fahmy A, Mohamed M, El A. 2023. β-caryophyllene oxide induces apoptosis and inhibits proliferation of A549 lung cancer cells. Medical Oncology 40: 1–10. doi: 10.1007/s12032-023-02022-9.

Shao LL, Lin KQ, Liu HF, Li ZY, Zhang N, Chen C, Pan WD, Lou HY, Li JY. 2024. Meliasanines A–L, tirucallane-type triterpenoids from *Melia toosendan* with anti-inflammatory properties via NF-κB signaling pathway. Phytochemistry 225: 114192. doi: 10.1016/j.phytochem.2024.114192.

Sim KY, Lee HT. 1972. Triterpenoid and other constituents from *Sandoricum indicum*. Phytochemistry 11: 3341–3343. doi: 10.1016/S0031-9422(00)86404-3.

Tanaka T, Koyano T, Kowithayakorn T, Fujimoto H, Okuyama E, Hayashi M, Komiyama K, Ishibashi M. 2001. New multiflorane-type triterpenoid acids from *Sandoricum indicum.* Journal of Natural Products 64: 1243–1245. doi: 10.1021/np010196w.

Teixidor-Toneu I, Jordan FM, Hawkins JA. 2018. Comparative phylogenetic methods and the cultural evolution of medicinal plant use. Nature Plants 4: 754-761. doi: 10.1038/s41477-018-0226-6.

Tukiran, Saidah, Suyatno, Hidayati N, Shimizu K. 2006. Brioninic acid from the hexane extract of *Sandoricum koetjape* Merr stem bark (meliaceae). Indo. J. Chem 6: 304–306.

Umar AH, Biringallo CSN, Tuyuwale PI, Kila A, Febyola KD, Syahruni R, Hendrarti W, Rafi M, Ratnadewi D. 2025. Unveiling the pharmacological mechanism of cosmos caudatus compounds as lung cancer drug candidates: pharmacology networking, molecular docking, and experimental validation. Journal of Pharmaceutical Innovation 20: 1–19. doi: 10.1007/s12247-025-09989-0.

Veber DF, Johnson SR, Cheng HY, Smith BR, Ward KW, Kopple KD. 2002. Molecular properties that influence the oral bioavailability of drug candidates. Journal of Medicinal Chemistry 45: 2615–2623. doi: 10.1021/jm020017n.

Wang J, Dempsey E, Corr SC, Kukula-Koch W, Sasse A, Sheridan H. 2022. The Traditional Chinese Medicine *Houttuynia cordata* Thunb decoction alters intestinal barrier function via an EGFR dependent MAPK (ERK1/2) signalling pathway. Phytomedicine 105: 154353. doi: 10.1016/j.phymed.2022.154353.

Wang X, Anwar T, Qureshi H, El-Beltagi HS, Sehar Z, Solieva D, Azizov B, Rebouh NY, Abbasov MA, Yakubov F, Alomran MM. 2025. Plant-based traditional remedies and their role in public health: ethnomedicinal perspectives for a growing population. Journal of Health, Population and Nutrition 44: 1-21. doi: 10.1186/s41043-025-01036-5.

Warsinah W, Kusumawati E, Sunarto S. 2015. Identification of compound antifungi of *Sandoricum koetjape* stem and activity to *Candida albicans*. Majalah Obat Tradisional (Traditional Medicine Journal) 16: 170–178. doi: 10.22146/TRADMEDJ.8055.

Wijaya MD. 2022. Ethnomedicinal, phytochemicals, and pharmacological aspects of sentul (*Sandoricum koetjape*). Journal of Biology, Medicine, & Natural Product Chemistry 11: 65–73. doi: 10.14421/biomedich.2022.111.65-73.

Xu X, Zhang W, Huang C, Li Y, Yu H, Wang Y. 2012. A novel chemometric method for the prediction of human oral bioavailability. International Journal of Molecular Sciences 13: 6964–6982. doi: 10.3390/ijms13066964.

Yadana, Lwin HH, Aung AA. Ethnomedicinal study of some edible plants in Kalwin Village, Myeik Township. J. Myanmar Acad. Arts. Sci 14: 425-433.

Zakaria MS. 2026. Ethnopharmacology at a crossroad: the vanishing link between nature and people. Research Connections 1: 1-4. doi: 10.1093/rescon/vmag043.

Supplementary Material

R Script for IC50 Statistical Analysis

```r
# ================================================================
# Supplementary Material S1
# R Script for IC50 Statistical Analysis
# Cross-cultural ethnobotanical knowledge of
# Sandoricum koetjape (Burm.f.) Merr.
# ================================================================

# Load packages
library(dplyr)
library(ggplot2)
library(FSA)
library(rcompanion)
library(car)

# Read data
data <- read.csv(
  "IC50_data.csv",
  sep = ";",
  stringsAsFactors = TRUE
)

data$Sample <- factor(data$Sample)

# Inspect data
str(data)
summary(data)

# ================================================================
# Descriptive statistics
# ================================================================

desc <- data %>%
  group_by(Sample) %>%
  summarise(
    n = n(),
    Mean = mean(IC50_ppm),
    SD = sd(IC50_ppm),
    Median = median(IC50_ppm),
    Min = min(IC50_ppm),
    Max = max(IC50_ppm)
  )

desc

# ================================================================
# Assumption tests
# ================================================================

model <- aov(IC50_ppm ~ Sample, data = data)

# Normality
shapiro.test(residuals(model))

# Homogeneity
leveneTest(IC50_ppm ~ Sample, data = data)

# ================================================================
# Non-parametric comparison
# ================================================================

kruskal.test(IC50_ppm ~ Sample, data = data)

# ================================================================
# Dunn post-hoc test
# ================================================================
```

```
65|
66| dunn <- dunnTest(
67|   IC50_ppm ~ Sample,
68|   data = data,
69|   method = "bh"
70| )
71|
72| dunn
73|
74| ######################################################################
75| # Group letters
76| ######################################################################
77|
78| letters <- cldList(
79|   P.adj ~ Comparison,
80|   data = dunn$res,
81|   threshold = 0.05
82| )
83|
84| ######################################################################
85| # Merge statistics
86| ######################################################################
87|
88| plot.data <- merge(
89|   desc,
90|   letters,
91|   by.x = "Sample",
92|   by.y = "Group"
93| )
94|
95| plot.data
96|
97| ######################################################################
98| # Figure
99| ######################################################################
100|
101| ggplot(
102|   plot.data,
103|   aes(
104|     x = Sample,
105|     y = Mean,
106|     fill = Sample
107|   )
108| ) +
109|   geom_col(
110|     width = 0.60,
111|     colour = "black",
112|     linewidth = 0.8
113|   ) +
114|   geom_errorbar(
115|     aes(
116|       ymin = Mean - SD,
117|       ymax = Mean + SD
118|     ),
119|     width = 0.15,
120|     linewidth = 0.8
121|   ) +
122|   geom_text(
123|     aes(
124|       y = (Mean + SD) * 1.35,
125|       label = Letter
126|     ),
127|     size = 7
128|   ) +
129|   scale_fill_manual(
130|     values = c(
131|       "Acarbose" = "#F8766D",
132|       "Fruit_Extract" = "#00BA38",
```

```
      "Leaves_Extract" = "#619CFF"
    )
  ) +
  scale_y_log10(
    expand = expansion(mult = c(0.05, 0.25))
  ) +
  coord_cartesian(clip = "off") +
  labs(
    x = "Sample",
    y = expression(IC[50] ~ "(ppm)")
  ) +
  theme_classic(base_size = 18) +
  theme(
    legend.position = "none",
    axis.title = element_text(face = "bold"),
    axis.text = element_text(
      colour = "black",
      size = 16
    ),
    axis.line = element_line(linewidth = 1),
    axis.ticks = element_line(linewidth = 1),
    plot.margin = margin(
      t = 20,
      r = 20,
      b = 10,
      l = 10
    )
  )
```

Table S1. Data Analysis

Type of data analysis	**p-Value (95%)**	**Intepretation**
Shapiro-wilk	0.005588	p < 0.05 = not distributed normal
Levene test	0.3864	p > 0.05 = data homogen
Kruskal-wallis	0.02732	p < 0.05 = significant within group
Dunn with Benjamini-Hochberg correction		
a. Acarbose-Fruit Extract	0.02187107	p < 0.05 = significantly different among group
b. Acarbose-Leaves Extract	0.17971249	p > 0.05 = not significantly different among group
c. Fruit Extract – Leaves Extract	0.26956874	p > 0.05 = not significantly different among group

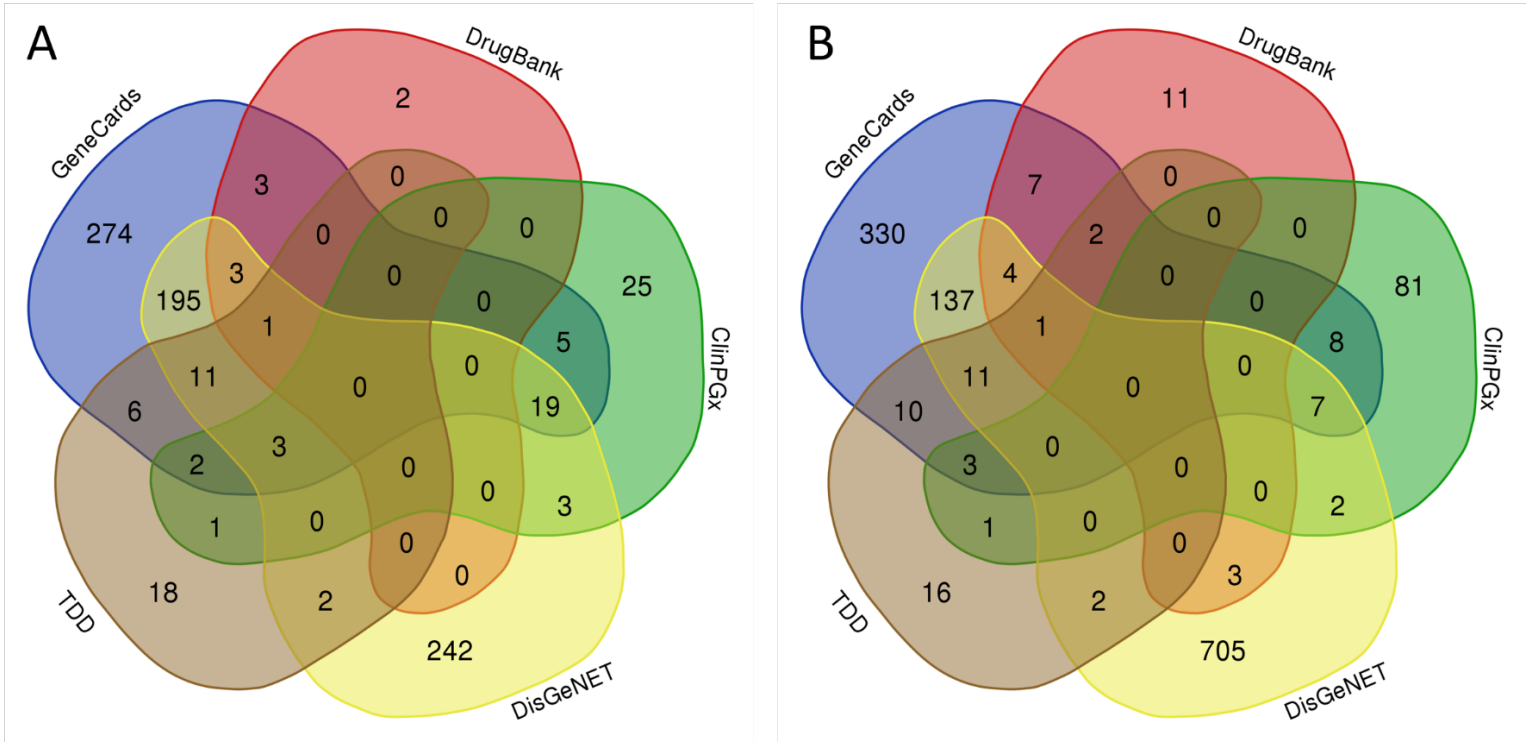

Figure S1. Venn diagram of diabetes (A) and breast cancer (B) targets using DrugBank, ClinPGx, DisGeNET, TDD, and GeneCard.

Table S2. Selection of *S. koetjape* triterpenoids compounds using Lipinski-veber rule, bioavailability and drug-likeness parameters

No	Compound Name	ID	MW	CLogP	HBD	HBA	tPSA	Rotable bonds	Lipinski/ Veber Violations	OB	DL
1	(–)-alloaromadendrene	10899740	204.35	4.34	0	0	0	0	0/0	0.55	-1.3
2	(–)-caryophyllene oxide	1742210	220.35	3.68	0	1	12.53	0	0/0	0.56	-1.5
3	(+)-spathulenol	92231	220.35	3.3	1	1	20.23	0	0/0	0.57	-0.96
4	[21α-methylmelianol (21R,23R) epoxy-24-hydroxy-21α-methoxyl]triucalla-7,25-dien-3-one	NA									
5	[2α-(2-methylbutanoyl)oxy]sandoricin	NA									
6	[2α-(2-methylpropanoyl)oxy]sandoricin	NA									
7	16R,22R-dihydroxycycloartenone	NA									
8	20-epikoetjapic acid*	10790564	470.68	6.06	2	4	74.6	5	1/0	0.84	0.42
9	3-epikatonic acid*	10434225	456.7	6.04	2	3	57.53	1	1/0	0.85	0.42
10	3-Oxo-olean-12-en-29-oic acid*	11970027	454.68	6.13	1	3	54.37	1	1/0	0.85	0.42
11	4,10,11-trihydroxy guaiane	NA									
12	6-hydroxysandoricin	196858	604.64	2.03	2	12	168.03	8	2/1	0.17	-0.31
13	Briononic acid	NA									
14	Bryonolic acid*	159970	456.7	6.06	2	3	57.53	1	1/0	0.85	0.46
15	Bryononic acid*	472768	456.7	6.1	2	3	57.53	1	1/0	0.86	0.46
16	Indicic acid	NA									
17	Katonic Acid*	9804114	456.7	6.04	2	3	57.53	1	1/0	0.85	0.42
18	Katononic acid*	9981416	454.68	6.06	1	3	54.37	1	1/0	0.85	0.42
19	Koetjapic Acid*	15513441	470.68	6.06	2	4	74.6	5	1/0	0.85	0.42
20	Koetjapin A	NA									
21	Koetjapin B	NA									
22	Koetjapin C	NA									
23	Koetjapin D	NA									
24	Phellochin*	14021541	488.74	5.45	2	4	66.76	6	1/0	0.55	0.48
25	Sandoricin	168012871	588.64	2.81	1	11	147.8	8	2/1	0.17	-0.46
26	Sandorinic Acid A*	10323147	486.68	4.54	3	5	94.83	1	0/0	0.56	0.57
27	Sandorinic acid B*	10323148	486.68	4.46	3	5	94.83	1	0/0	0.56	0.63
28	Sandorinic acid C*	11048975	470.68	5.23	2	4	74.6	1	1/0	0.85	0.51
29	Sandoripin A	102193789	720.76	2.34	2	15	207.49	12	2/2	0.17	-0.27
30	Sandoripin B	102193790	706.73	2.04	2	15	207.49	11	2/2	0.17	-0.43

31	Sandrapin A	273499464	660.66	1.95	1	14	191.17	10	2/2	0.17	-0.87
32	Sandrapin B	102193790	702.74	2.78	1	14	191.17	12	2/2	0.17	-0.46
33	Sandrapin C	C00057487	688.72	2.55	1	14	191.17	11	2/2	0.17	-0.65
34	Sandrapin D	12127458	700.73	2.65	1	14	191.17	11	2/2	0.17	-0.84
35	Sandrapin E	C00057570	686.7	2.5	1	14	191.17	11	2/2	0.17	-1
36	Sanjecumin A	NA									
37	Sanjecumin B	NA									
38	Secobryononic acid*	78101312	470.68	6.12	2	4	74.6	5	1/0	0.85	0.48
39	Secoisobryononic acid*	85082262	470.68	5.97	2	4	74.60	5	1/0	0.85	0.35
40	Sentulic Acid*	70683988	470.68	6.13	2	4	74.60	5	1/0	0.85	0.26

Notes: MW (molecular weight, g/mol); CLogP (lipophilicity); HBD (hydrogen bond donors); HBA (hydrogen bond acceptors); tPSA ($Å^2$); RB (rotatable bonds); OB (oral bioavailability, %); DL (drug-likeness score); * = qualify for all parameters.

Table S3. Topological features (Betweenness Centrality, Closeness Centrality, and Degree) of compounds from diabetic pharmacological network results.

Compound	Betweenness Centrality	Closeness Centrality	Degree
11970027	0.020486710231700466	0.33987603305785125	38
10323148	0.03278127339241809	0.378596087456847	37
10323147	0.03518655776237417	0.37133182844243795	36
10790564	0.009475859775548793	0.3299899699097292	36
70683988	0.010848789750857332	0.3306532663316583	35
15513441	0.009830841292716781	0.32671300893743793	35
9981416	0.010239221774638957	0.33401015228426395	35
9804114	0.0125452576067741	0.3391752577319588	35
11048975	0.015648708676240384	0.338477366255144	34
472768	0.006731322231383331	0.3231827111984283	34
159970	0.007049102509397238	0.3231827111984283	34
85082262	0.007980650429522689	0.32768924302788843	33
10434225	0.006474748316109881	0.3225490196078431	33
78101312	0.006146615509215727	0.3219178082191781	30
14021541	0.03466503055807607	0.3755707762557078	27

Tabel S4. Topological features (Betweenness Centrality, Closeness Centrality, and Degree) of targets from diabetic pharmacological network results.

Target	Betweenness Centrality	Closeness Centrality	Degree
PIK3CA	0.24356336563031544	0.4204472843450479	173
TP53	0.19645997965476084	0.39710319855159926	129
EGFR	0.15289519776482335	0.3947210557888422	123
MTOR	0.054835725778385996	0.37407617964752704	78
TNF	0.04847900909128986	0.3728045325779037	72
IL6	0.06056784870893898	0.36616583194212576	60
PRKAA2	0.03842221322157801	0.3637368711995577	50
CDK4	0.060258018722427975	0.3562533838657282	47
PTGS2	0.03620648079084685	0.3613399231191653	44
NOS2	0.03221490872173272	0.36054794520547945	42
PPARA	0.02472159621370033	0.36015325670498083	41
PTPN1	0.029444043736671303	0.35819270549809473	36
PPARG	0.01304808581103665	0.35780315388798256	35
FFAR1	0.03125156811192848	0.35319377348362857	33
ESR1	0.015656256483249083	0.35663956639566397	32
MMP9	0.019410196995138535	0.35395373856912316	31
PPARD	0.018598483021819153	0.3562533838657282	31
CYP17A1	0.013475488689425183	0.35586803677663603	30
G6PD	0.023960343838818843	0.35586803677663603	30
AR	0.020734030427255263	0.35586803677663603	30
CHRM2	0.014600672603118819	0.35319377348362857	29
HMGCR	0.014965286267179788	0.35548352242031334	29
MMP2	0.01534189661622462	0.35205992509363293	28
CYP19A1	0.011460712249883752	0.35509983810037776	28
SERPINE1	0.03167750508185743	0.3543349488422186	26
CYP2C19	0.02205811765361724	0.3543349488422186	26
CNR1	0.006938046488074112	0.3543349488422186	26
SCD	0.014695902051476603	0.3543349488422186	26
NR3C1	0.007822753032313511	0.3543349488422186	26
BCHE	0.01784712915980244	0.35243706480985537	26
NR1H4	0.010918417920391355	0.3341797866937532	25
TERT	0.023265726581810982	0.35395373856912316	25

HSD11B1	0.008574707247297081	0.35395373856912316	25
HSD11B2	0.00555211054989173	0.353573347662547	24
PTPN2	0.006566311851234252	0.353573347662547	24
AVPR2	0.027351310943756663	0.35130806193272823	23
PTGS1	0.0065865053465806195	0.30733302195235873	23
FABP4	0.0050218705025081335	0.35319377348362857	23
EDNRA	0.008911492478601178	0.3483324510322922	21
SREBF2	0.0030831180918751877	0.35055940330314334	21
NPC1L1	0.007677494485190844	0.35205992509363293	20
FABP3	0.0031486406499100818	0.35205992509363293	20
GCGR	0.012404478527145891	0.3509333333333334	18
SLC22A1	0.02908882100970391	0.35018626929217667	17
ACP1	7.95E+11	0.3509333333333334	17
EDNRB	0.0066194984976813975	0.3443223443223443	16
MME	0.01073028577744269	0.3421736869474779	16
CCKBR	0.00494928891524066	0.33691756272401435	15
P2RY12	0.013472802121217965	0.34146341463414637	14
CSF1R	0.002309260630615021	0.3390005151983514	14
AKR1B1	0.01993512255161738	0.3490716180371353	14
CYP27B1	0.01014527691063299	0.34110938310005184	13
RBP4	0.020477221380834833	0.3490716180371353	13
HNF4A	0.012088459621916871	0.3483324510322922	13
NR1I3	5.02E+11	0.3397005678884874	13
AGTR1	0.0020951150750334385	0.3487016428192899	11
NR1I2	4.05E+12	0.3390005151983514	11
REN	0.0035211317187849	0.3386515697375193	9
VDR	0.004080207143980576	0.33657289002557544	9
SLC10A2	0.003172183795530835	0.3281795511221945	9
ABCC8	0.008293344874377315	0.34722955145118733	9
ECE1	7.24E+11	0.3400516795865633	7
GC	0.002407660635094477	0.33657289002557544	6
DUT	0.009177617136336393	0.33451957295373663	6
ADAM17	6.88E+09	0.29949931725079654	2

Tabel S5. Topological features (Betweenness Centrality, Closeness Centrality, and Degree) of diseases from diabetic pharmacological network results.

Disease	Betweenness Centrality	Closeness Centrality	Degree
DM	0.11951793073401674	0.4544198895027624	47
Type 2 DM	0.05341449409434348	0.3875147232037691	31
Type 1 DM	0.003480093660947009	0.29639639639639637	11
DM Complications	3.14E+12	0.2655367231638418	4
Monogenic Diabetes	6.30E+10	0.265751211631664	3
Gestational Diabetes	3.60E+11	0.2781065088757396	3
Maturity Onset DM in Young	1.69E+11	0.2596685082872928	2
Prediabetes Syndrome	0.0	0.26813365933170336	1
Neonatal DM	0.0	0.25783699059561127	1
DM, Permanent Neonatal	0.0	0.25783699059561127	1

Table S6. Topological features (Betweenness Centrality, Closeness Centrality, and Degree) of diseases pathway from diabetic pharmacological network results.

Pathway	Betweenness Centrality	Closeness Centrality	Degree
Signal Transduction	0.06308894669154795	0.4306282722513089	29
Metabolism of lipids and lipoproteins	0.017423401686684593	0.3437826541274817	22
Generic Transcription Pathway	0.014017672095473459	0.3518716577540107	17
Gene Expression	0.014017672095473459	0.3518716577540107	17
Pathways in cancer	0.01768967538272527	0.38888888888888884	16
Immune System	0.014129637489190298	0.3812282734646582	14
Cytokine Signaling in Immune system	0.01089168330325434	0.3751425313568985	12
Signaling by GPCR	0.007808127205744808	0.3316532258064516	12
Metabolic pathways	0.0024381391492334756	0.28608695652173916	12
Developmental Biology	0.008765431603000199	0.35074626865671643	11
Nuclear Receptor transcription pathway	7.49E+11	0.28023850085178875	11
Signaling by Interleukins	0.008528109705876226	0.3704954954954955	10
GPCR ligand binding	8.53E+11	0.27554438860971525	10
GPCR downstream signaling	0.004542687218409322	0.3172613307618129	10
Class A/1 (Rhodopsin-like receptors)	6.70E+11	0.274395329441201	9
Fatty acid, triacylglycerol, and ketone body metabolism	6.01E+11	0.281437125748503	8
Proteoglycans in cancer	0.005251391092309827	0.3619361936193619	8
PI3K-Akt signaling	0.004982587053076012	0.3448637316561845	8
Endocrine resistance	0.005021780807196435	0.3564463705308776	8
Neuroactive ligand-receptor interaction	4.24E+12	0.2730290456431535	8
Metabolism of proteins	0.004392523823349113	0.3063314711359404	8
Interleukin-4 and 13 signaling	0.0031841380040702224	0.32097560975609757	7
Insulin resistance	0.003967779300121182	0.33640081799591	7
AMPK signaling pathway	0.0034990366597006765	0.3194174757281553	7
Innate Immune System	0.004663600594245575	0.35414424111948334	7
Gastrin-CREB signalling pathway via PKC and MAPK	0.0037840215150606003	0.3244575936883629	7
Hemostasis	0.005133186016901093	0.3395252837977296	6
Fluid shear stress and atherosclerosis	0.0033389504790249606	0.34522560335781743	6
PPAR signaling pathway	1.04E+12	0.27145214521452143	6
MicroRNAs in cancer	0.003649173825179364	0.35262593783494106	6
HIF-1 signaling pathway	0.0038507819310452888	0.338477366255144	6
Phase 1 - Functionalization of compounds	2.69E+11	0.271004942339374	6

Biological oxidations	2.69E+11	0.271004942339374	6
Transcriptional regulation of white adipocyte differentiation	0.0014265272220988859	0.2916666666666667	6
HTLV-I infection	0.006194714534783509	0.3518716577540107	6
Hepatitis B	0.00458790556933425	0.3488865323435843	6
Breast cancer	0.0036050935990043676	0.35149572649572647	6
AGE-RAGE signaling pathway in diabetic complications	0.004062897490941818	0.3319878910191726	6
G alpha (q) signalling events	0.0021004157409597367	0.3097928436911488	6
Calcium signaling pathway	0.0011005905056927082	0.29773755656108597	6
Platelet activation	0.0025548392582026326	0.3136320305052431	5
Longevity regulating	0.0018268412875348994	0.335030549898167	5
Non-alcoholic fatty liver disease (NAFLD)	0.0023516934457099045	0.3299899699097292	5
Chagas disease (American trypanosomiasis)	0.0026078697535849337	0.3263888888888889	5
Regulation of lipid metabolism by PPARalpha	7.94E+10	0.2707818930041152	5
PPARA activates gene expression	7.94E+10	0.2707818930041152	5
Signaling by SCF-KIT	0.002137415252553048	0.34270833333333334	5
Hepatitis C	0.00425541127590218	0.35838779956427014	5
Estrogen signaling pathway	0.0011908994643970773	0.3212890625	5
Central carbon metabolism in cancer	0.0033115114354330005	0.3459516298633018	5
Tuberculosis	0.0010232576331657322	0.2868352223190933	5
Cytochrome P450 - arranged by substrate type	2.03E+12	0.2698933552091879	5
Transcriptional misregulation in cancer	0.0011338323382771378	0.30834114339268975	5
Small cell lung cancer	0.003563493320099614	0.34093264248704663	5
Glioma	0.0029776008317763643	0.34558823529411764	5
Cellular responses to stress	0.0023979158262557817	0.31879844961240306	5
Bladder cancer	0.0020753903185968137	0.3206627680311891	5
Peptide ligand-binding receptors	1.02E+11	0.265751211631664	5
Prostate cancer	0.002816696360850278	0.34558823529411764	5
Metabolism of steroid hormones	1.49E+12	0.2668288726682887	5
Vesicle-mediated transport	0.0012784200997148123	0.3021120293847567	5
Circadian Clock	3.12E+12	0.2781065088757396	4
mTOR signalling	0.001250297329793753	0.320350535540409	4
Insulin signaling pathway	9.84E+11	0.3142311365807068	4
Apelin signaling pathway	6.77E+11	0.29012345679012347	4
Adipocytokine signaling pathway	7.82E+11	0.2990909090909091	4

Jak-STAT signaling pathway	9.41E+11	0.3178743961352657	4
IL-17 signaling pathway	5.56E+11	0.28884986830553117	4
Amoebiasis	0.0014258989708986055	0.3212890625	4
Regulation of cholesterol biosynthesis by SREBP (SREBF)	3.98E+09	0.26835236541598695	4
Bile secretion	3.31E+11	0.26835236541598695	4
Activation of gene expression by SREBF (SREBP)	3.98E+09	0.26835236541598695	4
Transcriptional Regulation by TP53	0.001178104572061989	0.30718954248366015	4
TP53 Regulates Metabolic Genes	0.001178104572061989	0.30718954248366015	4
Regulation of lipolysis in adipocytes	0.00122196124952179	0.30834114339268975	4
Thyroid hormone signaling pathway	0.0011320990936005127	0.3286713286713287	4
Signalling by NGF	0.001544908509131718	0.338477366255144	4
Signaling by Type 1 Insulin-like Growth Factor 1 Receptor (IGF1R)	8.80E+10	0.3206627680311891	4
Signaling by the B Cell Receptor (BCR)	0.001544908509131718	0.338477366255144	4
Signaling by PDGF	0.001544908509131718	0.338477366255144	4
Signaling by Insulin receptor	8.80E+10	0.3206627680311891	4
Signaling by EGFR	0.001544908509131718	0.338477366255144	4
Role of LAT2/NTAL/LAB on calcium mobilization	0.001544908509131718	0.338477366255144	4
PIP3 activates AKT signaling	0.001544908509131718	0.338477366255144	4
NGF signalling via TRKA from the plasma membrane	0.001544908509131718	0.338477366255144	4
MAPK signaling	0.002476039759506317	0.32899999999999996	4
IRS-related events triggered by IGF1R	8.80E+10	0.3206627680311891	4
IRS-mediated signalling	8.80E+10	0.3206627680311891	4
Insulin receptor signalling cascade	8.80E+10	0.3206627680311891	4
IGF1R signaling cascade	8.80E+10	0.3206627680311891	4
GAB1 signalosome	0.001544908509131718	0.338477366255144	4
FoxO signaling pathway	0.0016329415767662937	0.3286713286713287	4
Fc epsilon receptor (FCERI) signaling	0.001544908509131718	0.338477366255144	4
Downstream signal transduction	0.001544908509131718	0.338477366255144	4
Downstream signaling events of B Cell Receptor (BCR)	0.001544908509131718	0.338477366255144	4
Diseases of signal transduction	0.00232780240307077	0.31879844961240306	4
DAP12 signaling	0.001544908509131718	0.338477366255144	4
DAP12 interactions	0.001544908509131718	0.338477366255144	4
Choline metabolism in cancer	0.004469442361331505	0.320350535540409	4
Axon guidance	8.38E+11	0.31695568400770713	4

Adaptive Immune System	0.001544908509131718	0.338477366255144	4
Metabolism of vitamins and cofactors	3.40E+12	0.27011494252873564	4
Steroid hormone biosynthesis	1.28E+11	0.2648953301127214	4
Osteoclast differentiation	8.32E+11	0.31665062560153995	4
Hematopoietic cell lineage	3.65E+10	0.2811965811965812	4
Cytokine-cytokine receptor interaction	0.0010917512474177722	0.3051948051948052	4
Rap1 signaling pathway	6.14E+11	0.3172613307618129	4
cAMP signaling pathway	0.0010395324837773562	0.3115530303030303	4
Signaling by PTK6	0.00130224868186015	0.3018348623853211	4
Pancreatic cancer	0.0024308012522269444	0.3412863070539419	4
Non-small cell lung cancer	0.0024308012522269444	0.3412863070539419	4
Melanoma	0.0024308012522269444	0.3412863070539419	4
Measles	0.0024855008570865535	0.33743589743589747	4
Peptide hormone metabolism	1.68E+12	0.26835236541598695	4
Phospholipase D signaling pathway	0.001976033867388837	0.320350535540409	4
Membrane Trafficking	0.0011142557777833937	0.30128205128205127	4
Sphingolipid signaling pathway	0.0015335564322318965	0.3326592517694641	3
Signaling by MET	5.43E+11	0.30406654343807765	3
Apoptosis	0.0015335564322318965	0.3326592517694641	3
BMAL1:CLOCK,NPAS2 activates circadian gene expression	9.96E+09	0.27011494252873564	3
Leishmaniasis	2.45E+11	0.2821612349914237	3
Type II diabetes mellitus	7.73E+11	0.31483253588516746	3
Regulation of TP53 Activity	5.38E+11	0.3015582034830431	3
PI3K Cascade	3.68E+11	0.30718954248366015	3
PI3K/AKT activation	7.66E+11	0.3231827111984283	3
Autophagy - animal	3.68E+11	0.30718954248366015	3
Acute myeloid leukemia	6.39E+11	0.3089201877934272	3
Leukocyte transendothelial migration	3.51E+11	0.3023897058823529	3
Extracellular matrix organization	2.33E+12	0.26967213114754096	3
Toll-like receptor signaling pathway	9.44E+11	0.31513409961685823	3
TNF signaling	2.25E+12	0.2816780821917808	3
Pertussis	2.18E+12	0.28313253012048195	3
Interleukin-10 signaling	3.33E+12	0.28484848484848485	3
Influenza A	9.44E+11	0.31513409961685823	3

Hypertrophic cardiomyopathy (HCM)	4.11E+11	0.2868352223190933	3
Herpes simplex infection	0.0010730128093579367	0.3051948051948052	3
Glucagon signaling	1.83E+12	0.2757753562447611	3
Integration of energy metabolism	2.77E+11	0.27508361204013376	3
Lipid digestion, mobilization, and transport	3.85E+10	0.2621513944223108	3
VEGFA-VEGFR2 Pathway	3.92E+12	0.31573896353166986	3
Signaling by VEGF	3.92E+12	0.31573896353166986	3
Signaling by ERBB4	5.20E+09	0.31665062560153995	3
Oxytocin signaling pathway	7.03E+11	0.3015582034830431	3
ErbB signaling pathway	3.92E+12	0.31573896353166986	3
Endometrial cancer	0.0012080123049037599	0.33434959349593496	3
Serotonergic synapse	5.87E+11	0.2687908496732026	3
Chemical carcinogenesis	5.44E+10	0.2692307692307692	3
Arachidonic acid metabolism	5.87E+11	0.2687908496732026	3
Metabolism of fat-soluble vitamins	8.15E+10	0.26131850675139	3
Prolactin signaling pathway	7.65E+10	0.30718954248366015	3
Ovarian steroidogenesis	3.67E+10	0.2687908496732026	3
Glucocorticoid biosynthesis	5.74E+09	0.26425702811244983	3
Endogenous sterols	1.81E+10	0.265751211631664	3
C21-Steroid hormone biosynthesis	5.74E+09	0.26425702811244983	3
Ras signaling pathway	3.22E+12	0.3115530303030303	3
Regulation of actin cytoskeleton	6.51E+11	0.3160422670509126	3
G alpha (i) signalling events	5.54E+09	0.26596604688763137	3
Viral carcinogenesis	0.0013401739645014865	0.3260654112983152	3
T cell receptor signaling pathway	0.00130541606174795	0.31756756756756754	3
p53 signaling pathway	0.001277823185091968	0.29693140794223827	3
Chronic myeloid leukemia	0.0013401739645014865	0.3260654112983152	3
Cellular Senescence	0.001060935232704298	0.3029465930018416	3
Cell cycle	0.001229162647551283	0.2974683544303797	3
Clathrin-mediated endocytosis	6.40E+11	0.2921847246891652	3
Cargo recognition for clathrin-mediated endocytosis	6.40E+11	0.2921847246891652	3
Post-translational protein modification	4.30E+11	0.2927046263345196	3
Deubiquitination	4.30E+11	0.2927046263345196	3
Amyotrophic lateral sclerosis (ALS)	5.49E+11	0.2996357012750455	2

Regulation of IFNG signaling	2.78E+09	0.26425702811244983	2
Negative regulation of MET activity	2.78E+09	0.26425702811244983	2
Interferon gamma signaling	2.78E+09	0.26425702811244983	2
NF-kappa B signaling pathway	1.33E+12	0.27905004240882103	2
Synthesis of Prostaglandins (PG) and Thromboxanes (TX)	1.59E+10	0.2668288726682887	2
Regulation of TP53 Activity through Phosphorylation	3.33E+12	0.29533213644524237	2
Thyroid cancer	1.68E+12	0.2919254658385093	2
Huntington's disease	1.68E+12	0.2919254658385093	2
Wnt signaling	3.31E+12	0.2914083259521701	2
Import of palmitoyl-CoA into the mitochondrial matrix	5.30E+11	0.271900826446281	2
Organelle biogenesis and maintenance	4.56E+10	0.2730290456431535	2
Mitochondrial biogenesis	4.56E+10	0.2730290456431535	2
VEGF signaling pathway	4.10E+11	0.30547818012999073	2
TNF signaling	4.10E+11	0.30547818012999073	2
Platinum drug resistance	5.21E+11	0.31879844961240306	2
Neurotrophin signaling pathway	5.21E+11	0.31879844961240306	2
Natural killer cell mediated cytotoxicity	4.63E+12	0.3095014111006585	2
Fc epsilon RI signaling pathway	4.63E+12	0.3095014111006585	2
Epstein-Barr virus infection	5.21E+11	0.31879844961240306	2
Colorectal cancer	5.21E+11	0.31879844961240306	2
Recycling of bile acids and salts	6.89E+10	0.25703125	2
Bile acid and bile salt metabolism	6.89E+10	0.25703125	2
Toxoplasmosis	8.41E+10	0.2778716216216216	2
Regulation of TP53 Degradation	1.62E+12	0.29533213644524237	2
PKB-mediated events	4.39E+10	0.27834179357022	2
PI3K/AKT Signaling in Cancer	8.31E+10	0.3018348623853211	2
Macroautophagy	4.39E+10	0.27834179357022	2
Energy dependent regulation of mTOR by LKB1-AMPK	4.39E+10	0.27834179357022	2
EGFR tyrosine kinase inhibitor resistance	8.31E+10	0.3018348623853211	2
Costimulation by the CD28 family	8.31E+10	0.3018348623853211	2
CD28 dependent PI3K/Akt signaling	8.31E+10	0.3018348623853211	2
CD28 co-stimulation	8.31E+10	0.3018348623853211	2
EPH-Ephrin signaling	5.01E+09	0.26425702811244983	2
Degradation of the extracellular matrix	5.01E+09	0.26425702811244983	2

Collagen degradation	5.01E+09	0.26425702811244983	2
Activation of Matrix Metalloproteinases	5.01E+09	0.26425702811244983	2
Renin-angiotensin system	5.76E+09	0.2556332556332557	2
Neutrophil degranulation	3.84E+11	0.2653225806451613	2
Metabolism of Angiotensinogen to Angiotensins	5.76E+09	0.2556332556332557	2
Alzheimer's disease	1.10E+12	0.27416666666666667	2
Th17 cell differentiation	1.71E+12	0.2843560933448574	2
Salmonella infection	7.72E+10	0.27554438860971525	2
Rheumatoid arthritis	5.73E+10	0.2774030354131535	2
NOD-like receptor signaling pathway	5.73E+10	0.2774030354131535	2
Malaria	5.73E+10	0.2774030354131535	2
Legionellosis	5.73E+10	0.2774030354131535	2
Inflammatory bowel disease (IBD)	5.73E+10	0.2774030354131535	2
Graft-versus-host disease	5.73E+10	0.2774030354131535	2
Antifolate resistance	5.73E+10	0.2774030354131535	2
African trypanosomiasis	5.73E+10	0.2774030354131535	2
Aldosterone-regulated sodium reabsorption	2.66E+11	0.3021120293847567	2
Hormone-sensitive lipase (HSL)-mediated triacylglycerol hydrolysis	4.86E+08	0.2615262321144674	2
Ovarian tumor domain proteases	1.32E+12	0.2903795233892321	2
Endocrine and other factor-regulated calcium reabsorption	1.73E+11	0.26383319967923013	2
TFAP2 (AP-2) family regulates transcription	1.22E+12	0.2893579595426561	2
Signaling by Ligand-Responsive EGFR Variants in Cancer	2.17E+12	0.31067044381491976	2
Signaling by ERBB2	2.17E+12	0.31067044381491976	2
Signaling by EGFRvIII in Cancer	2.17E+12	0.31067044381491976	2
Signaling by EGFR in Cancer	2.17E+12	0.31067044381491976	2
RET signaling	2.17E+12	0.31067044381491976	2
PI5P, PP2A and IER3 Regulate PI3K/AKT Signaling	2.17E+12	0.31067044381491976	2
PI3K events in ERBB2 signaling	2.17E+12	0.31067044381491976	2
Negative regulation of the PI3K/AKT network	2.17E+12	0.31067044381491976	2
MAPK1/MAPK3 signaling	3.86E+11	0.295067264573991	2
Interleukin receptor SHC signaling	2.17E+12	0.31067044381491976	2
Interleukin-3, 5 and GM-CSF signaling	2.17E+12	0.31067044381491976	2
Interleukin-2 signaling	2.17E+12	0.31067044381491976	2
GnRH signaling pathway	1.20E+12	0.28809106830122594	2

Focal adhesion	2.17E+12	0.31067044381491976	2
EGFR TKI resistance	3.86E+11	0.295067264573991	2
Constitutive Signaling by Ligand-Responsive EGFR Cancer Variants	2.17E+12	0.31067044381491976	2
Constitutive Signaling by EGFRvIII	2.17E+12	0.31067044381491976	2
Constitutive Signaling by Aberrant PI3K in Cancer	2.17E+12	0.31067044381491976	2
Adherens junction	3.09E+12	0.29089301503094606	2
Renin secretion	1.70E+11	0.2621513944223108	2
cGMP-PKG signaling pathway	2.30E+09	0.25885129819040126	2
Vitamin D (calciferol) metabolism	4.21E+09	0.2546439628482972	2
C19/C18-Steroid hormone biosynthesis	1.56E+10	0.2632	2
Endocytosis	4.18E+10	0.2843560933448574	2
Retrograde endocannabinoid signaling	1.18E+11	0.26769731489015464	2
Cholinergic synapse	2.73E+12	0.3023897058823529	2
Tight junction	2.56E+11	0.27647058823529413	2
Oxidative Stress Induced Senescence	3.40E+11	0.2914083259521701	2
Oncogene Induced Senescence	3.40E+11	0.2914083259521701	2
Transmission across Chemical Synapses	6.45E+10	0.26446945337620575	2
Phospholipid metabolism	0.001036144303679151	0.3032258064516129	2
Neurotransmitter Clearance In The Synaptic Cleft	6.45E+10	0.26446945337620575	2
Neuronal System	6.45E+10	0.26446945337620575	2
Transmembrane transport of small molecules	2.95E+11	0.26446945337620575	2
G alpha (s) signalling events	3.78E+10	0.2632	2
Ub-specific processing proteases	2.85E+09	0.29063604240282687	2
Metabolism of carbohydrates	6.42E+10	0.2646822204344328	2
Vascular smooth muscle contraction	4.47E+09	0.2621513944223108	2
Mineral absorption	0.0	0.25191424196018375	1
Transcriptional activation of p53 responsive genes	0.0	0.2843560933448574	1
Transcriptional activation of cell cycle inhibitor p21	0.0	0.2843560933448574	1
TP53 regulates transcription of several additional cell death genes	0.0	0.2843560933448574	1
TP53 Regulates Transcription of Genes Involved in G2 Cell Cycle Arrest	0.0	0.2843560933448574	1
TP53 Regulates Transcription of Genes Involved in G1 Cell Cycle Arrest	0.0	0.2843560933448574	1
TP53 Regulates Transcription of Genes Involved in Cytochrome C Release	0.0	0.2843560933448574	1
TP53 Regulates Transcription of DNA Repair Genes	0.0	0.2843560933448574	1
TP53 Regulates Transcription of Death Receptors and Ligands	0.0	0.2843560933448574	1

TP53 Regulates Transcription of Cell Death Genes	0.0	0.2843560933448574	1
TP53 Regulates Transcription of Cell Cycle Genes	0.0	0.2843560933448574	1
TP53 Regulates Transcription of Caspase Activators and Caspases	0.0	0.2843560933448574	1
TP53 regulates transcription of additional cell cycle genes	0.0	0.2843560933448574	1
The role of GTSE1 in G2/M progression after G2 checkpoint	0.0	0.2843560933448574	1
SUMOylation	0.0	0.2843560933448574	1
SUMO E3 ligases SUMOylate target proteins	0.0	0.2843560933448574	1
Stabilization of p53	0.0	0.2843560933448574	1
Signaling by NOTCH	0.0	0.2843560933448574	1
Regulation of TP53 Expression	0.0	0.2843560933448574	1
Regulation of TP53 Activity through Methylation	0.0	0.2843560933448574	1
Regulation of TP53 Activity through Association with Co-factors	0.0	0.2843560933448574	1
Regulation of TP53 Activity through Acetylation	0.0	0.2843560933448574	1
Recruitment and ATM-mediated phosphorylation of repair and signaling proteins at DNA double strand breaks	0.0	0.2843560933448574	1
Protein folding	0.0	0.2843560933448574	1
Programmed Cell Death	0.0	0.2843560933448574	1
Pre-NOTCH Transcription and Translation	0.0	0.2843560933448574	1
Pre-NOTCH Expression and Processing	0.0	0.2843560933448574	1
PI5P Regulates TP53 Acetylation	0.0	0.2843560933448574	1
PI3K-AKT signaling	0.0	0.2843560933448574	1
p53-Dependent G1/S DNA damage checkpoint	0.0	0.2843560933448574	1
p53-Dependent G1 DNA Damage Response	0.0	0.2843560933448574	1
Mitotic G2-G2/M phases	0.0	0.2843560933448574	1
Mitophagy - animal	0.0	0.2843560933448574	1
Intrinsic Pathway for Apoptosis	0.0	0.2843560933448574	1
G2/M Transition	0.0	0.2843560933448574	1
G2/M DNA damage checkpoint	0.0	0.2843560933448574	1
G2/M Checkpoints	0.0	0.2843560933448574	1
G1/S DNA Damage Checkpoints	0.0	0.2843560933448574	1
Formation of Senescence-Associated Heterochromatin Foci (SAHF)	0.0	0.2843560933448574	1
Ferroptosis	0.0	0.2843560933448574	1
Factors involved in megakaryocyte development and platelet production	0.0	0.2843560933448574	1
DNA Repair	0.0	0.2843560933448574	1

DNA Double Strand Break Response	0.0	0.2843560933448574	1
DNA Damage/Telomere Stress Induced Senescence	0.0	0.2843560933448574	1
Chaperonin-mediated protein folding	0.0	0.2843560933448574	1
Basal cell carcinoma	0.0	0.2843560933448574	1
Autodegradation of the E3 ubiquitin ligase COP1	0.0	0.2843560933448574	1
Association of TriC/CCT with target proteins during biosynthesis	0.0	0.2843560933448574	1
Activation of PUMA and translocation to mitochondria	0.0	0.2843560933448574	1
Activation of NOXA and translocation to mitochondria	0.0	0.2843560933448574	1
Activation of BH3-only proteins	0.0	0.2843560933448574	1
Type I diabetes mellitus	0.0	0.27167630057803466	1
TNFR2 non-canonical NF-kB pathway	0.0	0.27167630057803466	1
TNFR1-mediated ceramide production	0.0	0.27167630057803466	1
TNFR1-induced proapoptotic signaling	0.0	0.27167630057803466	1
TNFR1-induced NFkappaB signaling pathway	0.0	0.27167630057803466	1
TGF-beta signaling pathway	0.0	0.27167630057803466	1
Systemic lupus erythematosus	0.0	0.27167630057803466	1
RIG-I-like receptor signaling pathway	0.0	0.27167630057803466	1
Regulation of TNFR1 signaling	0.0	0.27167630057803466	1
Dilated cardiomyopathy	0.0	0.27167630057803466	1
Death Receptor Signalling	0.0	0.27167630057803466	1
Asthma	0.0	0.27167630057803466	1
Antigen processing and presentation	0.0	0.27167630057803466	1
Allograft rejection	0.0	0.27167630057803466	1
Telomere Maintenance	0.0	0.2615262321144674	1
Telomere Extension By Telomerase	0.0	0.2615262321144674	1
TCF dependent signaling in response to WNT	0.0	0.2615262321144674	1
Signaling by Wnt	0.0	0.2615262321144674	1
Formation of the beta-catenin:TCF transactivating complex	0.0	0.2615262321144674	1
Extension of Telomeres	0.0	0.2615262321144674	1
Chromosome Maintenance	0.0	0.2615262321144674	1
Transport of glucose and other sugars	0.0	0.25946372239747634	1
SLC-mediated transmembrane transport	0.0	0.25946372239747634	1
Organic cation transport	0.0	0.25946372239747634	1
Organic cation/anion/zwitterion transport	0.0	0.25946372239747634	1

Norepinephrine Neurotransmitter Release Cycle	0.0	0.25946372239747634	1
Neurotransmitter Release Cycle	0.0	0.25946372239747634	1
Na+/Cl- dependent neurotransmitter transporters	0.0	0.25946372239747634	1
Abacavir transport and metabolism	0.0	0.25946372239747634	1
Transcriptional activity of SMAD2/SMAD3:SMAD4 heterotrimer	0.0	0.2617342879872713	1
SMAD2/SMAD3:SMAD4 heterotrimer regulates transcription	0.0	0.2617342879872713	1
Signaling by TGF-beta Receptor Complex	0.0	0.2617342879872713	1
Response to elevated platelet cytosolic Ca2+	0.0	0.2617342879872713	1
Platelet degranulation	0.0	0.2617342879872713	1
Hippo signaling pathway	0.0	0.2617342879872713	1
ECM proteoglycans	0.0	0.2617342879872713	1
Dissolution of Fibrin Clot	0.0	0.2617342879872713	1
Complement and coagulation cascades	0.0	0.2617342879872713	1
Triglyceride Biosynthesis	0.0	0.2617342879872713	1
Fatty Acyl-CoA Biosynthesis	0.0	0.2617342879872713	1
Fatty acid metabolism	0.0	0.2617342879872713	1
Biosynthesis of unsaturated fatty acids	0.0	0.2617342879872713	1
Visual phototransduction	0.0	0.25885129819040126	1
The canonical retinoid cycle in rods (twilight vision)	0.0	0.25885129819040126	1
Retinoid metabolism disease events	0.0	0.25885129819040126	1
Retinoid metabolism and transport	0.0	0.25885129819040126	1
Retinoid cycle disease events	0.0	0.25885129819040126	1
Diseases associated with visual transduction	0.0	0.25885129819040126	1
Regulation of IFNA signaling	0.0	0.26383319967923013	1
PTK6 Down-Regulation	0.0	0.26383319967923013	1
Platelet Aggregation	0.0	0.26383319967923013	1
Interferon alpha/beta signaling	0.0	0.26383319967923013	1
Integrin alphaIIb beta3 signaling	0.0	0.26383319967923013	1
Growth hormone receptor signaling	0.0	0.26383319967923013	1
Synthesis of 15-eicosatetraenoic acid derivatives	0.0	0.2655367231638418	1
Nicotinate metabolism	0.0	0.2655367231638418	1
Nicotinamide salvaging	0.0	0.2655367231638418	1
Metabolism of water-soluble vitamins and cofactors	0.0	0.2655367231638418	1
COX reactions	0.0	0.23516797712651896	1

Translocation of GLUT4 to the plasma membrane	0.0	0.2668288726682887	1
AMPK inhibits chREBP transcriptional activation activity	0.0	0.2668288726682887	1
Activation of PPARGC1A (PGC-1alpha) by phosphorylation	0.0	0.2668288726682887	1
The citric acid (TCA) cycle and respiratory electron transport	0.0	0.26277955271565495	1
Signaling by Retinoic Acid	0.0	0.26277955271565495	1
Regulation of pyruvate dehydrogenase (PDH) complex	0.0	0.26277955271565495	1
Pyruvate metabolism	0.0	0.26277955271565495	1
YAP1- and WWTR1 (TAZ)-stimulated gene expression	0.0	0.2648953301127214	1
Transcriptional activation of mitochondrial biogenesis	0.0	0.2648953301127214	1
RORA activates gene expression	0.0	0.2648953301127214	1
Tie2 Signaling	0.0	0.29612961296129614	1
TCR signaling	0.0	0.29612961296129614	1
Synthesis of PIPs at the plasma membrane	0.0	0.29612961296129614	1
Signaling pathways regulating pluripotency of stem cells	0.0	0.29612961296129614	1
Signaling by FGFR4	0.0	0.29612961296129614	1
Signaling by FGFR3	0.0	0.29612961296129614	1
Signaling by FGFR2	0.0	0.29612961296129614	1
Signaling by FGFR1	0.0	0.29612961296129614	1
Signaling by FGFR	0.0	0.29612961296129614	1
Signaling by cytosolic FGFR1 fusion mutants	0.0	0.29612961296129614	1
Role of phospholipids in phagocytosis	0.0	0.29612961296129614	1
Renal cell carcinoma	0.0	0.29612961296129614	1
Regulation of signaling by CBL	0.0	0.29612961296129614	1
Progesterone-mediated oocyte maturation	0.0	0.29612961296129614	1
PI Metabolism	0.0	0.29612961296129614	1
PI3K events in ERBB4 signaling	0.0	0.29612961296129614	1
PI-3K cascade:FGFR4	0.0	0.29612961296129614	1
PI-3K cascade:FGFR3	0.0	0.29612961296129614	1
PI-3K cascade:FGFR2	0.0	0.29612961296129614	1
PI-3K cascade:FGFR1	0.0	0.29612961296129614	1
PI3K-Akt signaling	0.0	0.29612961296129614	1
Phosphatidylinositol signaling system	0.0	0.29612961296129614	1
Nephrin interactions	0.0	0.29612961296129614	1
MET activates PI3K/AKT signaling	0.0	0.29612961296129614	1

Inositol phosphate metabolism	0.0	0.29612961296129614	1
Inflammatory mediator regulation of TRP channels	0.0	0.29612961296129614	1
GPVI-mediated activation cascade	0.0	0.29612961296129614	1
G-protein beta:gamma signalling	0.0	0.29612961296129614	1
G beta:gamma signalling through PI3Kgamma	0.0	0.29612961296129614	1
G alpha (12/13) signalling events	0.0	0.29612961296129614	1
FGFR1 mutant receptor activation	0.0	0.29612961296129614	1
Fc gamma R-mediated phagocytosis	0.0	0.29612961296129614	1
Fcgamma receptor (FCGR) dependent phagocytosis	0.0	0.29612961296129614	1
Downstream TCR signaling	0.0	0.29612961296129614	1
Downstream signaling of activated FGFR4	0.0	0.29612961296129614	1
Downstream signaling of activated FGFR3	0.0	0.29612961296129614	1
Downstream signaling of activated FGFR2	0.0	0.29612961296129614	1
Downstream signaling of activated FGFR1	0.0	0.29612961296129614	1
Chemokine signaling pathway	0.0	0.29612961296129614	1
Cell surface interactions at the vascular wall	0.0	0.29612961296129614	1
Cell-Cell communication	0.0	0.29612961296129614	1
Carbohydrate digestion and absorption	0.0	0.29612961296129614	1
B cell receptor signaling pathway	0.0	0.29612961296129614	1
Bacterial invasion of epithelial cells	0.0	0.29612961296129614	1
Signal amplification	0.0	0.2546439628482972	1
P2Y receptors	0.0	0.2546439628482972	1
Nucleotide-like (purinergic) receptors	0.0	0.2546439628482972	1
ADP signalling through P2Y purinoceptor 12	0.0	0.2546439628482972	1
PTK6 Expression	0.0	0.2617342879872713	1
Synthesis of bile acids and bile salts	0.0	0.25057121096725055	1
Trafficking of dietary sterols	0.0	0.2604908946951702	1
Fat digestion and absorption	0.0	0.2604908946951702	1
ROS, RNS production in phagocytes	0.0	0.26510878323932313	1
Platelet homeostasis	0.0	0.26510878323932313	1
Peroxisome	0.0	0.26510878323932313	1
Nitric oxide stimulates guanylate cyclase	0.0	0.26510878323932313	1
Arginine biosynthesis	0.0	0.26510878323932313	1
Arginine and proline metabolism	0.0	0.26510878323932313	1

VEGFR2 mediated vascular permeability	0.0	0.2723509933774835	1
Regulation of TP53 Expression	0.0	0.2723509933774835	1
mTORC1-mediated signalling	0.0	0.2723509933774835	1
HSF1-dependent transactivation	0.0	0.2723509933774835	1
Constitutive Signaling by AKT1 E17K in Cancer	0.0	0.2723509933774835	1
Collagen formation	0.0	0.2615262321144674	1
Assembly of collagen fibrils and other multimeric structures	0.0	0.2615262321144674	1
Regulation of IGF transport and uptake by IGFBPs	0.0	0.2604908946951702	1
Protein digestion and absorption	0.0	0.25503875968992246	1
Senescence pathways	0.0	0.26813365933170336	1
RAF-independent MAPK1/3 activation	0.0	0.26813365933170336	1
Prion diseases	0.0	0.26813365933170336	1
MAPK3 (ERK1) activation	0.0	0.26813365933170336	1
MAPK1 (ERK2) activation	0.0	0.26813365933170336	1
Intestinal immune network for IgA production	0.0	0.26813365933170336	1
Interleukin-6 signaling	0.0	0.26813365933170336	1
Interleukin-6 family signaling	0.0	0.26813365933170336	1
Cytosolic DNA-sensing pathway	0.0	0.26813365933170336	1
Metabolism of xenobiotics by cytochrome P450	0.0	0.2615262321144674	1
Regulation of gene expression in beta cells	0.0	0.2584446190102121	1
Regulation of beta-cell development	0.0	0.2584446190102121	1
Maturity onset diabetes of the young	0.0	0.2584446190102121	1
Terpenoid backbone biosynthesis	0.0	0.26236044657097285	1
Cholesterol biosynthesis	0.0	0.26236044657097285	1
C5 isoprenoid biosynthesis, mevalonate pathway	0.0	0.26236044657097285	1
Glucagon-type ligand receptors	0.0	0.2598736176935229	1
Class B/2 (Secretin family receptors)	0.0	0.2598736176935229	1
Pentose phosphate pathway (Pentose phosphate cycle)	0.0	0.26256983240223464	1
Pentose phosphate pathway, oxidative phase, glucose 6P => ribulose 5P	0.0	0.26256983240223464	1
Pentose phosphate pathway (hexose monophosphate shunt)	0.0	0.26256983240223464	1
Pentose phosphate pathway	0.0	0.26256983240223464	1
Glutathione metabolism	0.0	0.26256983240223464	1
Carbon metabolism	0.0	0.26256983240223464	1
Synthesis, secretion, and inactivation of GIP	0.0	0.26111111111111107	1

Synthesis, secretion, and inactivation of GLP-1	0.0	0.26111111111111107	1
Regulation of insulin secretion	0.0	0.26111111111111107	1
Insulin secretion	0.0	0.26111111111111107	1
Incretin synthesis, secretion, and inactivation	0.0	0.26111111111111107	1
Free fatty acids regulate insulin secretion	0.0	0.26111111111111107	1
Free fatty acid receptors	0.0	0.26111111111111107	1
Fatty Acids bound to GPR40 (FFAR1) regulate insulin secretion	0.0	0.26111111111111107	1
Nuclear signaling by ERBB4	0.0	0.26298960831334933	1
VEGFR2 proliferation	0.0	0.28313253012048195	1
SOS-mediated signalling	0.0	0.28313253012048195	1
Signal transduction by L1	0.0	0.28313253012048195	1
Signalling to RAS	0.0	0.28313253012048195	1
Signalling to p38 via RIT and RIN	0.0	0.28313253012048195	1
Signalling to ERKs	0.0	0.28313253012048195	1
Signaling by Overexpressed Wild-Type EGFR in Cancer	0.0	0.28313253012048195	1
Signaling by Leptin	0.0	0.28313253012048195	1
SHC1 events in ERBB2 signaling	0.0	0.28313253012048195	1
SHC1 events in EGFR signaling	0.0	0.28313253012048195	1
RAF/MAP kinase cascade	0.0	0.28313253012048195	1
PTK6 promotes HIF1A stabilization	0.0	0.28313253012048195	1
Prolonged ERK activation events	0.0	0.28313253012048195	1
PLCG1 events in ERBB2 signaling	0.0	0.28313253012048195	1
NCAM signaling for neurite out-growth	0.0	0.28313253012048195	1
L1CAM interactions	0.0	0.28313253012048195	1
Inhibition of Signaling by Overexpressed EGFR	0.0	0.28313253012048195	1
GRB2 events in ERBB2 signaling	0.0	0.28313253012048195	1
GRB2 events in EGFR signaling	0.0	0.28313253012048195	1
Gap junction	0.0	0.28313253012048195	1
Frs2-mediated activation	0.0	0.28313253012048195	1
FCERI mediated MAPK activation	0.0	0.28313253012048195	1
ERBB2 Regulates Cell Motility	0.0	0.28313253012048195	1
Epithelial cell signaling in Helicobacter pylori infection	0.0	0.28313253012048195	1
EGFR Transactivation by Gastrin	0.0	0.28313253012048195	1
EGFR interacts with phospholipase C-gamma	0.0	0.28313253012048195	1

EGFR downregulation	0.0	0.28313253012048195	1
Downregulation of ERBB2 signaling	0.0	0.28313253012048195	1
Dorso-ventral axis formation	0.0	0.28313253012048195	1
ARMS-mediated activation	0.0	0.28313253012048195	1
Melanogenesis	0.0	0.2562305295950156	1
Pyrimidine metabolism	0.0	0.2507621951219512	1
Pyrimidine biosynthesis	0.0	0.2507621951219512	1
Metabolism of nucleotides	0.0	0.2507621951219512	1
Xenobiotics	0.0	0.2617342879872713	1
Synthesis of epoxy (EET) and dihydroxyeicosatrienoic acids (DHET)	0.0	0.2617342879872713	1
Synthesis of (16-20)-hydroxyeicosatetraenoic acids (HETE)	0.0	0.2617342879872713	1
Linoleic acid metabolism	0.0	0.2617342879872713	1
Drug metabolism - cytochrome P450	0.0	0.2617342879872713	1
CYP2E1 reactions	0.0	0.2617342879872713	1
Steroid biosynthesis	0.0	0.25444702242846096	1
Cholecalciferol biosynthesis	0.0	0.25444702242846096	1
Estrogen biosynthesis	0.0	0.2621513944223108	1
Androgen biosynthesis	0.0	0.26256983240223464	1
Muscarinic acetylcholine receptors	0.0	0.26111111111111107	1
Amine ligand-binding receptors	0.0	0.26111111111111107	1
Ubiquitin-dependent degradation of Cyclin D1	0.0	0.26277955271565495	1
Ubiquitin-dependent degradation of Cyclin D	0.0	0.26277955271565495	1
S Phase	0.0	0.26277955271565495	1
Senescence-Associated Secretory Phenotype (SASP)	0.0	0.26277955271565495	1
SCF(Skp2)-mediated degradation of p27/p21	0.0	0.26277955271565495	1
RMTs methylate histone arginines	0.0	0.26277955271565495	1
PTK6 Regulates Cell Cycle	0.0	0.26277955271565495	1
Mitotic G1-G1/S phases	0.0	0.26277955271565495	1
Meiotic recombination	0.0	0.26277955271565495	1
Meiosis	0.0	0.26277955271565495	1
G1/S Transition	0.0	0.26277955271565495	1
G1 Phase	0.0	0.26277955271565495	1
Cyclin E associated events during G1/S transition	0.0	0.26277955271565495	1
Cyclin D associated events in G1	0.0	0.26277955271565495	1

Cyclin A:Cdk2-associated events at S phase entry	0.0	0.26277955271565495	1
Chromatin organization	0.0	0.26277955271565495	1
Chromatin modifying enzymes	0.0	0.26277955271565495	1
Gastric acid secretion	0.0	0.2521072796934866	1
Synthesis, secretion, and deacylation of Ghrelin	0.0	0.26069730586370843	1
Synthesis of PC	0.0	0.26069730586370843	1
Glycerophospholipid biosynthesis	0.0	0.26069730586370843	1
Vasopressin regulates renal water homeostasis via Aquaporins	0.0	0.2600790513833992	1
Vasopressin-regulated water reabsorption	0.0	0.2600790513833992	1
Vasopressin-like receptors	0.0	0.2600790513833992	1
SLC transporter disorders	0.0	0.2600790513833992	1
Disorders of transmembrane transporters	0.0	0.2600790513833992	1
Defective AVP causes NDI	0.0	0.2600790513833992	1
Aquaporin-mediated transport	0.0	0.2600790513833992	1
Signaling by Rho GTPases	0.0	0.26256983240223464	1
RHO GTPases activate PKNs	0.0	0.26256983240223464	1
RHO GTPase Effectors	0.0	0.26256983240223464	1
Oocyte meiosis	0.0	0.26256983240223464	1
Activated PKN1 stimulates transcription of AR	0.0	0.26256983240223464	1
Pregnenolone biosynthesis	0.0	0.25885129819040126	1
Pentose and glucuronate interconversions	0.0	0.25885129819040126	1
Glycerolipid metabolism	0.0	0.25885129819040126	1
Galactose metabolism	0.0	0.25885129819040126	1
Fructose metabolism	0.0	0.25885129819040126	1
Fructose biosynthesis	0.0	0.25885129819040126	1

Table S7. Topology features (Betweenness Centrality, Closeness Centrality, and Degree) of protein-protein interactions related to diabetic from network results.

Target	**Betweenness Centrality**	**Closeness Centrality**	**Degree**
IL6	0.1381421829486726	0.7590361445783133	43
TNF	0.12371863048142633	0.7325581395348837	41
PPARG	0.10110316008327061	0.7411764705882352	41
TP53	0.028820728434824087	0.6363636363636364	29
PPARA	0.07787587941352304	0.6363636363636364	28
PTGS2	0.06699414852269733	0.6237623762376238	27

REN	0.028815026443161723	0.63	27
EGFR	0.032934510520416085	0.6176470588235294	26
ESR1	0.015481154391247207	0.6116504854368933	25
MMP9	0.012364329617339754	0.6116504854368933	25
HMGCR	0.035560127343249086	0.6116504854368933	24
AGTR1	0.06947276022864865	0.5779816513761468	22
MTOR	0.00855929882369915	0.5779816513761468	21
NR3C1	0.013920783582336662	0.5727272727272728	19
MMP2	0.005615370993725807	0.5727272727272728	18
HNF4A	0.02119861356347412	0.5575221238938053	18
AR	0.004163830676405386	0.5575221238938053	18
CYP19A1	0.014972958512310734	0.5575221238938053	18
PPARD	0.009025397954293544	0.5575221238938053	17
CDK4	0.0017982492560065524	0.525	15
SERPINE1	0.0035497032317147333	0.5526315789473684	15
CYP27B1	0.01833260054868795	0.5478260869565218	15
NR1H4	0.010546512102653558	0.5338983050847458	14
TERT	7.26E+11	0.525	13
NOS2	0.007852841344837462	0.525	12
FABP4	0.005810196743146044	0.525	12
CYP2C19	0.019429301338511524	0.49606299212598426	12
NR1I2	0.02432192361014312	0.5294117647058824	12
SCD	0.0022205559016974835	0.525	12
SREBF2	0.002238227163541004	0.525	12
PIK3CA	5.64E+11	0.5080645161290323	11
G6PD	0.019854557833792138	0.5338983050847458	11
PTGS1	0.002013858807285456	0.5163934426229508	10
CSF1R	0.0012884495603389613	0.504	10
PTPN1	0.0147123614131385	0.5121951219512195	10
CYP17A1	0.0030337244526304286	0.4921875	9
HSD11B1	0.00394028573064669	0.5	9
AKR1B1	0.0014981136829595252	0.525	9
EDNRA	0.005875810680809337	0.4921875	8
ADAM17	5.36E+10	0.5	8

HSD11B2	0.0035036159962327372	0.47368421052631576	8
SLC10A2	0.007996865411845452	0.44366197183098594	8
MME	6.41E+11	0.49606299212598426	8
RBP4	0.0024696244226380063	0.4921875	7
P2RY12	0.002480557199220818	0.49606299212598426	7
NPC1L1	8.30E+10	0.4632352941176471	6
EDNRB	0.0031627221500029703	0.4809160305343511	6
FABP3	3.54E+12	0.4666666666666667	6
NR1I3	8.11E+11	0.42	5
GC	7.71E+10	0.4809160305343511	5
GCGR	0.002006834816979248	0.4666666666666667	5
FFAR1	0.003269061844727928	0.48461538461538456	5
CNR1	2.22E+12	0.504	5
AVPR2	0.0012308105603488272	0.411764705882353	5
BCHE	2.68E+11	0.4632352941176471	4
PRKAA2	0.0	0.45652173913043476	4
PTPN2	0.003296665099773438	0.44999999999999996	4
ECE1	2.30E+12	0.4012738853503185	4
SLC22A1	1.68E+12	0.3727810650887574	3
ABCC8	3.58E+12	0.44366197183098594	3
ACP1	4.75E+12	0.3620689655172414	3
CHRM2	9.12E+11	0.4632352941176471	3
DUT	0.0	0.391304347826087	1
CCKBR	0.0	0.3684210526315789	1

Table S8. Topological features (Betweenness Centrality, Closeness Centrality, and Degree) of compounds from breast cancer pharmacological network results.

Compound	Betweenness Centrality	Closeness Centrality	Degree
9804114	0.010444607957830783	0.3618507202095155	34
14021541	0.04076512498133304	0.4188984335522991	33
70683988	0.01119102352388005	0.3571736320551486	32
10323147	0.027000546777136737	0.4118231495280676	32
9981416	0.008638055146909273	0.35594675826534994	31
10323148	0.01683252178594518	0.38648018648018645	30
11048975	0.008298715610779045	0.357481673134972	29
11970027	0.009177392004553218	0.354122170012815	29
85082262	0.00572452443650379	0.3435557397430585	28
15513441	0.0056413514106829635	0.34185567010309276	27
472768	0.0054610611763558185	0.34129271305063813	27
10434225	0.00583617707094697	0.3449854348730753	27
10790564	0.005266760404833572	0.3415739596209312	27
159970	0.005306214434118055	0.34101192924722334	26
78101312	0.004569772286534708	0.33850551245406285	25

Tabel S9. Topological features (Betweenness Centrality, Closeness Centrality, and Degree) of targets from breast cancer pharmacological network results.

Target	Betweenness Centrality	Closeness Centrality	Degree
MAPK3	0.24248929858223459	0.4275399690562145	243
PIK3CA	0.14173635894006784	0.39913336543091	174
TP53	0.12217677041553589	0.3854021385402138	137
PRKCA	0.12181497407089445	0.3829099307159353	130
EGFR	0.07229532627132186	0.37871174052078577	126
EP300	0.1082516583286339	0.3749434644957033	107
MAPK14	0.062170886609427795	0.3719156572454015	105
MDM2	0.03459772078214465	0.36632788334069816	81
MTOR	0.030200839499041645	0.36122004357298476	76
TNF	0.05049983786722306	0.3631187034603592	71
HDAC1	0.046483120931449094	0.3550321199143469	60
IL6	0.03051422808958474	0.3584089926502378	57
PLA2G4A	0.04924176002271246	0.3565591397849462	54
CDK4	0.034922321277293784	0.35261590812420246	49
PRKAA2	0.023834671382206025	0.35594675826534994	49
PTGS2	0.023749092824579227	0.3550321199143469	45
NOS2	0.01709639479390144	0.35381988903115663	41
PPARG	0.009492992551888946	0.3523161920951976	36
PTPN1	0.022438879015970394	0.3520169851380042	35
ABL1	0.020715830322803535	0.3490526315789474	34
ESR1	0.00617282615212386	0.3514200932598559	33
MMP9	0.008295995804128242	0.3452728029987505	32
ALOX5	0.009174987696435793	0.3511224057602711	32
AGTR1	0.010676283283573318	0.350825222175201	31
CYP17A1	0.013425355494006972	0.350825222175201	31
PSEN2	0.02011099368897203	0.3499366821443647	30
CDC25B	0.016062617945397265	0.34729786342689567	30
AR	0.008245578469063855	0.35052854122621563	30
CDK6	0.007315242368484565	0.3376782077393075	29
MMP2	0.006198866821139588	0.34758909853249476	29
ADAM17	0.015397746801771646	0.3435557397430585	28
CYP19A1	0.010266943172127844	0.3499366821443647	28

SLC6A3	0.020034433508229647	0.3490526315789474	27
PTGER1	0.006442441853221685	0.3467168548724383	27
SERPINE1	0.016739922691871675	0.34613778705636744	26
KDR	0.014130832736134623	0.3464270789803594	25
CYP2C19	0.014940338763569037	0.3244618395303327	25
TOP2A	0.0052648183810081045	0.3415739596209312	25
PGR	0.0025800655206036165	0.3490526315789474	25
TERT	0.011848942762444173	0.34584897788902796	25
NR3C1	0.0053986873375691325	0.3490526315789474	25
ESR2	0.0015714393137820156	0.3487589398401346	24
HSD11B1	0.006975877408578266	0.3487589398401346	24
AVPR2	0.022208762239957724	0.34700711594809547	23
MMP1	0.006903113898217705	0.3484657419083648	23
MMP3	0.004694754089637411	0.34788082249265634	23
FABP4	0.00655425151156488	0.3484657419083648	23
CTSD	0.013645240877993046	0.34817303653926923	22
EDNRA	0.004339748704549688	0.34788082249265634	21
SMO	0.023812203501746856	0.34298717418287133	20
SREBF2	0.006668026589117942	0.3379535262943335	20
FAAH	9.98E+11	0.34758909853249476	20
TOP1	0.0017698788341780013	0.32471602036819425	18
PTGFR	0.003387478994465238	0.3421378456458935	16
F10	0.022297305066947225	0.33989339893398934	15
CSF1R	0.0010169250121196917	0.33467904723455794	14
ALOX5AP	0.0019965392639415057	0.3242080563159953	13
KEAP1	0.005475301495655343	0.3319983980776932	12
MMP8	7.02E+11	0.33387031816351187	10
VDR	0.0028343928780000887	0.34412619344126194	9
MMP14	4.77E+11	0.33279807306302694	8
THRB	3.38E+12	0.3231968810916179	8

Tabel S10. Topological features (Betweenness Centrality, Closeness Centrality, and Degree) of diseases from breast cancer pharmacological network results.

Disease	Betweenness Centrality	Closeness Centrality	Degree
Breast Cancer	0.050457089507989904	0.4628699050809603	39
Malignant neoplasm of breast	0.03725427946431391	0.38975082275505407	31
Breast Carcinoma	0.0013075922723243558	0.3242080563159953	7
Ductal Breast Carcinoma	2.17E+11	0.2654498879282741	3
Adenocarcinoma of breast	1.89E+12	0.3031078610603291	2
Breast Neoplasms	3.25E+10	0.2713584288052373	2
Triple Negative Breast Neoplasms	4.90E+09	0.26159671820763647	2

Tabel S11. Topological features (Betweenness Centrality, Closeness Centrality, and Degree) of pathway from breast cancer pharmacological network results.

Pathway	Betweenness Centrality	Closeness Centrality	Degree
Signal Transduction	0.05545453875847384	0.4618384401114206	34
Immune System	0.022365217454072543	0.42188295165394407	25
Pathways in cancer	0.022702347446076347	0.42360756259580995	25
Gene Expression	0.01130988081718405	0.38756428237494156	19
Generic Transcription Pathway	0.006492149489011145	0.3553364766395199	17
Cytokine Signaling in Immune system	0.007067022745365119	0.3692650334075724	16
Developmental Biology	0.012477720454443402	0.39270487920416863	16
Innate Immune System	0.009988708630290572	0.3953266571292322	15
Metabolism of lipids and lipoproteins	0.006771888307679431	0.33387031816351187	15
Hemostasis	0.01879103949650849	0.40340632603406323	14
Proteoglycans in cancer	0.008558577755077505	0.38504412447747327	14
Signaling by Interleukins	0.005050438514935272	0.36280087527352295	14
Metabolism	0.005177205988596745	0.31872356785851597	13
MicroRNAs in cancer	0.008075130466390527	0.3763050385837494	13
Endocrine resistance	0.0037995680135201764	0.36343708899605437	12
Metabolism of proteins	0.0036799922927611218	0.309212980231257	12
Signaling by GPCR	0.0072983412605552725	0.3553364766395199	12
Extracellular matrix organization	0.0019126436003238912	0.295122819508722	11
PI3K-AKT signaling	0.00486698319537881	0.36407553798858144	11
Signalling by NGF	0.00747016535142685	0.38361869504858864	11
AGE-RAGE signaling pathway in diabetic complications	0.0048090919390997066	0.36280087527352295	10
Axon guidance	0.0048638261290342676	0.35442496793501493	10
Breast cancer	0.0025195662823979752	0.3520169851380042	10
Cellular responses to stress	0.004600488547634091	0.36122004357298476	10
Hepatitis B	0.006331068379874741	0.38648018648018645	10
Interleukin-4 and 13 signaling	0.0016064138979743283	0.3066962634110248	10
TNF signaling	0.0030471159506411717	0.3415739596209312	10
Thyroid hormone signaling	0.005487264789738615	0.37802097583219335	10
Cell Cycle	0.004352179712583809	0.36122004357298476	9
Cell cycle	0.0027523414756303955	0.31318473743860975	9
Diseases of signal transduction	0.004873198177665552	0.3621668851026649	9
Fluid shear stress and atherosclerosis	0.0030189355459411434	0.33712891419276125	9

Gastrin-CREB signalling pathway via PKC and MAPK	0.002120149156559575	0.3415739596209312	9
Glioma	0.00357016685871879	0.3673017279574657	9
HIF-1 signaling pathway	0.004784530018714114	0.3702545779365788	9
Phospholipase D signaling pathway	0.0050741704356493346	0.3523161920951976	9
Post-translational protein modification	0.002478840398371435	0.3035518125228854	9
Adaptive Immune System	0.002901865037257798	0.3499366821443647	8
Bladder cancer	0.001833241734326513	0.3396149119213437	8
Cell Cycle, Mitotic	0.0039597096772662635	0.3596529284164859	8
Chronic myeloid leukemia	0.0031256406222156165	0.3547282841249465	8
Collagen degradation	2.37E+11	0.26959349593495935	8
Degradation of the extracellular matrix	2.37E+11	0.26959349593495935	8
Fc epsilon RI signaling pathway	0.003742004112488721	0.3529161345253299	8
FoxO signaling pathway	0.0035089197309673323	0.3631187034603592	8
IL-17 signaling pathway	0.0014701534266034428	0.32548095798979193	8
MAPK signaling pathway	0.0052175573517818956	0.36568151742390825	8
NGF signalling via TRKA from the plasma membrane	0.002988148680262386	0.36632788334069816	8
Nuclear Receptor transcription pathway	1.01E+12	0.2671608121173058	8
Prostate cancer	0.003106389156637759	0.36248360297332755	8
Ras signaling	0.0032869627525818484	0.3490526315789474	8
Signaling by EGFR	0.0031923864032500486	0.3647162340519138	8
Signaling by SCF-KIT	0.002562086957748102	0.3631187034603592	8
Transcriptional misregulation in cancer	0.001284877572392739	0.30646950092421443	8
Tuberculosis	0.003020489744206932	0.34101192924722334	8
Viral carcinogenesis	0.003904065719641192	0.36280087527352295	8
Calcium signaling pathway	7.88E+11	0.3026652062796641	7
Cellular Senescence	0.0019120318256676818	0.3396149119213437	7
Chagas disease (American trypanosomiasis)	0.0020821129127926684	0.3376782077393075	7
DAP12 interactions	0.002249369824587144	0.36027813993915686	7
DAP12 signaling	0.002249369824587144	0.36027813993915686	7
Downstream signal transduction	0.002249369824587144	0.36027813993915686	7
Estrogen signaling pathway	7.39E+11	0.3275385223231924	7
GPCR downstream signaling	0.0016267198241944338	0.3117713426100038	7
GnRH signaling pathway	0.002154984302941433	0.33712891419276125	7
HTLV-I infection	0.0031267084893465457	0.33850551245406285	7

Influenza A	0.003854448785651226	0.36697653829127935	7
Melanoma	0.0019387521682617246	0.3496415014761704	7
Neuroactive ligand-receptor interaction	2.11E+12	0.266131621187801	7
Non-small cell lung cancer	0.0027919710352043697	0.36280087527352295	7
Rap1 signaling	0.0018262946297672165	0.3446985446985447	7
Regulation of TP53 Activity	0.002249168637836882	0.3285770907649624	7
Signaling by PDGF	0.002249369824587144	0.36027813993915686	7
Signaling by VEGF	0.0020067639201433386	0.34758909853249476	7
Sphingolipid signaling	0.0035339736772037737	0.36697653829127935	7
Transcriptional Regulation by TP53	0.002249168637836882	0.3285770907649624	7
VEGF signaling pathway	0.0030838603861648817	0.3490526315789474	7
VEGFA-VEGFR2 Pathway	0.0020067639201433386	0.34758909853249476	7
Activation of Matrix Metalloproteinases	4.50E+11	0.26376073814826595	6
Apelin signaling pathway	0.0010266660708672022	0.31872356785851597	6
Arachidonic acid metabolism	3.53E+11	0.27314662273476115	6
Choline metabolism in cancer	0.0022316045822308793	0.3464270789803594	6
Deubiquitination	7.73E+11	0.29981916817359855	6
Downstream signaling events of B Cell Receptor (BCR)	0.0012733389933953592	0.34613778705636744	6
Epstein-Barr virus infection	0.002366889172679896	0.34185567010309276	6
ErbB signaling	0.0015277421557358757	0.3435557397430585	6
Fc epsilon receptor (FCERI) signaling	0.0012733389933953592	0.34613778705636744	6
GAB1 signalosome	0.0012733389933953592	0.34613778705636744	6
GPCR ligand binding	3.61E+11	0.266816865143225	6
Hepatitis C	0.002078817308467978	0.35442496793501493	6
Insulin resistance	0.001227517069212583	0.31083614548181476	6
Neurotrophin signaling pathway	0.0024096034271432016	0.34758909853249476	6
Osteoclast differentiation	0.0011064801392095826	0.33279807306302694	6
Oxidative Stress Induced Senescence	0.0013920792173800082	0.3333333333333333	6
Oxytocin signaling pathway	0.002244750267494593	0.3396149119213437	6
PIP3 activates AKT signaling	0.0012733389933953592	0.34613778705636744	6
Pancreatic cancer	0.0016693226292708605	0.34700711594809547	6
Platelet activation	0.0023847431803828536	0.33522038010513544	6
Prolactin signaling pathway	0.0010331021055803424	0.3277975484381178	6
Role of LAT2/NTAL/LAB on calcium mobilization	0.0012733389933953592	0.34613778705636744	6

Serotonergic synapse	0.0022960586293163335	0.3288377627925426	6
Signaling by ERBB4	9.16E+11	0.3078351281099146	6
Signaling by the B Cell Receptor (BCR)	0.0012733389933953592	0.34613778705636744	6
Small cell lung cancer	0.0014125829287984476	0.31921447824412785	6
Transcriptional regulation of white adipocyte differentiation	0.0011162625695244237	0.29617720614505183	6
Amoebiasis	0.0011453318174693154	0.3199536858355847	5
Apoptosis	0.0016964599284392718	0.3444121312837557	5
Central carbon metabolism in cancer	0.0010487835444201934	0.343840729987557	5
Class A/1 (Rhodopsin-like receptors)	7.24E+09	0.26409684612934053	5
Cytokine-cytokine receptor interaction	5.05E+11	0.29345132743362834	5
Focal adhesion	0.0011482524769112598	0.3374033374033374	5
G alpha (q) signalling events	3.29E+12	0.2928293889085129	5
IGF1R signaling cascade	7.35E+11	0.3290988487495038	5
IRS-mediated signalling	7.35E+11	0.3290988487495038	5
IRS-related events triggered by IGF1R	7.35E+11	0.3290988487495038	5
Insulin receptor signalling cascade	7.35E+11	0.3290988487495038	5
Insulin signaling pathway	9.50E+10	0.32573673870333986	5
Leishmaniasis	8.08E+11	0.3202008497489378	5
Leukocyte transendothelial migration	7.44E+11	0.3211933359163115	5
Measles	9.43E+11	0.3158095238095238	5
Membrane Trafficking	0.0010984871556246809	0.29702615549982087	5
Neutrophil degranulation	2.98E+12	0.2826457551994545	5
Oncogene Induced Senescence	8.66E+11	0.32676389436342135	5
Ovarian steroidogenesis	3.14E+11	0.2736876857048531	5
PI3K/AKT activation	9.29E+11	0.3393368808841588	5
Pertussis	7.72E+11	0.3194605009633911	5
Platinum drug resistance	9.77E+11	0.3379535262943335	5
Progesterone-mediated oocyte maturation	0.0010114310469776717	0.32548095798979193	5
Retrograde endocannabinoid signaling	9.24E+09	0.3262495080676899	5
Signaling by Insulin receptor	7.35E+11	0.3290988487495038	5
Signaling by NOTCH	0.0012374713209254652	0.3022238425082027	5
Signaling by Type 1 IGF1R	7.35E+11	0.3290988487495038	5
T cell receptor signaling pathway	0.0014019066152709773	0.33522038010513544	5
Toll-like receptor signaling pathway	0.0010809669450469253	0.3317326930772309	5

Toxoplasmosis	6.96E+11	0.31872356785851597	5
Vascular smooth muscle contraction	0.0011085716005316533	0.3244618395303327	5
Vesicle-mediated transport	0.0010984871556246809	0.29702615549982087	5
p53 signaling	5.82E+09	0.290571328426218	5
AMPK signaling pathway	2.82E+12	0.2985235866042492	4
Adherens junction	0.0012365853750967144	0.32936034962256655	4
Adrenergic signaling in cardiomyocytes	7.01E+11	0.32471602036819425	4
Alzheimer's disease	9.31E+11	0.31484998101025446	4
Autophagy - animal	4.96E+11	0.3231968810916179	4
Circadian Clock	4.13E+10	0.2859606760952052	4
EGFR TKI resistance	5.63E+11	0.3031078610603291	4
EPH-Ephrin signaling	1.42E+12	0.26871961102106967	4
Endocytosis	1.89E+12	0.2877473099618188	4
Endometrial cancer	8.43E+11	0.34073160706946154	4
Factors involved in megakaryocyte development and platelet production	7.48E+11	0.30047118521203336	4
Fatty acid, triacylglycerol, and ketone body metabolism	3.56E+12	0.2841960918752143	4
Fc gamma R-mediated phagocytosis	0.0013316740773097833	0.33712891419276125	4
Herpes simplex infection	9.24E+11	0.3048915042294962	4
Huntington's disease	5.67E+11	0.30047118521203336	4
Inflammatory mediator regulation of TRP channels	0.0010917503884480277	0.3221919937815779	4
Jak-STAT signaling pathway	8.57E+11	0.3136587211502081	4
Longevity regulating	2.82E+12	0.2985235866042492	4
Mitotic G1-G1/S phases	2.48E+12	0.27550681289464934	4
NOD-like receptor signaling pathway	5.68E+11	0.3172598545732874	4
Natural killer cell mediated cytotoxicity	0.001072971256748193	0.3382292941656467	4
Non-alcoholic fatty liver disease (NAFLD)	5.55E+11	0.30444362835108335	4
Notch signaling	4.92E+11	0.28341880341880343	4
Nuclear signaling by ERBB4	9.66E+10	0.2678513731825525	4
Platelet activation, signaling and aggregation	0.001107766895156798	0.3277975484381178	4
RET signaling	7.56E+11	0.33549170376365844	4
Regulation of TP53 Activity through Phosphorylation	5.28E+11	0.305565794323627	4
Rheumatoid arthritis	1.19E+12	0.27441244620986427	4
SUMO E3 ligases SUMOylate target proteins	1.47E+12	0.2843910806174957	4
SUMOylation	1.47E+12	0.2843910806174957	4

Salmonella infection	4.46E+12	0.31556909021697754	4
Signaling by NOTCH1	4.92E+11	0.28341880341880343	4
Signaling by PTK6	4.30E+11	0.28955640936081034	4
Signaling by Wnt	0.0010811911828521785	0.3028863719400804	4
Th17 cell differentiation	4.70E+11	0.3184786784479447	4
Type II diabetes mellitus	6.58E+11	0.32676389436342135	4
Ub-specific processing proteases	2.33E+12	0.2851737186102511	4
cAMP signaling pathway	0.0011465950140625899	0.3357634669906845	4
Acute myeloid leukemia	2.26E+12	0.31921447824412785	3
Adipocytokine signaling pathway	2.12E+11	0.2830317514510072	3
African trypanosomiasis	4.05E+11	0.29179866244280184	3
Alcoholism	8.41E+11	0.3124764417640407	3
Aldosterone-regulated sodium reabsorption	5.19E+11	0.330147351652728	3
Amphetamine addiction	7.80E+11	0.290571328426218	3
Amyotrophic lateral sclerosis (ALS)	4.71E+12	0.3026652062796641	3
BMAL1:CLOCK,NPAS2 activates circadian gene expression	1.73E+12	0.2790306294177045	3
Biological oxidations	1.93E+11	0.261761919797916	3
Cargo recognition for clathrin-mediated endocytosis	2.83E+12	0.28206873086083706	3
Chemical carcinogenesis	4.15E+10	0.2649408756791307	3
Cholinergic synapse	5.19E+11	0.330147351652728	3
Chromatin modifying enzymes	3.71E+11	0.2843910806174957	3
Chromatin organization	3.71E+11	0.2843910806174957	3
Clathrin-mediated endocytosis	2.83E+12	0.28206873086083706	3
Colorectal cancer	5.74E+10	0.33387031816351187	3
Constitutive Signaling by NOTCH1 HD+PEST Domain Mutants	2.62E+11	0.28073145953267864	3
Constitutive Signaling by NOTCH1 PEST Domain Mutants	2.62E+11	0.28073145953267864	3
Cytochrome P450 - arranged by substrate type	1.93E+11	0.261761919797916	3
DNA Repair	4.15E+12	0.29554367201426024	3
Dopaminergic synapse	7.13E+11	0.29702615549982087	3
EGFR Transactivation by Gastrin	2.09E+12	0.2963889882016446	3
EGFR tyrosine kinase inhibitor resistance	2.26E+12	0.31921447824412785	3
EPH-ephrin mediated repulsion of cells	5.61E+10	0.2657903174094261	3
Endocrine and other factor-regulated calcium reabsorption	1.78E+11	0.2828386216308427	3
Epithelial cell signaling in Helicobacter pylori infection	3.02E+11	0.2949128424048381	3

Fcgamma receptor (FCGR) dependent phagocytosis	3.84E+11	0.3189688341669873	3
Formation of the beta-catenin:TCF transactivating complex	2.35E+12	0.2809217214503558	3
G2/M Transition	4.16E+12	0.29575454869782375	3
Gap junction	3.90E+12	0.3216918897943345	3
Glutamatergic synapse	7.20E+10	0.3216918897943345	3
Growth hormone receptor signaling	3.95E+12	0.30624307351311414	3
Hematopoietic cell lineage	4.80E+10	0.2717141920681744	3
Hypertrophic cardiomyopathy (HCM)	1.83E+12	0.27790814616158227	3
Interleukin receptor SHC signaling	2.49E+11	0.3216918897943345	3
Interleukin-10 signaling	1.25E+12	0.27624125291569473	3
Interleukin-2 signaling	2.49E+11	0.3216918897943345	3
Interleukin-3, 5 and GM-CSF signaling	2.49E+11	0.3216918897943345	3
Long-term depression	7.20E+10	0.3216918897943345	3
Long-term potentiation	0.001023865620394091	0.3336016096579477	3
MAPK family signaling cascades	2.89E+11	0.3141341417203486	3
MAPK1/MAPK3 signaling	2.89E+11	0.3141341417203486	3
Melanogenesis	0.001023865620394091	0.3336016096579477	3
Metabolism of steroid hormones	3.88E+10	0.2606098711097139	3
Mitotic G2-G2/M phases	4.16E+12	0.29575454869782375	3
Negative regulation of the PI3K/AKT network	2.49E+11	0.3216918897943345	3
Neuronal System	4.55E+12	0.29118370214260625	3
Oocyte meiosis	8.94E+10	0.3022238425082027	3
Organelle biogenesis and maintenance	4.70E+11	0.2824531516183986	3
PI3K Cascade	1.54E+10	0.29345132743362834	3
PI5P, PP2A and IER3 Regulate PI3K/AKT Signaling	2.49E+11	0.3216918897943345	3
PPAR signaling pathway	2.40E+10	0.26426522154925086	3
PPARA activates gene expression	1.34E+11	0.27753598928691	3
Peptide ligand-binding receptors	2.88E+11	0.26225877886744703	3
Phase 1 - Functionalization of compounds	1.93E+11	0.261761919797916	3
Platelet homeostasis	3.05E+11	0.28537005163511187	3
RHO GTPase Effectors	2.30E+11	0.30511593669488407	3
Regulation of TP53 Activity through Acetylation	4.18E+12	0.2963889882016446	3
Regulation of TP53 Activity through Methylation	2.72E+11	0.29470316388197654	3
Regulation of TP53 Degradation	1.05E+12	0.2893542757417103	3

Regulation of actin cytoskeleton	2.49E+11	0.3216918897943345	3
Regulation of lipolysis in adipocytes	2.74E+12	0.29324372125928544	3
Renal cell carcinoma	9.27E+11	0.33387031816351187	3
Senescence-Associated Secretory Phenotype (SASP)	2.90E+11	0.30624307351311414	3
Shigellosis	2.96E+11	0.30990654205607476	3
Signaling by ERBB2	3.54E+11	0.3115370161593386	3
Signaling by NOTCH1 HD+PEST Domain Mutants in Cancer	2.62E+11	0.28073145953267864	3
Signaling by NOTCH1 PEST Domain Mutants in Cancer	2.62E+11	0.28073145953267864	3
Signaling by Rho GTPases	2.30E+11	0.30511593669488407	3
Signaling pathways regulating pluripotency of stem cells	3.15E+12	0.3219417475728155	3
Signalling to ERKs	2.33E+11	0.31484998101025446	3
Signalling to RAS	2.33E+11	0.31484998101025446	3
Steroid hormone biosynthesis	3.88E+10	0.2606098711097139	3
TCF dependent signaling in response to WNT	2.35E+12	0.2809217214503558	3
TGF-beta signaling pathway	8.54E+11	0.32599292174596933	3
TP53 Regulates Metabolic Genes	2.23E+12	0.2903677758318739	3
Thyroid cancer	3.92E+11	0.32144241954245834	3
Transmission across Chemical Synapses	4.55E+12	0.29118370214260625	3
VEGFR2 proliferation	2.44E+11	0.29470316388197654	3
Wnt signaling	8.34E+11	0.3124764417640407	3
cGMP-PKG signaling pathway	1.71E+11	0.30332967435053054	3
mTOR signaling	6.10E+11	0.3231968810916179	3
mTOR signalling	1.54E+10	0.29345132743362834	3
p75 NTR receptor-mediated signalling	1.57E+12	0.27064968984655563	3
ADP signalling through P2Y purinoceptor 1	1.62E+12	0.28016221696519095	2
ARMS-mediated activation	6.90E+10	0.3078351281099146	2
Activated NOTCH1 Transmits Signal to the Nucleus	2.00E+11	0.26225877886744703	2
Activated TLR4 signalling	7.56E+09	0.3066962634110248	2
Activation of PPARGC1A (PGC-1alpha) by phosphorylation	7.88E+10	0.2794068082237951	2
Activation of the AP-1 family of transcription factors	7.56E+09	0.3066962634110248	2
Aldosterone synthesis and secretion	7.07E+09	0.28073145953267864	2
Antifolate resistance	2.06E+11	0.27064968984655563	2
Assembly of collagen fibrils and other multimeric structures	1.63E+10	0.2614317250078839	2
B cell receptor signaling pathway	1.20E+12	0.3153290224419931	2

Basal cell carcinoma	3.47E+11	0.28130302002035973	2
C19/C18-Steroid hormone biosynthesis	7.52E+08	0.2601192343897082	2
C21-Steroid hormone biosynthesis	1.46E+10	0.26028257456828885	2
CD28 co-stimulation	3.58E+10	0.2893542757417103	2
CD28 dependent PI3K/Akt signaling	3.58E+10	0.2893542757417103	2
CDO in myogenesis	7.86E+10	0.27550681289464934	2
Ca-dependent events	1.68E+11	0.2828386216308427	2
Cell Cycle Checkpoints	2.00E+10	0.2818769126147569	2
Cell surface interactions at the vascular wall	8.34E+10	0.2885485555168813	2
Cell-Cell communication	1.20E+12	0.29981916817359855	2
Cellular response to heat stress	4.41E+12	0.31774626293599084	2
Chemokine signaling pathway	1.20E+12	0.3153290224419931	2
Circadian entrainment	2.13E+12	0.31461100569259964	2
Collagen formation	1.63E+10	0.2614317250078839	2
Complement and coagulation cascades	1.36E+12	0.2612669398046013	2
Constitutive Signaling by AKT1 E17K in Cancer	1.96E+11	0.27550681289464934	2
Constitutive Signaling by Aberrant PI3K in Cancer	5.98E+10	0.29617720614505183	2
Constitutive Signaling by EGFRvIII	5.98E+10	0.29617720614505183	2
Constitutive Signaling by Ligand-Responsive EGFR Cancer Variants	5.98E+10	0.29617720614505183	2
Costimulation by the CD28 family	3.58E+10	0.2893542757417103	2
Cyclin A:Cdk2-associated events at S phase entry	7.56E+10	0.2673331183489197	2
Cyclin D associated events in G1	4.90E+09	0.26159671820763647	2
DNA Double Strand Break Response	1.09E+12	0.282260810350698	2
Death Receptor Signalling	7.84E+10	0.2701205604431411	2
Dorso-ventral axis formation	6.90E+10	0.3078351281099146	2
EGFR interacts with phospholipase C-gamma	1.08E+12	0.29303640862495584	2
ERK/MAPK targets	7.56E+09	0.3066962634110248	2
Eicosanoid ligand-binding receptors	7.36E+08	0.25801431683784626	2
Endogenous sterols	7.52E+08	0.2601192343897082	2
Energy dependent regulation of mTOR by LKB1-AMPK	1.97E+11	0.2717141920681744	2
Epigenetic regulation of gene expression	8.17E+10	0.2777219430485762	2
FCERI mediated MAPK activation	6.90E+10	0.3078351281099146	2
Frs2-mediated activation	6.90E+10	0.3078351281099146	2
G-protein mediated events	1.68E+11	0.2828386216308427	2

G0 and Early G1	3.77E+11	0.2680245716133204	2
G1 Phase	4.90E+09	0.26159671820763647	2
G1/S DNA Damage Checkpoints	2.00E+10	0.2818769126147569	2
GRB2 events in EGFR signaling	6.90E+10	0.3078351281099146	2
Glucocorticoid biosynthesis	1.46E+10	0.26028257456828885	2
Glutamate Binding, Activation of AMPA Receptors and Synaptic Plasticity	8.02E+10	0.2875476933749566	2
Graft-versus-host disease	2.06E+11	0.27064968984655563	2
HSF1-dependent transactivation	1.21E+11	0.2840013703323056	2
Inflammatory bowel disease (IBD)	2.06E+11	0.27064968984655563	2
Integration of energy metabolism	2.16E+10	0.28556665518429214	2
L1CAM interactions	6.90E+10	0.3078351281099146	2
Legionellosis	2.06E+11	0.27064968984655563	2
Linoleic acid metabolism	9.93E+10	0.2664738026358084	2
Longevity regulating pathway	5.93E+10	0.2836127266507013	2
M Phase	2.13E+12	0.31461100569259964	2
MAP kinase activation in TLR cascade	7.56E+09	0.3066962634110248	2
MAPK targets/ Nuclear events mediated by MAP kinases	7.56E+09	0.3066962634110248	2
MAPK3 (ERK1) activation	1.30E+11	0.30601698043558506	2
Macroautophagy	1.97E+11	0.2717141920681744	2
Malaria	2.06E+11	0.27064968984655563	2
Mitochondrial biogenesis	7.88E+10	0.2794068082237951	2
Mitotic Prophase	2.13E+12	0.31461100569259964	2
MyD88 cascade initiated on plasma membrane	7.56E+09	0.3066962634110248	2
MyD88 dependent cascade initiated on endosome	7.56E+09	0.3066962634110248	2
MyD88-independent TLR3/TLR4 cascade	7.56E+09	0.3066962634110248	2
MyD88:Mal cascade initiated on plasma membrane	7.56E+09	0.3066962634110248	2
Myogenesis	7.86E+10	0.27550681289464934	2
NCAM signaling for neurite out-growth	6.90E+10	0.3078351281099146	2
NF-kappa B signaling pathway	5.49E+10	0.27207088939940927	2
NOTCH1 Intracellular Domain Regulates Transcription	8.17E+10	0.2777219430485762	2
Neurotransmitter Receptor Binding And Downstream Transmission	8.02E+10	0.2875476933749566	2
Nuclear Events (kinase and transcription factor activation)	7.56E+09	0.3066962634110248	2
Opioid Signalling	1.68E+11	0.2828386216308427	2
Ovarian tumor domain proteases	3.40E+10	0.28206873086083706	2

PI3K events in ERBB2 signaling	5.98E+10	0.29617720614505183	2
PI5P Regulates TP53 Acetylation	1.72E+12	0.2913884007029877	2
PKB-mediated events	1.97E+11	0.2717141920681744	2
PLC beta mediated events	1.68E+11	0.2828386216308427	2
Pathogenic Escherichia coli infection	1.26E+12	0.2811122414377755	2
Phosphatidylinositol signaling system	1.86E+12	0.3022238425082027	2
Phospholipid metabolism	3.06E+11	0.2936592277718739	2
Platelet sensitization by LDL	1.62E+12	0.28016221696519095	2
Positive epigenetic regulation of rRNA expression	8.17E+10	0.2777219430485762	2
Pre-NOTCH Expression and Processing	1.72E+12	0.2913884007029877	2
Pre-NOTCH Transcription and Translation	1.72E+12	0.2913884007029877	2
Prion diseases	1.30E+11	0.30601698043558506	2
Prolonged ERK activation events	6.90E+10	0.3078351281099146	2
Prostanoid ligand receptors	7.36E+08	0.25801431683784626	2
RAF-independent MAPK1/3 activation	1.30E+11	0.30601698043558506	2
RAF/MAP kinase cascade	6.90E+10	0.3078351281099146	2
RHO GTPases Activate WASPs and WAVEs	1.42E+12	0.3031078610603291	2
RIG-I-like receptor signaling pathway	8.76E+10	0.2811122414377755	2
RNA Polymerase I Promoter Clearance	3.55E+11	0.3094438223217618	2
RNA Polymerase I Transcription	3.55E+11	0.3094438223217618	2
RNA Polymerase I, RNA Polymerase III, and Mitochondrial Transcription	3.55E+11	0.3094438223217618	2
Recruitment and ATM-mediated phosphorylation	1.09E+12	0.282260810350698	2
Regulated proteolysis of p75NTR	2.00E+11	0.26225877886744703	2
Regulation of IGF transport and uptake by IGFBPs	2.38E+10	0.2607738282478767	2
Regulation of TP53 Expression and Degradation	2.00E+10	0.2818769126147569	2
Regulation of actin dynamics for phagocytic cup formation	1.42E+12	0.3031078610603291	2
Regulation of lipid metabolism by PARalpha	4.18E+11	0.27697961911125957	2
Regulation of lipid metabolism by PPARalpha	4.97E+09	0.2612669398046013	2
Regulation of mRNA stability by proteins that bind AU-rich elements	1.50E+12	0.2922100810715545	2
Renin secretion	1.43E+10	0.2606098711097139	2
Response to elevated platelet cytosolic Ca2+	1.47E+12	0.2803517078119716	2
S Phase	7.56E+10	0.2673331183489197	2
SHC1 events in EGFR signaling	6.90E+10	0.3078351281099146	2
SHC1 events in ERBB2 signaling	1.08E+12	0.29303640862495584	2

SMAD2/SMAD3:SMAD4 heterotrimer regulates transcription	6.29E+10	0.266131621187801	2
SOS-mediated signalling	6.90E+10	0.3078351281099146	2
SUMOylation of DNA replication proteins	1.53E+10	0.25930559899906164	2
SUMOylation of transcription factors	2.00E+10	0.2818769126147569	2
Signal amplification	1.62E+12	0.28016221696519095	2
Signal transduction by L1	6.90E+10	0.3078351281099146	2
Signaling by EGFR in Cancer	5.98E+10	0.29617720614505183	2
Signaling by EGFRvIII in Cancer	5.98E+10	0.29617720614505183	2
Signaling by FGFR	1.20E+12	0.3153290224419931	2
Signaling by FGFR1	1.20E+12	0.3153290224419931	2
Signaling by FGFR2	1.20E+12	0.3153290224419931	2
Signaling by FGFR3	1.20E+12	0.3153290224419931	2
Signaling by FGFR4	1.20E+12	0.3153290224419931	2
Signaling by Hedgehog	8.73E+10	0.26028257456828885	2
Signaling by Leptin	6.90E+10	0.3078351281099146	2
Signaling by Ligand-Responsive EGFR Variants in Cancer	5.98E+10	0.29617720614505183	2
Signaling by MET	1.68E+12	0.290571328426218	2
Signaling by NOTCH2	1.18E+12	0.27624125291569473	2
Signaling by TGF-beta Receptor Complex	6.29E+10	0.266131621187801	2
Signalling to p38 via RIT and RIN	6.90E+10	0.3078351281099146	2
Stabilization of p53	2.00E+10	0.2818769126147569	2
Synthesis of 5-eicosatetraenoic acids	1.75E+10	0.26028257456828885	2
Synthesis of Leukotrienes (LT) and Eoxins (EX)	1.75E+10	0.26028257456828885	2
Synthesis of Lipoxins (LX)	1.75E+10	0.26028257456828885	2
TFAP2 (AP-2) family regulates transcription	2.41E+11	0.2805414551607445	2
TP53 Regulates Transcription of Cell Cycle Genes	1.72E+12	0.2913884007029877	2
TP53 Regulates Transcription of Genes Involved in G2 Cell Cycle Arrest	1.72E+12	0.2913884007029877	2
TRAF6 mediated induction of NFkB and MAP kinases upon TLR7/8 or 9 activation	7.56E+09	0.3066962634110248	2
TRIF-mediated TLR3/TLR4 signaling	7.56E+09	0.3066962634110248	2
Th1 and Th2 cell differentiation	7.56E+09	0.3066962634110248	2
Tight junction	1.14E+12	0.27064968984655563	2
Toll Like Receptor 10 (TLR10) Cascade	7.56E+09	0.3066962634110248	2
Toll Like Receptor 2 (TLR2) Cascade	7.56E+09	0.3066962634110248	2
Toll Like Receptor 3 (TLR3) Cascade	7.56E+09	0.3066962634110248	2

Toll Like Receptor 4 (TLR4) Cascade	7.56E+09	0.3066962634110248	2
Toll Like Receptor 5 (TLR5) Cascade	7.56E+09	0.3066962634110248	2
Toll Like Receptor 7/8 (TLR7/8) Cascade	7.56E+09	0.3066962634110248	2
Toll Like Receptor 9 (TLR9) Cascade	7.56E+09	0.3066962634110248	2
Toll Like Receptor TLR1:TLR2 Cascade	7.56E+09	0.3066962634110248	2
Toll Like Receptor TLR6:TLR2 Cascade	7.56E+09	0.3066962634110248	2
Toll-Like Receptors Cascades	7.56E+09	0.3066962634110248	2
Trafficking of AMPA receptors	8.02E+10	0.2875476933749566	2
Transcriptional activity of SMAD2/SMAD3:SMAD4 heterotrimer	6.29E+10	0.266131621187801	2
Transmembrane transport of small molecules	1.44E+12	0.26275752773375594	2
Ubiquitin mediated proteolysis	3.62E+11	0.26906848425835767	2
p53-Dependent G1 DNA Damage Response	2.00E+10	0.2818769126147569	2
p53-Dependent G1/S DNA damage checkpoint	2.00E+10	0.2818769126147569	2
AKT phosphorylates targets in the cytosol	0.0	0.26819799417664186	1
AMPK inhibits chREBP transcriptional activation activity	0.0	0.26259106746911626	1
Acetylcholine regulates insulin secretion	0.0	0.27697961911125957	1
Activated PKN1 stimulates transcription of AR regulated genes KLK2 and KLK3	0.0	0.25963044159098025	1
Activation of BH3-only proteins	0.0	0.27828130245048677	1
Activation of HOX genes during differentiation	0.0	0.27278710102007236	1
Activation of NOXA and translocation to mitochondria	0.0	0.27828130245048677	1
Activation of PUMA and translocation to mitochondria	0.0	0.27828130245048677	1
Activation of SMO	0.0	0.2554699537750385	1
Activation of anterior HOX genes in hindbrain development during early embryogenesis	0.0	0.27278710102007236	1
Activation of gene expression by SREBF (SREBP)	0.0	0.25266686985675096	1
Activation of the TFAP2 (AP-2) family of transcription factors	0.0	0.27278710102007236	1
Acyl chain remodeling of CL	0.0	0.2629241991753885	1
Acyl chain remodelling of PC	0.0	0.2629241991753885	1
Acyl chain remodelling of PE	0.0	0.2629241991753885	1
Acyl chain remodelling of PG	0.0	0.2629241991753885	1
Acyl chain remodelling of PI	0.0	0.2629241991753885	1
Acyl chain remodelling of PS	0.0	0.2629241991753885	1
Advanced glycosylation endproduct receptor signaling	0.0	0.29960245753523673	1
Allograft rejection	0.0	0.2664738026358084	1
Androgen biosynthesis	0.0	0.25979316828580384	1

Antigen processing and presentation	0.0	0.2664738026358084	1
Antigen processing: Ubiquitination & Proteasome degradation	0.0	0.2493233082706767	1
Antiviral mechanism by IFN-stimulated genes	0.0	0.29960245753523673	1
Aquaporin-mediated transport	0.0	0.2576935032639105	1
Arginine and proline metabolism	0.0	0.2614317250078839	1
Arginine biosynthesis	0.0	0.2614317250078839	1
Association of TriC/CCT with target proteins during biosynthesis	0.0	0.27828130245048677	1
Asthma	0.0	0.2664738026358084	1
Attenuation phase	0.0	0.27278710102007236	1
Autodegradation of the E3 ubiquitin ligase COP1	0.0	0.27828130245048677	1
Autophagy	0.0	0.25833593019632284	1
B-WICH complex positively regulates rRNA expression	0.0	0.27278710102007236	1
BBSome-mediated cargo-targeting to cilium	0.0	0.2554699537750385	1
Bacterial invasion of epithelial cells	0.0	0.28537005163511187	1
Basigin interactions	0.0	0.2584970377299657	1
Beta-catenin independent WNT signaling	0.0	0.27697961911125957	1
C-type lectin receptors (CLRs)	0.0	0.27278710102007236	1
CD209 (DC-SIGN) signaling	0.0	0.27278710102007236	1
COPI-independent Golgi-to-ER retrograde traffic	0.0	0.2629241991753885	1
CYP2E1 reactions	0.0	0.2450487732781555	1
Ca2+ pathway	0.0	0.27697961911125957	1
CaM pathway	0.0	0.27697961911125957	1
Calmodulin induced events	0.0	0.27697961911125957	1
Carbohydrate digestion and absorption	0.0	0.28537005163511187	1
Cargo trafficking to the periciliary membrane	0.0	0.2554699537750385	1
Cell cycle - G1/S transition	0.0	0.2525129454766981	1
Cell death signalling via NRAGE, NRIF and NADE	0.0	0.25930559899906164	1
Cellular response to hypoxia	0.0	0.27278710102007236	1
Chaperonin-mediated protein folding	0.0	0.27828130245048677	1
Chromosome Maintenance	0.0	0.25705426356589145	1
Cilium Assembly	0.0	0.2554699537750385	1
Class B/2 (Secretin family receptors)	0.0	0.2554699537750385	1
Class I MHC mediated antigen processing & presentation	0.0	0.2493233082706767	1
Cocaine addiction	0.0	0.2588198563846394	1

Common Pathway of Fibrin Clot Formation	0.0	0.253749617385981	1
Constitutive Signaling by NOTCH1	0.0	0.25578525146559705	1
Cyclin A/B1 associated events during G2/M transition	0.0	0.2578538102643857	1
Cyclin B2 mediated events	0.0	0.2578538102643857	1
Cyclin E associated events during G1/S transition	0.0	0.2607738282478767	1
Cytosolic DNA-sensing pathway	0.0	0.26392868513212353	1
Cytosolic sensors of pathogen-associated DNA	0.0	0.27278710102007236	1
DAG and IP3 signaling	0.0	0.27697961911125957	1
DNA Damage/Telomere Stress Induced Senescence	0.0	0.27828130245048677	1
DNA damage-induced cell cycle checkpoints	0.0	0.2578538102643857	1
DSCAM interactions	0.0	0.2711808963035656	1
Deactivation of the beta-catenin transactivating complex	0.0	0.2620929497312678	1
Defective AVP causes neurohypophyseal diabetes insipidus (NDI)	0.0	0.2576935032639105	1
Degradation of beta-catenin by the destruction complex	0.0	0.2620929497312678	1
Depolymerisation of the Nuclear Lamina	0.0	0.27697961911125957	1
Deregulated CDK5 triggers multiple neurodegenerative pathways in Alzheimer's disease models	0.0	0.2578538102643857	1
Dilated cardiomyopathy	0.0	0.2664738026358084	1
Disinhibition of SNARE formation	0.0	0.27697961911125957	1
Disorders of transmembrane transporters	0.0	0.2576935032639105	1
Dissolution of Fibrin Clot	0.0	0.25721377598510703	1
Dopamine clearance from the synaptic cleft	0.0	0.2588198563846394	1
Downregulation of ERBB2 signaling	0.0	0.27477626781571096	1
Downregulation of SMAD2/3:SMAD4 transcriptional activity	0.0	0.2620929497312678	1
Downstream TCR signaling	0.0	0.28537005163511187	1
Downstream signaling of activated FGFR1	0.0	0.28537005163511187	1
Downstream signaling of activated FGFR2	0.0	0.28537005163511187	1
Downstream signaling of activated FGFR3	0.0	0.28537005163511187	1
Downstream signaling of activated FGFR4	0.0	0.28537005163511187	1
Drug metabolism - cytochrome P450	0.0	0.2450487732781555	1
Dual incision in TC-NER	0.0	0.27278710102007236	1
ECM proteoglycans	0.0	0.25721377598510703	1
EGFR downregulation	0.0	0.27477626781571096	1
EPHA-mediated growth cone collapse	0.0	0.25737348649487735	1

ERBB2 Activates PTK6 Signaling	0.0	0.27477626781571096	1
ERBB2 Regulates Cell Motility	0.0	0.27477626781571096	1
ERCC6 (CSB) and EHMT2 (G9a) positively regulate rRNA expression	0.0	0.2620929497312678	1
ERKs are inactivated	0.0	0.29960245753523673	1
Estrogen biosynthesis	0.0	0.25930559899906164	1
Ether lipid metabolism	0.0	0.2629241991753885	1
Extension of Telomeres	0.0	0.25705426356589145	1
Extrinsic Pathway of Fibrin Clot Formation	0.0	0.253749617385981	1
FGFR1 mutant receptor activation	0.0	0.28537005163511187	1
Ferroptosis	0.0	0.27828130245048677	1
Formation of Fibrin Clot (Clotting Cascade)	0.0	0.253749617385981	1
Formation of Senescence-Associated Heterochromatin Foci (SAHF)	0.0	0.27828130245048677	1
Formation of TC-NER Pre-Incision Complex	0.0	0.27278710102007236	1
G alpha (12/13) signalling events	0.0	0.28537005163511187	1
G alpha (s) signalling events	0.0	0.2576935032639105	1
G alpha (z) signalling events	0.0	0.27697961911125957	1
G beta:gamma signalling through PI3Kgamma	0.0	0.28537005163511187	1
G-protein beta:gamma signalling	0.0	0.28537005163511187	1
G1/S Transition	0.0	0.2607738282478767	1
G2/M Checkpoints	0.0	0.27828130245048677	1
G2/M DNA damage checkpoint	0.0	0.27828130245048677	1
GABAergic synapse	0.0	0.27697961911125957	1
GPVI-mediated activation cascade	0.0	0.28537005163511187	1
GRB2 events in ERBB2 signaling	0.0	0.27477626781571096	1
Gamma carboxylation, hypusine formation and arylsulfatase activation	0.0	0.253749617385981	1
Gamma-carboxylation of protein precursors	0.0	0.253749617385981	1
Gamma-carboxylation, transport, and amino-terminal cleavage of proteins	0.0	0.253749617385981	1
Gap-filling DNA repair synthesis and ligation in TC-NER	0.0	0.27278710102007236	1
Gastric acid secretion	0.0	0.27697961911125957	1
Glucagon signaling	0.0	0.26259106746911626	1
Glucagon signaling pathway	0.0	0.27278710102007236	1
Glycerophospholipid biosynthesis	0.0	0.2629241991753885	1
Glycerophospholipid metabolism	0.0	0.2629241991753885	1
Golgi Cisternae Pericentriolar Stack Reorganization	0.0	0.29960245753523673	1

Golgi-to-ER retrograde transport	0.0	0.2629241991753885	1
HATs acetylate histones	0.0	0.27278710102007236	1
HDACs deacetylate histones	0.0	0.2620929497312678	1
HDR through Homologous Recombination (HR)	0.0	0.2588198563846394	1
HDR through Single Strand Annealing (SSA)	0.0	0.2588198563846394	1
Hedgehog 'off' state	0.0	0.2554699537750385	1
Hedgehog 'on' state	0.0	0.2554699537750385	1
Hedgehog ligand biogenesis	0.0	0.25578525146559705	1
Hedgehog signaling	0.0	0.2554699537750385	1
Hedgehog signaling pathway	0.0	0.2554699537750385	1
Hippo signaling pathway	0.0	0.25721377598510703	1
Homology Directed Repair	0.0	0.2588198563846394	1
Hormone-sensitive lipase (HSL)-mediated triacylglycerol hydrolysis	0.0	0.2584970377299657	1
HuR (ELAVL1) binds and stabilizes mRNA	0.0	0.27697961911125957	1
Hydrolysis of LPC	0.0	0.2629241991753885	1
ISG15 antiviral mechanism	0.0	0.29960245753523673	1
Import of palmitoyl-CoA into the mitochondrial matrix	0.0	0.26259106746911626	1
Inactivation, recovery and regulation of the phototransduction cascade	0.0	0.27697961911125957	1
Inhibition of Signaling by Overexpressed EGFR	0.0	0.27477626781571096	1
Inositol phosphate metabolism	0.0	0.28537005163511187	1
Insulin secretion	0.0	0.27697961911125957	1
Integrin alphaIIb beta3 signaling	0.0	0.2604461200125668	1
Integrin cell surface interactions	0.0	0.25737348649487735	1
Interferon Signaling	0.0	0.29960245753523673	1
Interferon alpha/beta signaling	0.0	0.2604461200125668	1
Interferon gamma signaling	0.0	0.2604461200125668	1
Interleukin-6 family signaling	0.0	0.26392868513212353	1
Interleukin-6 signaling	0.0	0.26392868513212353	1
Intestinal immune network for IgA production	0.0	0.26392868513212353	1
Intra-Golgi and retrograde Golgi-to-ER traffic	0.0	0.2629241991753885	1
Intrinsic Pathway for Apoptosis	0.0	0.27828130245048677	1
Intrinsic Pathway of Fibrin Clot Formation	0.0	0.253749617385981	1
KSRP (KHSRP) binds and destabilizes mRNA	0.0	0.2711808963035656	1
LRR FLII-interacting protein 1 (LRRFIP1) activates type I IFN production	0.0	0.27278710102007236	1

Lipid digestion, mobilization, and transport	0.0	0.2584970377299657	1
Longevity regulating pathway - multiple species	0.0	0.2620929497312678	1
Lysosome	0.0	0.25833593019632284	1
MAP2K and MAPK activation	0.0	0.29960245753523673	1
MAPK (ERK1/2) signaling	0.0	0.29960245753523673	1
MAPK (p38) signaling	0.0	0.2711808963035656	1
MAPK1 (ERK2) activation	0.0	0.26392868513212353	1
MET activates PI3K/AKT signaling	0.0	0.28537005163511187	1
MHC class II antigen presentation	0.0	0.25833593019632284	1
Meiosis	0.0	0.2607738282478767	1
Meiotic recombination	0.0	0.2607738282478767	1
Metabolism of Angiotensinogen to Angiotensins	0.0	0.25833593019632284	1
Metabolism of vitamins and cofactors	0.0	0.2620929497312678	1
Metabolism of water-soluble vitamins and cofactors	0.0	0.2620929497312678	1
Metabolism of xenobiotics by cytochrome P450	0.0	0.2586583463338533	1
Metalloprotease DUBs	0.0	0.27278710102007236	1
Mineral absorption	0.0	0.256101328390485	1
Mitophagy - animal	0.0	0.27828130245048677	1
Morphine addiction	0.0	0.27697961911125957	1
NOD1/2 Signaling Pathway	0.0	0.2711808963035656	1
NOTCH2 Activation and Transmission of Signal to the Nucleus	0.0	0.25930559899906164	1
NOTCH2 intracellular domain regulates transcription	0.0	0.27278710102007236	1
NRIF signals cell death from the nucleus	0.0	0.25930559899906164	1
Na+/Cl- dependent neurotransmitter transporters	0.0	0.2588198563846394	1
Negative epigenetic regulation of rRNA expression	0.0	0.2620929497312678	1
Negative feedback regulation of MAPK pathway	0.0	0.29960245753523673	1
Negative regulation of FGFR1 signaling	0.0	0.29960245753523673	1
Negative regulation of FGFR2 signaling	0.0	0.29960245753523673	1
Negative regulation of FGFR3 signaling	0.0	0.29960245753523673	1
Negative regulation of FGFR4 signaling	0.0	0.29960245753523673	1
Negative regulation of MAPK pathway	0.0	0.29960245753523673	1
Negative regulation of MET activity	0.0	0.2604461200125668	1
Nephrin interactions	0.0	0.28537005163511187	1
Neurodegenerative Diseases	0.0	0.2578538102643857	1

Neurophilin interactions with VEGF and VEGFR	0.0	0.25737348649487735	1
Neurotransmitter Clearance In The Synaptic Cleft	0.0	0.2588198563846394	1
Nicotinamide salvaging	0.0	0.2620929497312678	1
Nicotinate metabolism	0.0	0.2620929497312678	1
Nitric oxide stimulates guanylate cyclase	0.0	0.2614317250078839	1
NoRC negatively regulates rRNA expression	0.0	0.2620929497312678	1
Non-integrin membrane-ECM interactions	0.0	0.27697961911125957	1
Nuclear Envelope Breakdown	0.0	0.27697961911125957	1
Nucleotide Excision Repair	0.0	0.27278710102007236	1
Nucleotide-binding domain, leucine rich repeat containing receptor (NLR) signaling	0.0	0.2711808963035656	1
Oncogenic MAPK signaling	0.0	0.29960245753523673	1
PCP/CE pathway	0.0	0.27697961911125957	1
PI Metabolism	0.0	0.28537005163511187	1
PI-3K cascade:FGFR1	0.0	0.28537005163511187	1
PI-3K cascade:FGFR2	0.0	0.28537005163511187	1
PI-3K cascade:FGFR3	0.0	0.28537005163511187	1
PI-3K cascade:FGFR4	0.0	0.28537005163511187	1
PI3K events in ERBB4 signaling	0.0	0.28537005163511187	1
PI3K-Akt signaling	0.0	0.28537005163511187	1
PLC-gamma1 signalling	0.0	0.27697961911125957	1
PLCG1 events in ERBB2 signaling	0.0	0.27477626781571096	1
PTK6 Down-Regulation	0.0	0.2604461200125668	1
PTK6 Expression	0.0	0.2588198563846394	1
PTK6 Regulates Cell Cycle	0.0	0.2607738282478767	1
PTK6 promotes HIF1A stabilization	0.0	0.27477626781571096	1
Pancreatic secretion	0.0	0.27697961911125957	1
Paradoxical activation of RAF signaling by kinase inactive BRAF	0.0	0.29960245753523673	1
Parkinson's disease	0.0	0.2588198563846394	1
Peptide hormone metabolism	0.0	0.25833593019632284	1
Peroxisome	0.0	0.2614317250078839	1
Platelet Aggregation	0.0	0.2604461200125668	1
Platelet degranulation	0.0	0.25721377598510703	1
Polo-like kinase mediated events	0.0	0.27278710102007236	1
Programmed Cell Death	0.0	0.27828130245048677	1

Protein folding	0.0	0.27828130245048677	1
RHO GTPases activate PKNs	0.0	0.25963044159098025	1
RIG-I/MDA5 mediated induction of IFN-alpha/beta pathways	0.0	0.27278710102007236	1
RMTs methylate histone arginines	0.0	0.2607738282478767	1
RNA Polymerase I Promoter Opening	0.0	0.29960245753523673	1
RNA Polymerase I Transcription Initiation	0.0	0.2620929497312678	1
RORA activates gene expression	0.0	0.27278710102007236	1
ROS, RNS production in phagocytes	0.0	0.2614317250078839	1
Regulation of HSF1-mediated heat shock response	0.0	0.29960245753523673	1
Regulation of Hypoxia-inducible Factor (HIF) by oxygen	0.0	0.27278710102007236	1
Regulation of IFNA signaling	0.0	0.2604461200125668	1
Regulation of IFNG signaling	0.0	0.2604461200125668	1
Regulation of KIT signaling	0.0	0.27697961911125957	1
Regulation of TNFR1 signaling	0.0	0.2664738026358084	1
Regulation of TP53 Activity through Association with Co-factors	0.0	0.27828130245048677	1
Regulation of TP53 Expression	0.0	0.27828130245048677	1
Regulation of TP53 Expression	0.0	0.2654498879282741	1
Regulation of cholesterol biosynthesis by SREBP (SREBF)	0.0	0.25266686985675096	1
Regulation of gene expression by Hypoxia-inducible Factor	0.0	0.27278710102007236	1
Regulation of insulin secretion	0.0	0.27697961911125957	1
Regulation of signaling by CBL	0.0	0.28537005163511187	1
Release of Hh-Np from the secreting cell	0.0	0.25578525146559705	1
Removal of aminoterminal propeptides from gamma-carboxylated proteins	0.0	0.253749617385981	1
Renin-angiotensin system	0.0	0.25979316828580384	1
Repression of WNT target genes	0.0	0.2620929497312678	1
Role of Abl in Robo-Slit signaling	0.0	0.2588198563846394	1
Role of phospholipids in phagocytosis	0.0	0.28537005163511187	1
SCF(Skp2)-mediated degradation of p27/p21	0.0	0.2607738282478767	1
SLC transporter disorders	0.0	0.2576935032639105	1
SLC-mediated transmembrane transport	0.0	0.2588198563846394	1
Salivary secretion	0.0	0.27697961911125957	1
Senescence pathways	0.0	0.26392868513212353	1
Signal attenuation	0.0	0.29960245753523673	1
Signaling by BRAF and RAF fusions	0.0	0.29960245753523673	1

Signaling by NOTCH3	0.0	0.25930559899906164	1
Signaling by NOTCH4	0.0	0.25930559899906164	1
Signaling by Overexpressed Wild-Type EGFR in Cancer	0.0	0.27477626781571096	1
Signaling by RAS mutants	0.0	0.29960245753523673	1
Signaling by Robo receptor	0.0	0.2588198563846394	1
Signaling by cytosolic FGFR1 fusion mutants	0.0	0.28537005163511187	1
Signaling by high-kinase activity BRAF mutants	0.0	0.29960245753523673	1
Signaling by moderate kinase activity BRAF mutants	0.0	0.29960245753523673	1
Spry regulation of FGF signaling	0.0	0.29960245753523673	1
Syndecan interactions	0.0	0.27697961911125957	1
Synthesis of 15-eicosatetraenoic acid derivatives	0.0	0.2620929497312678	1
Synthesis of HETE	0.0	0.2450487732781555	1
Synthesis of PA	0.0	0.2629241991753885	1
Synthesis of PIPs at the plasma membrane	0.0	0.28537005163511187	1
Synthesis of Prostaglandins (PG) and Thromboxanes (TX)	0.0	0.2620929497312678	1
Synthesis of epoxy (EET) and DHET	0.0	0.2450487732781555	1
Systemic lupus erythematosus	0.0	0.2664738026358084	1
TCR signaling	0.0	0.28537005163511187	1
TNFR1-induced NFkappaB signaling pathway	0.0	0.2664738026358084	1
TNFR1-induced proapoptotic signaling	0.0	0.2664738026358084	1
TNFR1-mediated ceramide production	0.0	0.2664738026358084	1
TNFR2 non-canonical NF-kB pathway	0.0	0.2664738026358084	1
TP53 Regulates Transcription of Caspase Activators and Caspases	0.0	0.27828130245048677	1
TP53 Regulates Transcription of Cell Death Genes	0.0	0.27828130245048677	1
TP53 Regulates Transcription of DNA Repair Genes	0.0	0.27828130245048677	1
TP53 Regulates Transcription of Death Receptors and Ligands	0.0	0.27828130245048677	1
TP53 Regulates Transcription of Genes Involved in Cytochrome C Release	0.0	0.27828130245048677	1
TP53 Regulates Transcription of Genes Involved in G1 Cell Cycle Arrest	0.0	0.27828130245048677	1
TP53 regulates transcription of additional cell cycle genes	0.0	0.27828130245048677	1
TP53 regulates transcription of several additional cell death genes	0.0	0.27828130245048677	1
TRAF3-dependent IRF activation pathway	0.0	0.27278710102007236	1
TRAF6 mediated IRF7 activation	0.0	0.27278710102007236	1
Telomere Extension By Telomerase	0.0	0.25705426356589145	1
Telomere Maintenance	0.0	0.25705426356589145	1

The phototransduction cascade	0.0	0.27697961911125957	1
The role of GTSE1 in G2/M progression after G2 checkpoint	0.0	0.27828130245048677	1
Thrombin signalling through proteinase activated receptors (PARs)	0.0	0.29960245753523673	1
Thyroid hormone synthesis	0.0	0.27697961911125957	1
Tie2 Signaling	0.0	0.28537005163511187	1
Trafficking of GluR2-containing AMPA receptors	0.0	0.27697961911125957	1
Transcription-Coupled Nucleotide Excision Repair (TC-NER)	0.0	0.27278710102007236	1
Transcriptional activation of cell cycle inhibitor p21	0.0	0.27828130245048677	1
Transcriptional activation of p53 responsive genes	0.0	0.27828130245048677	1
Transcriptional regulation by the AP-2 (TFAP2) family of transcription factors	0.0	0.27278710102007236	1
Translocation of GLUT4 to the plasma membrane	0.0	0.26259106746911626	1
Transport of gamma-carboxylated protein precursors	0.0	0.253749617385981	1
Transport of glucose and other sugars	0.0	0.2588198563846394	1
Type I diabetes mellitus	0.0	0.2664738026358084	1
Ubiquitin-dependent degradation of Cyclin D	0.0	0.2607738282478767	1
Ubiquitin-dependent degradation of Cyclin D1	0.0	0.2607738282478767	1
VEGF binding	0.0	0.25737348649487735	1
VEGF binds to VEGFR leading to receptor dimerization	0.0	0.25737348649487735	1
VEGFR2 mediated cell proliferation	0.0	0.29960245753523673	1
VEGFR2 mediated vascular permeability	0.0	0.2654498879282741	1
Vasopressin regulates renal water homeostasis via Aquaporins	0.0	0.2576935032639105	1
Vasopressin-like receptors	0.0	0.2576935032639105	1
Vasopressin-regulated water reabsorption	0.0	0.2576935032639105	1
Vibrio cholerae infection	0.0	0.27697961911125957	1
Viral myocarditis	0.0	0.2588198563846394	1
Visual phototransduction	0.0	0.27697961911125957	1
WNT5A-dependent internalization of FZD4	0.0	0.27697961911125957	1
Xenobiotics	0.0	0.2450487732781555	1
activated TAK1 mediates p38 MAPK activation	0.0	0.2711808963035656	1
alpha-Linolenic acid metabolism	0.0	0.2629241991753885	1
mTORC1-mediated signalling	0.0	0.2654498879282741	1
p38MAPK events	0.0	0.2711808963035656	1
p75NTR negatively regulates cell cycle via SC1	0.0	0.2620929497312678	1
phospho-PLA2 pathway	0.0	0.2629241991753885	1

Table S12. Topology features (Betweenness Centrality, Closeness Centrality, and Degree) of protein-protein interactions related to breast cancer from network results.

Display name	Betweenness Centrality	Closeness Centrality	Degree
TNF	0.08203510120401204	0.7922077922077921	45
IL6	0.07664593584902715	0.7922077922077921	45
TP53	0.06892097633765197	0.7625000000000001	43
MAPK3	0.06178192745323669	0.7349397590361446	39
PTGS2	0.11260972537942408	0.7261904761904762	38
EGFR	0.05563670873384328	0.7093023255813954	37
PPARG	0.038331403086102896	0.7176470588235294	37
ESR1	0.026687272871164597	0.6931818181818181	35
MMP9	0.020732050643469807	0.6853932584269663	33
MTOR	0.013202470173742818	0.6421052631578947	28
MAPK14	0.019197409090722744	0.6421052631578947	27
MMP2	0.014260940946889969	0.6354166666666666	27
PGR	0.012401676708198826	0.6354166666666666	27
EP300	0.011840014252488274	0.6354166666666666	27
CDK4	0.015037107233611034	0.6224489795918368	26
MDM2	0.00590170836723569	0.6224489795918368	26
KDR	0.006131677431457982	0.6224489795918368	25
PIK3CA	0.007653365609872588	0.6039603960396039	24
AR	0.0050309825881093995	0.61	24
HDAC1	0.008148626232172728	0.6039603960396039	23
SERPINE1	0.01477759749146393	0.5980392156862745	22
PRKCA	0.03970269439578474	0.5980392156862745	21
ABL1	0.009140174411262452	0.5700934579439253	20
ESR2	0.0034947704662392854	0.5865384615384616	20
TERT	0.0013763952272328956	0.5700934579439253	20
CYP19A1	0.012297516718787798	0.580952380952381	19
MMP3	0.005512410005158533	0.5922330097087378	19
NR3C1	0.004660905398285098	0.580952380952381	19
CDK6	0.0038170438316212653	0.5545454545454546	18
AGTR1	0.018287298678450654	0.5648148148148149	16
KEAP1	0.0026605338954568103	0.5596330275229358	15
ADAM17	0.03407929516793642	0.5545454545454546	14

MMP1	4.67E+12	0.5596330275229358	14
MMP14	3.12E+11	0.5545454545454546	13
NOS2	7.92E+10	0.5495495495495495	13
TOP2A	0.007197003843095863	0.5126050420168068	12
CTSD	2.58E+12	0.516949152542373	12
ALOX5	0.010293346566186955	0.5213675213675214	11
PLA2G4A	0.010022662958530233	0.5350877192982456	11
CYP27B1	0.004110545228120938	0.5258620689655172	11
PTPN1	0.0013172427600089613	0.5213675213675214	11
CSF1R	6.23E+11	0.5304347826086956	11
EDNRA	0.0036689993672474512	0.49593495934959353	8
CYP17A1	0.0010719881700844156	0.4803149606299213	8
MMP8	2.90E+10	0.48800000000000004	8
SREBF2	0.0	0.5041322314049587	7
CDC25B	4.14E+11	0.4765625	7
THRB	5.49E+10	0.49593495934959353	7
TOP1	1.22E+12	0.4728682170542636	6
SMO	2.82E+11	0.4728682170542636	6
FABP4	9.52E+10	0.48800000000000004	6
PTGER1	0.0010971246422066096	0.44525547445255476	5
CYP2C19	7.36E+11	0.4552238805970149	5
HSD11B1	4.23E+11	0.4765625	5
AVPR2	0.0011039871271517744	0.4586466165413534	4
PRKAA2	0.0	0.4586466165413534	3
PTGFR	0.0	0.4357142857142857	3
ALOX5AP	0.0	0.4357142857142857	3
FAAH	8.45E+10	0.4552238805970149	3
F10	0.0	0.4485294117647059	2
SLC6A3	0.0	0.3765432098765432	1
PSEN2	0.0	0.3588235294117647	1